Two-dimensional Gas Chromatography: a novel technique for Iron Low Temperature Fischer-Tropsch selectivity studies

By

THELMA GROBLER

Hons. B.Sc. (CHEM) (Potchefstroom University)
B.Sc. (CHEM) (Potchefstroom University)

Supervisor: Prof. Eric van Steen, UCT
Co-Supervisor: Dr Matthys Janse van Vuuren, Sasol

Thesis submitted for the degree of
Masters in Chemical Engineering
at the University of Cape Town

December 2008

DECLARATION

I know the meaning of plagiarism and declare that all the work in the document, save for that which is properly acknowledged, is my own.

Thelma Grobler
December 2008

ACKNOWLEDGEMENTS

I would like to seize this opportunity to thank all the people and organisations who contributed to the execution of this research project. I truly believe that what I have achieved is due to the fact that I was “standing on the shoulders of giants” (Isaac Newton).

I would especially like to thank Prof. Eric van Steen, my supervisor, for all his guidance and time. I really appreciate your valuable inputs. My co-supervisor, Dr Matthys Janse van Vuuren, for his guidance and support as well as providing me the opportunity to grow as a scientists. Bernadette Murray, a colleague at Sasol Technology who assisted me with the operation of the micro-reactor. I would not have been able to perform this project without your assistance. Thank you for all your time and effort.

Furthermore I would like to thank Sasol Technology, Research and Development for funding this research project and allowing me the opportunity to further my education.

I also would like to thank John Swinley & Rouan Volsteedt from Scientific Supply Services for their technical support especially with regards to the set-up of the GCxGC instrumentation, a colleague, Riaan Bekker, for his expertise regarding GCxGC method development and all other colleagues at Sasol Technology for their support and motivation.

On a personnel level I would like to thank my husband, Daniel Grobler, for his support through out the entire project. I really appreciate the fact that you are always willing to listen and give advice. You are my rock.

I would also like to thank my parents Gert and Marlene Venter for always supporting me and teaching me the value of hard work and education.

Lastly I would like to thank God for providing me with the ability to explore the wonders of his creation.

SYNOPSIS

Fischer-Tropsch synthesis is a process that catalytically converts hydrogen and carbon monoxide into a large variety of hydrocarbons and oxygenated products. Over the years many researchers have attempted to describe the full product spectrum (ranging from C_1 to C_{100+}) but due to the complexity of the product and shortcomings of certain analytical techniques (or equipment) most researchers were only able to construct product distributions from extrapolations of data recorded from analysis of the C_1 to C_5 fraction of the Fischer-Tropsch product.

With recent advances in analytical technology and the development of comprehensive two-dimensional gas chromatography (GCxGC) it may now be possible to analyze the complex Fischer-Tropsch products in a relatively short time while delivering good separation of even minor compounds such as oxygenates and branched compounds.

The aim of this study was to investigate if two-dimensional gas chromatography (GCxGC) really results in improved separation and identification of compounds in the complex Fischer-Tropsch product spectrum and will lead to a more complete product distribution especially of the minor compounds such as branched hydrocarbons, ketones, aldehydes and acids.

For this study GCxGC equipment, supplied by Zoex Corporation, was connected to a micro slurry phase reactor system to provide for both on-line gas analysis as well as off-line product analysis. GCxGC methods were developed to analyze the hot tail gas and oil products from Fischer-Tropsch synthesis. Thereafter a test sample (C_6 to C_{30} oil product from Fischer-Tropsch synthesis process) was injected several times into both the GCxGC and 1D GC systems. The purpose of this was to compare the detection ability and accuracy of the two instruments.

To display the benefit of using GCxGC for Fischer-Tropsch research, synthesis experiments at various temperatures and H_2/CO feed gas ratios were performed and the products collected were analyzed using GCxGC. The data was then compared to data collected from one-dimensional gas chromatography (1D GC) analyses to establish the differences between the two methods. To highlight the benefits of GCxGC technique for the study of Fischer-Tropsch selectivity at a fundamental level, trends were constructed from the GCxGC data collected of the runs at various temperatures and H_2/CO feed ratios.

TABLE OF CONTENTS

LIST OF TABLES

LIST OF FIGURES

LIST OF SCHEMES

NOMENCLATURE

ABBREVIATIONS

1D	One-dimensional
2D	Two-dimensional
1D GC	One-dimensional Gas Chromatography
AOAC	Association of Analytical Communities
ARGE	Arbeidsgemeinshaft
ASF	Anderson-Schulz-Flory
BASF	Badische Anilin und Soda Fabrik
cat.	Catalyst
CFB	Circulating Fluidised Bed
CI	Confidence Interval
CSTR	Continuously Stirred Tank Reactor
ECD	Electron Capture Detection
FCV	Flow Control Valve
FIC	Flow Indicated Controller
FID	Flame Ionization Detector
FT	Flow Transmitter
FT	Fischer-Tropsch
FT-ICR	Fourier Transform Ion Cyclotron Resonance
FTS	Fischer-Tropsch Synthesis
GC	Gas Chromatography
GC-AED	Gas Chromatograph Atomic Emission Detector
GC-FID	Gas Chromatograph Flame Ionization Detector
GC-TCD	Gas Chromatograph Thermal Conductivity Detector
GCxGC	Two-dimensional Gas Chromatography
GHSV	Gas Hourly Space Velocity (ml/g_{cat}/hr)
GTL	Gas-To-Liquids
HCV	Hand Control Valve
HTFT	High Temperature Fischer-Tropsch
HTGC	High Temperature Gas Chromatography

IFE	In-line Flow Element
ID	Internal Diameter
LIAD	Laser-Induced Acoustic Desorption
LMCS	Longitudinally Modulating Cryogenic System
LTFT	Low Temperature Fischer-Tropsch
MFC	Mass Flow Controller
NCD	Nitrogen Chemiluminescence Detection
NRV	Non Return Valve
P&ID	Piping and Instrumentation Diagram
PAH	Pressure Alarm High
PCV	Pressure Control Valve
PI	Pressure Indicator
PT	Pressure Transmitter
rpm	revolutions per minute
RSD	Relative Standard Deviation
RV	Relief Valve
SAS	Sasol Advanced Synthol
Sasol	South African Coal, Oil and Gas Corporation
SCD	Sulphur Chemiluminescence Detection
SIC	Stirrer Indicated Controller
ST	Stirrer Transmitter
STP	Standard Temperature and Pressure [P=101.3 kPa, T=273.1 K]
Syngas	Synthesis Gas
TCD	Thermal Conductivity Detector
TE	Temperature Emitter
TIC	Temperature Indicated Controller
TSHH	Temperature Set point High
TV	Temperature Variable
WCOT	Wall Coated Open Tubular
WGS	Water Gas Shift
WHSV	Weight Hourly Space Velocity [ml (STP)/g-cat./hr]
wt%	Weight percentage

SYMBOLS

a	Kinetic parameter	[-]
A_i	Peak area count of compound i in GC-TCD or GC-FID trace	[-]
A_s	Peak area count of methane standard in GC-TCD or GC-FID trace	[-]
A_{C36}	Area of C_{36} n-paraffin with internal standard	[-]
$A_{C36calc}$	Calculated area of C_{36} n-paraffin	[-]
$\sum A_i$ =	Sum of component areas	[-]
C_{Ar}	Internal standard (argon) concentration	[mole %]
C_i	Concentration of component i (gas analysis)	[mole %]
C_i	Concentration of component i (oil analysis)	[mass%]
C_s	Concentration of external standard	[mole %]
C_{36conc}	Concentration of internal C_{36}	[mass%]
C_{36add}	C_{36} stock solution added to sample	[mass%]
$C_{36stockconc}$	C_{36} stock solution concentration	[mass%]
F_i	Flow rate of compound i	[mole/hr]
F_{Ar}	Flow rate of internal standard, Argon	[ml_n/min]
F_{TG}	Total flow rate of outlet gas (tail gas)	[ml_n/min]
F_{H2O}	Total Flow rate of H_2O	[ml_n/min]
$F_{CO,feed}$	Flow rate of CO in feed gas	[ml_n/min]
$F_{CO,tail}$	Flow rate of CO in outlet gas	[ml_n/min]
$F_{CO2,feed}$	Flow rate of CO_2 in feed gas	[ml_n/min]
$F_{CO2,tail}$	Flow rate of CO_2 in outlet gas	[ml_n/min]
$F_{i,FF}$	Flow rate of component in feed gas	[ml_n/min]
$F_{i,TG}$	Flow rate of component in outlet gas	[ml_n/min]
M_i	Mass percent of component I	[mass%]
M_{cat}	Mass of unreduced catalyst	[g]
M_{wax}	Mass of wax sample in sample solution	[g]
n	Average number of carbon atoms per hydrocarbon molecule	[-]
P	Pressure	[bar]
$P_{reactor}$	Total reactor pressure	[bar]

R	Universal gas constant	8.314 [J/mol/K]
RF	Response factor	[-]
RF_{1D}	Response factor for component separated	
	On one-dimensional GCxGC channel	[-]
RF_{2D}	Response factor for component separated	
	on two-dimensional GCxGC channel	[-]
r_{FT}	Fischer-Tropsch reaction rate	[mol/g-cat/s]
r_{wgs}	Water Gas Shift reaction rate	[mol/g-cat/s]
S_i	Selectivity of component i	[C atom]
T	Temperature	[ºC]
X	A factor for used in wax analysis calculations	[-]
$X_{i,overall}$	Overall conversion of each component	[%]

GREEK LETTERS

α	Chain growth probability	[-]
α	Position of double bond for olefins	[-]

SUPERSCRIPTS AND SUBSCRIPTS

1D	One-dimensional
2D	Two-dimensional
cat	Catalyst
FF	Fresh Feed gas
FT	Fischer-Tropsch
i	Component i
n	Carbon number
WGS	Water Gas Shift

CHAPTER 1

INTRODUCTION

Fischer-Tropsch synthesis is a process that catalytically converts hydrogen and carbon monoxide into a complex array of hydrocarbons and oxygenates which can be used in the production of fuels and high value chemicals. Realising the commercial potential of Fischer-Tropsch synthesis researchers have embarked on many studies to find optimal catalysts, reactor systems and process conditions that will produce the desired product (Dry et al., 1981; Schulz, 1985).

A huge variety of products of different chain lengths and different functionality is produced by Fischer-Tropsch synthesis. Over the years many researchers (Donnelly and Satterfield, 1981; Friedel and Anderson, 1950) have attempted to describe the full product spectrum (ranging from C_1 to C_{100+}) but due to the complexity of the product and shortcomings of certain analytical techniques (or equipment) most researchers were only able to construct product distributions from extrapolations of data recorded from analysis of the C_1 to C_5 fraction of the Fischer-Tropsch synthesis product (Weitkamp, et al., 1953). In most cases the selectivity information focused on the major compounds present in the products such as linear paraffins, olefins and alcohols whereas limited information was captured with regards to the minor compounds such as acids, aldehydes, ketones and branched hydrocarbons.

Over the last decade researchers have shown more interest in the minor compounds believing that knowledge of these compounds can help them with catalyst optimization initiatives, reactor design issues and fundamental studies regarding reaction kinetics and reaction mechanisms (Tau et al., 1991; Xu et al., 1997; Dry, 2004; Liu et al., 2007).

For most of the selectivity research reported in literature, gas chromatographic (GC) methods were used to separate the compounds in

the Fischer-Tropsch products. Gas chromatographic methods can be performed in a relatively short time (ranging from 10 min to 80 min depending on the product analyzed) and in general delivers good separation but when interest shifts to the detection and quantification of oxygenates, problems may be encountered. If oxygenates and other minor compounds are not separated from the hydrocarbon product into functional groups prior to GC analysis, it may be difficult to identify the individual oxygenated compounds. In most cases the compounds co-elute with some of the major compounds making accurate quantifications difficult.

With recent advances in analytical technology and the development of comprehensive two-dimensional gas chromatography (GCxGC) it may now be possible to analyze the complex Fischer-Tropsch products in a relatively short time (approximately 80 minutes) while delivering good separation of even the minor compound such as oxygenates and branched hydrocarbons (Dallüge et. al., 2003; Vendeuvre et. al., 2005).

The aim of this study was to investigate if two-dimensional gas chromatography (GCxGC) really presents improved separation in comparison to 1D GC and if so, what benefits GCxGC will provide to Fischer-Tropsch research.

CHAPTER 2

LITERATURE REVIEW

Fischer-Tropsch synthesis is a surprising phenomenon in heterogeneous catalysis that has attracted the interest of world experts for the past 100 years. Most of the research conducted over this period focused on topics such as catalyst and reactor development, influence of reaction conditions on activity and selectivity and reaction pathway analysis. Because knowledge regarding product selectivity can provide valuable insight in fundamental aspects of the Fischer-Tropsch synthesis (Schulz, 1985), many researchers captured selectivity data. Unfortunately due to the complexity of the Fischer-Tropsch synthesis products, the analytical techniques available and the time and effort needed to collect selectivity data most publications report only on the major products such as paraffins, olefins and alcohols. In recent years researchers such as Davis et al. (1991), Yang et al. (2004), Schulz et al. (1990), Xu et al. (1997) and Schulz et al. (1994) to name just a few, have shown interest in the minor products produced and have made an effort to develop analytical methods and systems to analyze these product compounds.

The following sections will give a short overview of the Fischer-Tropsch synthesis process and its development, the effect of operating conditions on product distribution and Fischer-Tropsch product analysis.

2.1. FISCHER-TROPSCH SYNTHESIS

The demand for fuel and energy resources is increasing especially amongst developing countries like China and India. According to the International Energy Agency, the world will need approximately 60% more energy in 2030 than it needed in 2002 (BBC News, 2004). Up until now, oil has been the greatest fuel resource for many countries, but due to depleting reserves and increasing costs, countries have started to search for alternative energy resources and technologies.

Fischer-Tropsch Synthesis (FTS), the process that catalytically converts carbon monoxide and hydrogen (synthesis gas) into automotive fuel or chemicals is an alternative technology that countries may consider as the synthesis gas needed for Fischer-Tropsch synthesis can be derived from coal, natural gas or biomass, resources that are abundantly available in many developing countries (Bartholomew and Farrauto, 2006).

Fischer-Tropsch Synthesis is not a new technology and has been around for nearly a century but its development has often been neglected due to the availability and popularity of crude oil as a fuel source.

2.1.1. Historical background and development

A few discoveries were made in the early 1900s that led to the conception of Fischer-Tropsch synthesis. Sabatier and Senderens (1902) were the first to synthesize methane from synthesis gas over reduced nickel and cobalt catalysts. Later in 1913 'Badische Anilin und Soda Fabrik' (BASF) went a step further and was the first to patent a process where liquid hydrocarbons and oxygenated products were produced from synthesis gas over a cobalt catalyst under high pressure. In 1923 Fischer and Tropsch reported their success in synthesizing a liquid hydrocarbon product rich in oxygenated compounds from synthesis gas at high pressures (100 -150 atm) and temperatures (400ºC - 450ºC) over an alkali treated iron catalyst. Subsequent to this work, Fischer and Tropsch (1925) succeeded in producing hydrocarbon liquids and solid paraffins on cobalt and iron catalysts under mild conditions of 1 atm and 250 - 300ºC which marked the official beginning of Fischer-Tropsch synthesis (Bartholomew and Farrauto, 2006).

During the 1930s and 1940s most of the Fischer-Tropsch process developments occurred in Germany. The Germans realised that it would be to their advantage if they became more independent of external resources

for energy by producing liquid fuels from their own vast coal reserves. The construction of commercial-size Ruhrchemie licensed Fischer-Tropsch plants started in 1935 and reached a climax towards the end of World War II (1944) when a total annual capacity of approximately 570 000 metric tons of automotive fuel, oxygenated hydrocarbons, soft waxes and heavy oils were produced (Stranges, 2003). Initially the plants operated with cobalt catalysts at atmospheric pressure and at temperatures between 180 – 200ºC, but in order to enhance catalyst performance and increase catalyst lifetime the operating pressures were increased to pressures of 5-20 bar (Dry, 1981).

After World War II, research and development on the Fischer-Tropsch synthesis continued in the United States, Great Britain and Germany due to the perceived petroleum shortage and the fear that crude oil prices would increase. Most of the work was based on inexpensive iron catalyst developed towards the end of the war in Germany (Bartholomew and Farrauto, 2006).

With the objective to maximise gasoline production, several firms in the United States developed High Temperature Fischer-Tropsch (HTFT) fluidised bed reactor technology. In Brownsville Texas the first commercial Fischer-Tropsch based Gas-to-Liquids (GTL) plant was constructed in 1951 and operated until 1957 by a Texaco-led consortium (Zhang and Davis, 2000; Bartholomew and Farrauto, 2006). In this GTL process, fused iron catalyst was loaded in a fluidised bed reactor, a technology later to be implemented at Sasol. Although GTL processes have their roots in the United States, the technology never caught on there; the GTL applications were not economically viable due to the high gas prices and low cost crude oil imports from the Middle East (Zhang and Davis, 2000).

From the 1950s to the 1980s most of the Fischer-Tropsch technology development occurred in South Africa. Due to its apartheid policies, South Africa feared being boycotted and wished to become independent of external oil supplies. At that stage Fischer-Tropsch technology was an

economical viable option due to the existence of extremely large coal deposits in the country which could be mined at low cost (Masters, 1979).

In 1950 the South African Government founded Sasol (South African Coal, Oil and Gas Corporation) and in 1955 began to produce liquid fuels and coal based chemicals in Sasolburg at their Sasol I plant. The circulating fluidized bed (CFB) reactor technology used for Fischer-Tropsch synthesis was developed by Kellogg. Initially some problems occurred with the use of the CFB technology and therefore the license for the technology was transferred to Sasol. The problems were eventually solved and the process was renamed the 'Synthol' (Sasol Synthol^{TM}) process (Steynberg, 2004). In the early 1980s Sasol further embarked on the construction of two coal-based plants in Secunda (Sasol II), South Africa. Initially CFB reactors were used for Fischer-Tropsch synthesis at this complex, but later the reactors were replaced at Sasol Advanced Synthol (SAS) reactors which increased capacity significantly. Today the plant continues to produce 140,000 bbl/d (Steynberg et al., 1999; Dry, 2002). Furthermore, Sasol constructed a 25 000 bbl/d GTL plant using the CFB technology in Mosselbay, South Africa (Dancuart and Steynberg, 2004).

Although South Africa was leading the way in Fischer-Tropsch commercialization, research and development on the Fischer-Tropsch synthesis was revived in the United States and Europe after the 1973 oil embargo (Bartholomew and Farrauto, 2006). Between 1975 and 1990 several researchers actively studied topics regarding Fischer-Tropsch catalysts, kinetics, mechanisms and catalyst deactivation. Building on previous work, significant progress was made in the area of relating Fischer-Tropsch synthesis activity and selectivity with catalyst properties. Sophisticated methods and tools were used to conduct fundamental studies leading to the rational design of catalysts. Research by companies like Gulf Oil, Exxon, Shell and Statoil all contributed to the development of high-surface-area, high-activity, promoted Co/Al_2O_3 catalysts. New insights and innovations improved Fischer-Tropsch process economics and paved the way for advanced Fischer-Tropsch technology development, especially in

diesel production using a combination of GTL and cobalt catalyst technology (Bartholomew and Farrauto, 2006). In 1993 a 10,000 bbl/d Fischer-Tropsch plant was constructed by Shell in Bintulu, Malaysia using a cobalt based catalyst, in which wax production is optimized which is subsequently hydro-cracked (Dancuart and Steynberg, 2004).

In the modern day era, Fischer-Tropsch technology has once again received revived interest globally due to increasing energy demands from fast developing countries like China and India, rising crude oil prices (reaching prices beyond $140 per barrel in 2008) and the shift towards low sulphur diesel to reduce the impact diesel engine usage have on the environment.

Going into the new millennium, it seems to be an exciting time for Fischer-Tropsch technology. In 2006 the 34 000 bbl/d Oryx plant in Qatar was commissioned (in a joint venture with Qatar General Petroleum and Sasol) and currently construction is underway of a 34 000 bbl/d plant in Nigeria (a Sasol-Chevron joint venture). Many companies are also embarking on feasibility studies to construct Fischer-Tropsch plants in China, India, Australia and the United States (Davies, 2005; Hill, 2007; Van der Merwe, 2008) and with the focus on cleaner fuel technologies, Fischer-Tropsch technology is even being considered as a non-conventional bio-diesel synthesis pathway (Holbein et al., 2004).

2.1.2. Stoichiometry of Fischer-Tropsch products

In general the Fischer-Tropsch synthesis is described as a highly exothermic polymerisation reaction that converts hydrogen and carbon monoxide to hydrocarbons and water. Stoichiometrically, the Fischer-Tropsch synthesis can be described by the following equation (Dry 2004):

$$nCO + 2nH_2 \rightarrow (-CH_2-)_n + nH_2O \qquad (2.1)$$

As presented in equation 2.1 the stoichiometry is primarily concerned with the ratio of consumption (2:1) of hydrogen and carbon monoxide. The main products produced are linear paraffins, α-olefins, linear alcohols (see equation 2.2) and as a by-product, water.

$$nCO + 2nH_2 \rightarrow C_nH_{2n+2}O + (n-1)\ H_2O \qquad (2.2)$$

Depending on the type of catalyst, the gas composition and the synthesis conditions, different side reactions can also occur. The Water-Gas-Shift (WGS) reaction is a side reaction that converts carbon monoxide and water into carbon dioxide and hydrogen (see equation 2.3). When using an iron-based catalyst at low temperatures with a hydrogen lean feed gas, a significant amount of carbon dioxide is produced. However at high reaction temperatures the WGS reaction approaches equilibrium and carbon dioxide and hydrogen can be consumed to produce water and carbon monoxide. Over cobalt and ruthenium catalysts the extent of the WGS reaction is negligible and this reaction may be treated as a one way reaction producing a small amount of carbon dioxide (Dry, 2004).

$$CO + H_2O \leftrightarrow CO_2 + H_2 \qquad (2.3)$$

Thermodynamically the production of methane is favoured above the production of heavier molecular weight hydrocarbons; however experiments at typical Fischer-Tropsch conditions deliver a product distribution ranging from C_1 to C_{100+} indicating that reaction kinetics rather than thermodynamics drives the Fischer-Tropsch synthesis (Bartholomew and Farrauto, 2006; Dry, 1981; Dry, 2004).

2.1.3. Fischer-Tropsch products

2.1.3.1. Classification of Fischer-Tropsch products

Knowledge of the composition of the Fischer-Tropsch derived products is essential for efficient utilization of these products and for developing improvements of the process. Analysis of the products may also provide clues to the reaction mechanisms involved which in turn may result in optimised production processes.

A huge variety of products of different chain lengths and different functionality is formed in Fischer-Tropsch synthesis. The actual composition or product distribution of a Fischer-Tropsch process depends on many reaction variables such as reaction conditions, the reactor system used, as well as the catalyst formulation and physical properties of a catalyst.

In general mainly linear olefins and paraffins are produced during the Fischer-Tropsch synthesis, but some oxygenates and branched compounds are also formed (Claeys and Van Steen, 2004). The oxygenates can include alcohols, aldehydes, ketones and carboxylic acids.

Different types of product can form when different catalysts are used. Ruthenium catalysts yield waxes of high molecular weight, cobalt catalysts produce products consisting mainly of linear olefins for the low carbon number product and paraffinic waxes and the products from iron catalysts are largely olefinic and contain significant proportions of branched isomers and oxygenated compounds (Weitkamp et al., 1953).

Generally cobalt and iron catalysts are used for the commercial Fischer-Tropsch synthesis process. Studies conducted over these catalysts have revealed that primary formed products are olefins, paraffins and alcohols. Linear paraffins and α-olefins are primary products of the Fischer-Tropsch synthesis and can be present in more than 60 wt% of the total Fischer-Tropsch synthesis product. Depending on reaction conditions, α-olefins can

re-adsorb on the catalyst surface and undergo secondary reactions like hydrogenation, isomerisation (double bond shift), re-insertion, hydrogenolysis and hydroformylation (Schulz and Claeys, 1999b; Dry, 1999; Weitkamp and Frye, 1953).

Branched compounds are also produced during Fischer-Tropsch synthesis via primary and secondary reactions. It has been reported that for the Low Temperature Fischer-Tropsch (LTFT) process over an iron catalyst approximately 5 wt% of the hydrocarbons obtained are branched while half of those from the High Temperature Fischer-Tropsch (HTFT) process are branched (Jager, 1998).

Relative to the amount of olefins and paraffins produced from Fischer-Tropsch synthesis, oxygenated products are regarded as minor synthesis products. Little is known about the formation of oxygenated compounds, but it is believed that linear alcohols and aldehydes are the primary formed products (Weitkamp and Frye, 1953). Early works also reported the presence of straight-chain alcohols, acids, aldehydes and ketones present in the water stream. Esters, cyclic ketones and branched-chain alcohols, aldehydes and acids are present in minor fractions (Steitz and Barnes, 1953). With regards to oxygenated compounds in the oil stream the main oxygenated components are acids, alcohols and carbonyl compounds of the aliphatic series. Alcohols appear to be more closely related structurally to the aliphatic hydrocarbons than the acids and branched isomers are more prevalent in the acids. (Cain et al., 1953).

Aromatics are also formed in the Fischer-Tropsch synthesis, but the formation mechanism is still unknown. Dry (1981) reported that the production of aromatics over an iron catalyst at 227ºC is virtually zero but as the operating temperature of the Fischer-Tropsch synthesis increase, more aromatics are produced in the gasoline product (approximately 25 wt% aromatics at 337ºC). Steynberg et al. (1999) reported similar results for the HTFT process where 15 wt% of the products formed were aromatics.

2.1.3.2. Fischer-Tropsch product distributions

The Fischer-Tropsch synthesis is a surface polymerisation reaction that yields a distinctive recognizable product distribution pattern (Herington, 1946). Anderson (1950) and Flory (1936) were the first to develop the chain growth model from which a mathematical model, known as the Anderson-Schulz-Flory (ASF) distribution, was derived (Dry, 2004). The ASF distribution model is depicted by the following equation:

$$\lg\left(\frac{W_n}{N_c}\right) = N_c \cdot \lg\left(p_g\right) + \lg\left(\frac{1-p_g}{p_g}\right) \tag{2.6}$$

Where W_n is the weight fraction of the species with carbon number n. According to the equation the ASF distribution should yield a straight line and from the slope of the plot a single value can be obtained known as the chain growth probability (p_g) or α (see equation 2.7 where r_g = rate of chain growth and r_d = rate of desorption).

$$p_g = \frac{r_g}{r_g + r_d} \tag{2.7}$$

The entire product spectrum can be readily calculated from α-values ranging from zero to one, assuming that the chain growth probability is independent of chain length (see Figure 2.1).

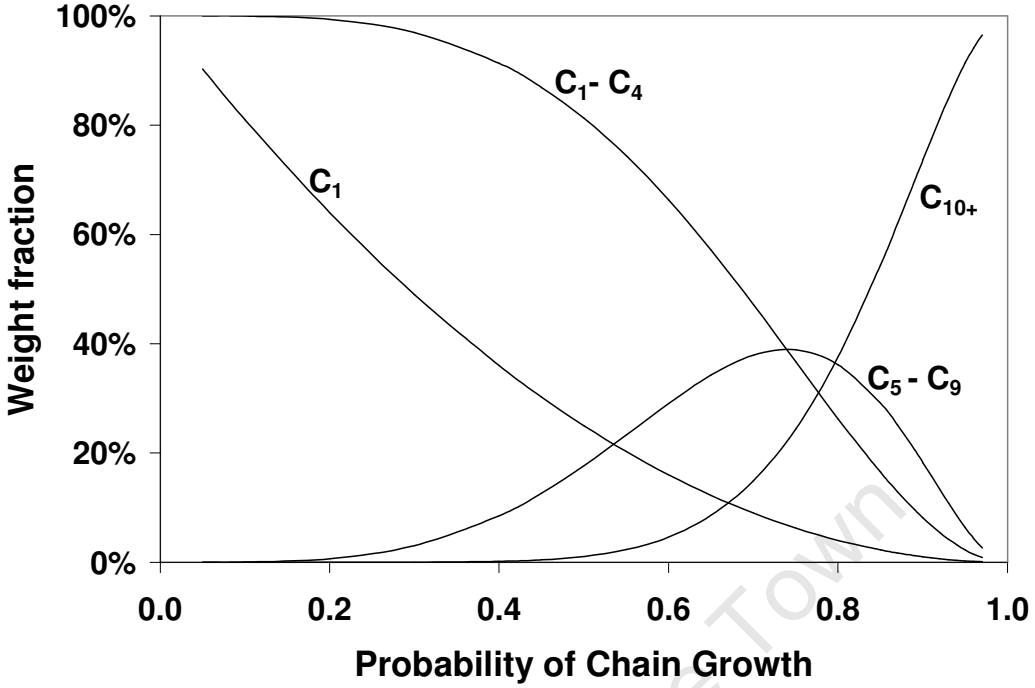

Figure 2.1: Product selectivity as a function of chain growth probability according to the ideal Anderson-Schulz-Flory model (Janse van Vuuren et al., 2008)

The ASF distribution model approximates an ideal molecular weight distribution but this ideal case is often not experimentally observed. The following deviations have been observed (Davis, 2003; Van der Laan and Beenackers, 1999):

- a relatively higher than expected methane yield.
- the total C_2 selectivity is lower than expected.
- the chain growth probability (α) increases with carbon number and
- the olefin-to-paraffin ration decreases with increasing carbon number.

Many researchers have conducted work to explain the deviations observed. In general the following explanations are mentioned in literature (Davis, 2003; Van der Laan and Beenackers, 1999; Puskas and Hurlbut, 2003):

- The existence of two α-values can be attributed to the existence of two different types of catalytic sites or two mechanisms that are occurring simultaneously.

- Olefins are re-adsorbed on the catalyst surface and undergo further secondary reactions.
- Higher molecular weight or longer chain species are less likely to desorb, thus they will remain longer on the catalyst surface and can undergo further chain growth thereby resulting in the higher chain growth probability observed.

2.1.4. Mechanisms in Fischer-Tropsch synthesis

Fischer-Tropsch synthesis is classified as a polymerisation reaction where the monomers are produced in-situ from the gaseous reactants hydrogen and carbon monoxide. All the reaction pathways consist of three steps: the generation of the chain initiator, chain growth and chain termination. It is generally accepted that Fischer-Tropsch (FT) synthesis is a complex process that comprises more than one reaction pathway on the catalyst surface and reactions may occur in parallel. The four reaction mechanisms accepted by most are: the “alkyl”, the “alkenyl”, the “enol” and the “CO-insertion” mechanism (Claeys and van Steen, 2004).

2.1.4.1. The Alkyl mechanism

The alkyl mechanism (Figure 2.2) has been conceptualised from the so-called “carbide”-mechanism and has been the most widely accepted mechanism for the Fischer-Tropsch synthesis (Claeys and Van Steen, 2004). Chain initiation occurs when dissociated CO is chemisorbed to form surface carbon and surface oxygen species. The surface oxygen is removed from the catalyst surface by either reacting with adsorbed hydrogen to form water or adsorbed carbon monoxide to form carbon dioxide. Subsequently, surface carbon is hydrogenated yielding sequentially CH, CH_2 and CH_3 hydrocarbon species. In this reaction mechanism, the CH_2 species functions as the monomer responsible for chain growth and is successively incorporated while the CH_3 is regarded as the chain initiator. The third step is product formation. Primary products are formed either by

β-hydrogen elimination or hydrogen addition forming α-olefins and n-paraffins. The formation of branched hydrocarbons are not described by the main reaction pathway of the alkyl mechanism but Schulz et al. (1990) proposed a reaction pathway involving the reaction of an alkylidene species and methyl surface corresponding to the alkyl mechanism. The formation of oxygenated compounds cannot be explained by the alkyl mechanism, but Johnston and Joyner (1993) proposed the involvement of surface hydroxyl groups in the formation of oxygenates.

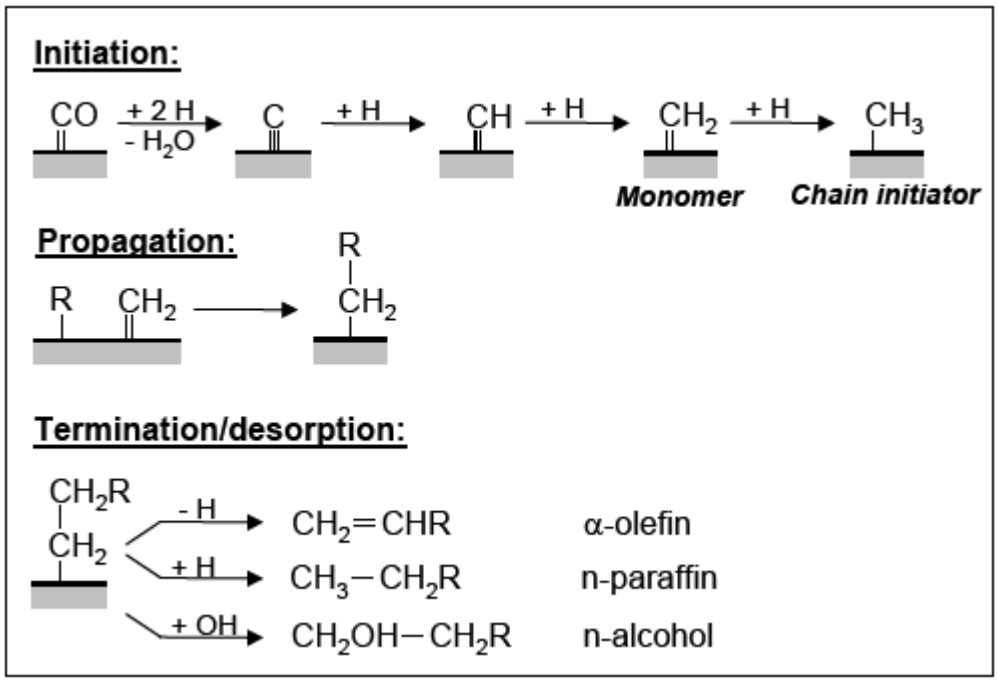

Figure 2.2: Reaction steps in the Fischer-Tropsch synthesis according to the alkyl mechanism (R = C_nH_{2n+1} with $n \geq 0$) (Claeys and van Steen, 2004)

2.1.4.2. The Alkenyl mechanism

An alternative reaction pathway (see Figure 2.3) for Fischer-Tropsch synthesis, which predicted olefin formation, was proposed by Maitlis and co-workers (1996 and 1999). The initial activation of carbon monoxide and its transformation into CH_x surface species are identical to the proposed alkyl mechanism. In the case of this mechanism the chain initiator is a vinyl species ($CH=CH_2$). Chain propagation involves the addition of a methylene species to a surface vinyl species yielding a surface allyl species. This is

followed by an allyl-vinyl isomerisation forming an alkenyl species. Product desorption involves hydrogen addition to an alkenyl species yielding an α-olefin. The mechanism fails to explain the primary formation of n-paraffins and requires the co-existence of an alternative chain growth mechanism.

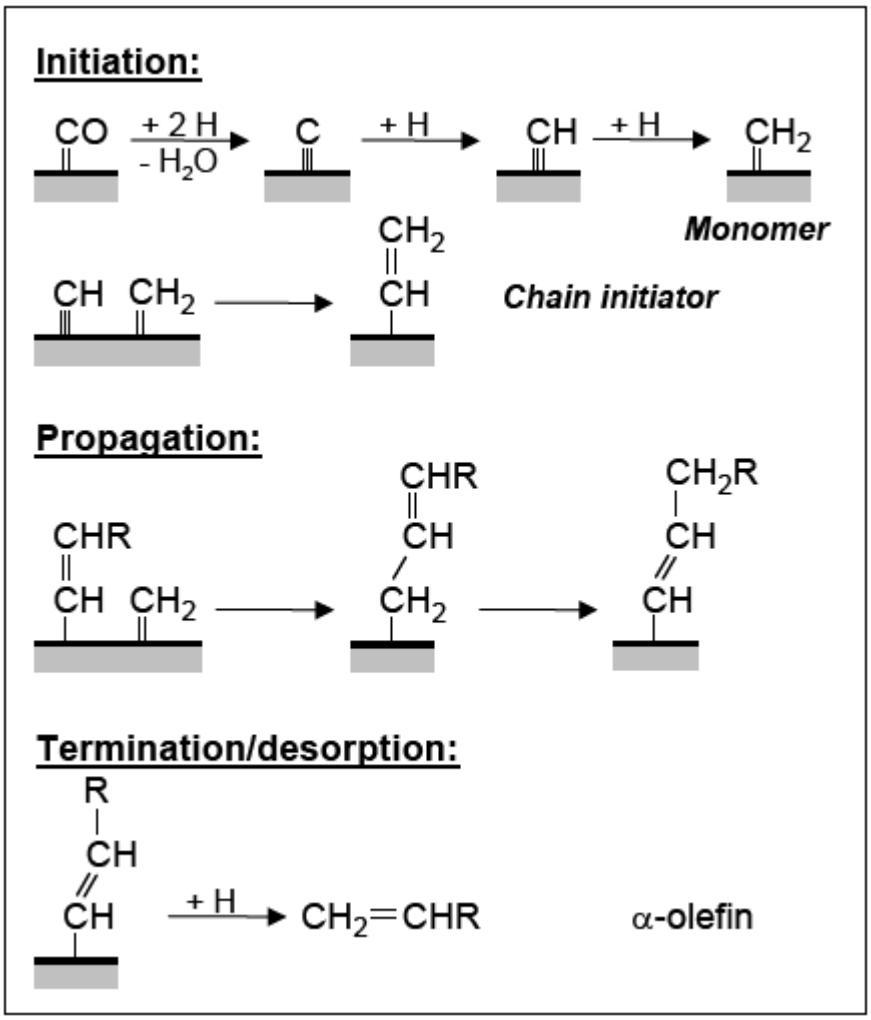

Figure 2.3: Reaction steps in the Fischer-Tropsch synthesis according to the alkenyl mechanism (R = C_nH_{2n+1} with $n \geq 0$) (Maitlis et al., 1996 and 1999)

2.1.4.3. The Enol mechanism

Storch et al. (1951) proposed an alternative reaction mechanism involving oxygenated (enol) species as the chain initiator (see Figure 2.4). According to the mechanism chemisorbed carbon monoxide is hydrogenated to enol surface species. Chain growth occurs through a condensation reaction between enol species under elimination of water. Termination of the chain

growth process yields oxygenates (aldehydes and alcohols) and α-olefins. According to the mechanism, n-paraffins are formed secondarily by hydrogenation of primarily formed olefins. The primary formation of n-paraffins would require an alternative reaction pathway.

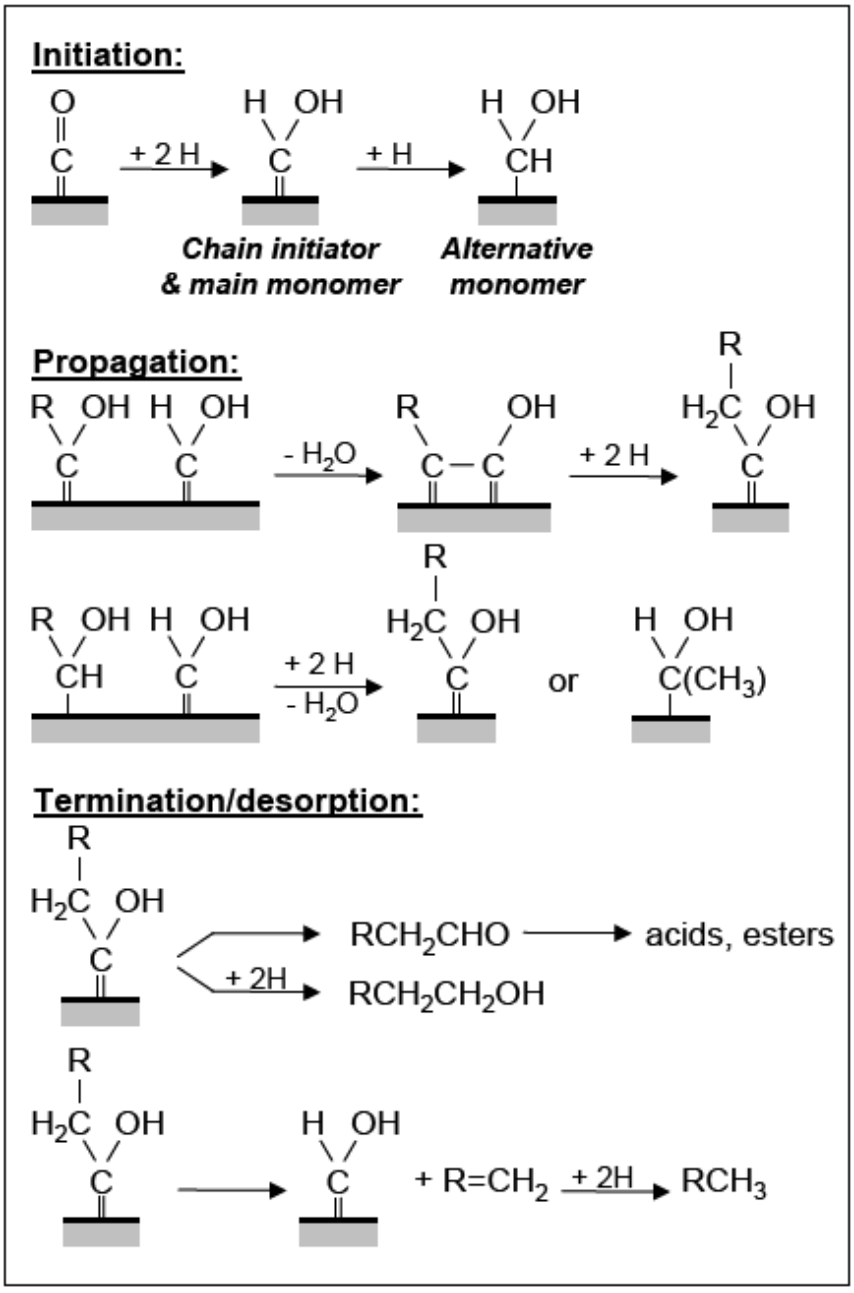

Figure 2.4: Reaction steps in the Fischer-Tropsch synthesis according to the enol mechanism (R = C_nH_{2n+1} with $n \geq 0$) (Storch et al., 1951)

2.1.4.4. The CO insertion mechanism

The CO insertion mechanism was originally proposed by Sternberg and Wender (1959) and Roginski (1965) and later fully developed by Pichler and Schulz (1970). The monomer in this mechanism is chemisorbed carbon monoxide. The chain initiator is thought to be a surface methyl species. The reaction pathway leading to the formation of the surface methyl species differs from the alkyl-mechanism at the time of the oxygen elimination from the surface species. Chain growth takes place by CO-insertion in a metal-alkyl bond leading to a surface acyl species. The elimination of oxygen from surface species leads to the formation of the enlarged alkyl species. Desorption of these species can either lead to α-olefins or n-paraffin formation (this has been proposed by the alkyl-mechanism) or to the formation of aldehydes and alcohols from oxygen containing surface species.

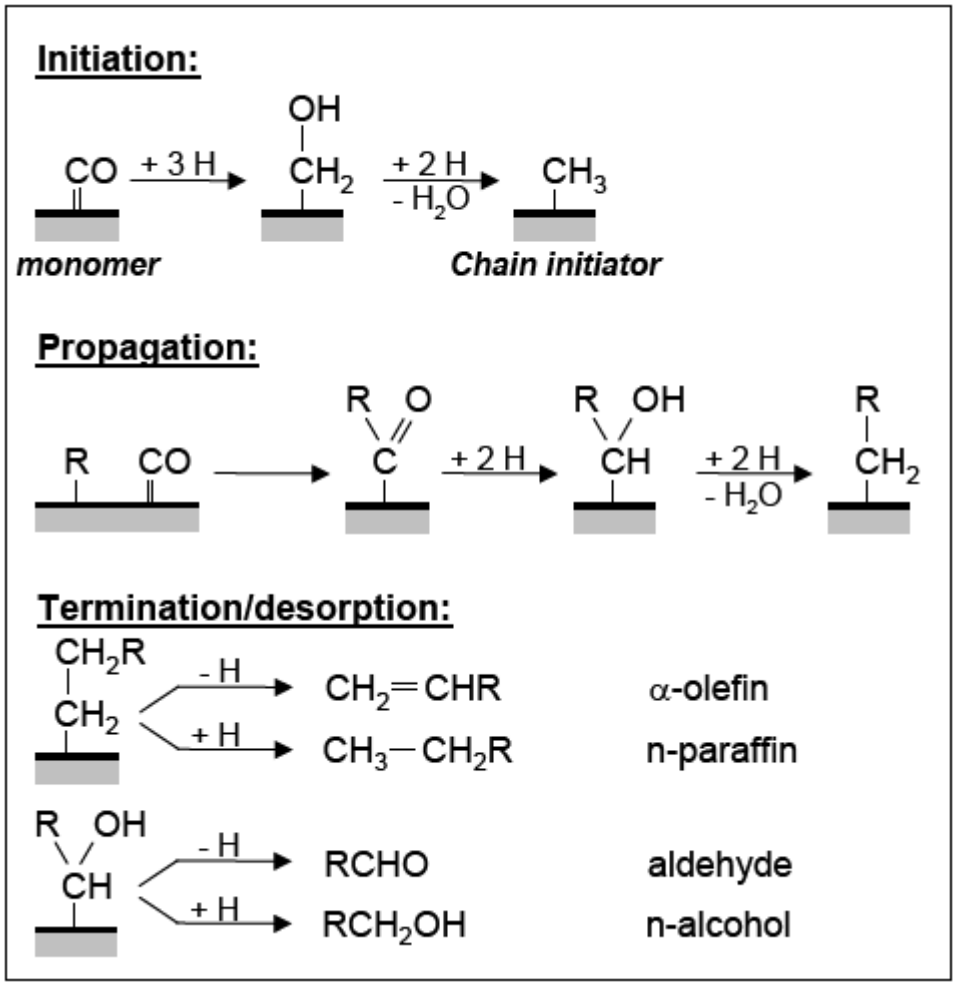

Figure 2.5: Reaction steps in the Fischer-Tropsch synthesis according to the CO-insertion mechanism (Pichler and Schulz, 1970; Claeys and van Steen, 2004)

2.1.5. Fischer-Tropsch synthesis catalysts

The catalysts commonly used for Fischer-Tropsch synthesis consist of the group VII metals (Van der Laan, Beenackers, 1999). Of these metals Fe is an attractive option due to its low cost in comparison to the other active metals like Co, Ru and Ni (Rao et al., 1992). For commercial low temperature Fischer-Tropsch operations, Co and Fe catalyst are predominantly used (Adesina, 1996), but the choice between various Fischer-Tropsch synthesis catalysts is mostly determined by the feed gas composition and the desired product selectivity

Cobalt catalysts are relatively expensive catalysts (Rao et al., 1992) usually employed in gas-to-liquid (GTL) processes where hydrogen rich syngas is generated from natural gas. Cobalt catalysts normally have extended catalyst lifetime (Chaumette et al., 1995), high wax selectivity and achieve high per pass conversions (van Berge and Everson, 1997).

In general iron catalysts have relatively low Fischer-Tropsch synthesis activity, a tendency for rapid deactivation, high water-gas-shift (WGS) reaction activity and high selectivity to olefins (Jager and Espinoza, 1995; Kölbel and Ralek, 1980). The catalyst is typically used for coal-to-liquids (CTL) operations as the high WGS activity makes the catalyst suitable for the low H_2: CO ratio coal derived synthesis gas (Xu et al., 1998).

2.2. THE EFFECT OF OPERATING CONDITIONS ON PRODUCT DISTRIBUTION

Fischer-Tropsch product selectivity can be influenced by process conditions and the type of catalyst used. The influence of temperature, partial pressures and residence time will be discussed briefly. Table 2.1 shows the general influence of different process parameters on Fischer-Tropsch synthesis product selectivity.

Table 2.1: Influence of process parameters on the Fischer-Tropsch product selectivity

Increasing parameter	Chain length	Chain branching	Methane selectivity	Olefin selectivity	Oxygenate selectivity
Temperature [1,2]	↓	↑	↑	*	↓
Pressure (Total)[1,2]	↑	↓	↓	*	↑
H_2/CO[1,2]	↓	↑	↑	↓	↓
H_2 partial pressure[2]	↓	*	↑	↓	
CO partial pressure[2]	↑	*	↓	↑	
Conversion[1]	*	*	↑	↓	↓
Space velocity[1,2]	*	*	↓[1],↑[2]	↓[1],↑[2]	↓[1],↑[2]

*Note: Increase with increasing parameter: ↑. Decrease with increasing parameter: ↓. Complex relation: * Sources: [1]Roper (1983) and [2]Claeys (1997)*

2.2.1. The effect of temperature

In general, irrespective of the type of catalyst used, if the Fischer-Tropsch synthesis operating temperature is raised the Fischer-Tropsch product spectrum shifts to a lower carbon number and a lighter product is obtained. One explanation for this observation is that the rate of desorption increases at higher synthesis temperatures thus limiting surface species growth. Hence a lighter product will be produced (Dry, 2004). As the temperature increases, the Fischer-Tropsch system also becomes more hydrogenating

and therefore the olefin-to-paraffin ratio decreases (Dry, 2004; Dictor and Bell, 1986). Contrary to this Donnelly and Satterfield (1989) reported an increase in the olefin-to-paraffin ratio as temperature was raised.

Concerning oxygenate selectivity various different observation has been captured in literature. Dry (1981) compared the iron-based High Temperature Fischer-Tropsch (HTFT) and Low Temperature Fischer-Tropsch (LTFT) processes, and observed the differences in oxygenate selectivity (see Table 2.2). The High Temperature Fischer-Tropsch process does not only produce more oxygenates than the Low Temperature Fischer-Tropsch process, the oxygenated product is also more diverse, i.e. it consisted out of large amounts of ketones, iso-alcohols, acids and aromatics. Of the alcohols, aldehydes and acids produced the most abundant species on a carbon atom basis are the C_2 compounds, namely, ethanol, acetaldehyde and acetic acid. The most abundant ketone produced is acetone. With regards to acids Dry (2004) reported that at 500 K the production of aromatics over and iron based catalyst is virtually zero but when operating at 650 K the amount of aromatics formed increases to ca. 25% in the gasoline cut.

Table 2.2: Observed oxygenate selectivity differences between HTFT and LTFT processes.

Fischer-Tropsch synthesis process	Oxygenates	Primary Alcohols	Methanol	Ketones, iso-alcohols, Acids	Aromatics
LTFT (240 ºC)	Lower	Higher	Higher	Lower	None
HTFT (340 ºC)	Higher	Lower	Lower	Higher	Higher

In more recent years researchers such as Liu et al. (2007) conducted experiments with an iron-manganese catalyst over a temperature range of

260ºC – 280ºC and reported that the overall oxygenate selectivity increased as temperature increased. This was in contrast with observations made by Roper (1983) and Claeys (1997) that oxygenate selectivity decrease as temperature increase. Dry (1981) however noted that as the operating conditions move from LTFT to HTFT conditions (over an iron based catalyst), oxygenate selectivity increases.

Liu et al. (2007) also reported that as the Fischer-Tropsch synthesis temperature increases, the alcohol selectivity in the water product increases, this is in contrast with Roper's observations (Roper, 1983) that alcohol selectivity decreases as temperature increase. Furthermore Liu et al. (2007) reported that the acid selectivity in the water product decreases, aldehyde selectivity increases and the ketone selectivity did not vary as temperature was raised. Dry (1981) reported when he investigated selectivity at various temperature over the HTFT range (310ºC – 380ºC) that the acid selectivity decreases, this is in accordance with Liu et al. (2007), but regarding his observation of ketones selectivity he noticed an increase where Liu et al. (2007) noted no variation as temperature increase.

According to Roper (1983) and Claeys (1997) the selectivity towards branched products increase as Fischer-Tropsch synthesis reaction temperature is raised. Pichler and Schulz (1970) made a similar observation regarding the degree of branching stating that the degree of branching increases as synthesis temperatures increase over an iron catalyst at 320ºC.

2.2.2. The effect of H_2 and CO partial pressure

Gas composition, partial pressures of the gaseous components and total pressure are all interlink and will have an influence on Fischer-Tropsch product selectivity if these parameters change. The most relevant partial pressures are those of H_2 and CO. When CO partial pressure is high the coverage of adsorbed catalyst monomers are high, this will promote chain

growth. On the other hand when CO partial pressure is low, surface coverage of monomers are lower and the probability of desorption increases. Thus in general it can be argued that when the H_2/CO ratio increases the probability of chain termination increases leading to lighter hydrocarbons (Dry, 2004).

When observing the effect of H_2/CO ratios on selectivity, Donnelly and Satterfield (1989) noticed a decrease of the olefin-to-paraffin ratio by increasing the H_2/CO ratio. According to Roper (1983) and Claeys (1997) the total oxygenate selectivity decreases as H_2/CO ratio increases. Dry (2004) reported increasing alcohol selectivity with increasing H_2/CO ratios.

Dry (1981) reported that over an iron based catalyst, the acid selectivity for Fischer-Tropsch synthesis over a pressure range of 8 – 60 bar, increased with increasing total pressure. Work conducted by Anderson et al. (1952) found that over a fused iron catalyst, increased pressure delivered higher oxygenate production. Liu et al. (2007) observed the same trend for experiments conducted over an iron-manganese catalyst.

During Fischer-Tropsch synthesis the actual situation on the catalyst surface is quite complex for the surface coverage by CO and H_2 could also depend on competition for vacant sites by other gases such as CO_2 and H_2O. As CO chemisorption is much stronger than H_2 chemisorption, CO_2 and H_2O partial pressures might have a greater negative effect on the amount of hydrogen adsorbed than the amount of CO.

2.2.3. The effect of residence time

Residence time and space velocity is interlinked for the residence time of reactants that take part in Fischer-Tropsch synthesis can be changed by changing the space velocity. Iglesia et al. (1993) performed Fischer-Tropsch synthesis runs over Co/TiO_2 catalysts and reported that as residence time increases (decrease in space velocity), CO conversion and C_{5+} selectivity

increases while methane selectivity decreases. Similar results were reported for Ru catalysts. They also reported that the paraffin content increased when residence time increased.

Contradictory to the above findings, Bukur et al. (1990) performed Fischer-Tropsch experiments on a commercial supported iron catalyst and measured no effect of the space velocity on the molecular weight of hydrocarbons.

Elbashir and Roberts (2004) reported that an increase in residence time of α-olefins inside catalyst pores, can lead to secondary reactions of the olefins such as hydrogenation and isomerisation to form normal paraffins and branched products. Iglesia et al. (1991) also observed a decrease in olefins with an increase in residence time (decrease in space velocity).

The following observations were made with regards to the influence of residence time on oxygenate selectivity. Liu et al. (2007) reported that over a Fe-Mn catalyst the overall oxygenate formation rate increased when space velocity was increased (residence time decreased). But when the space velocity was increased further, the overall oxygenate formation rate decreased to some extent. Roper (1983) observed a decrease in oxygenate selectivity while Claeys (1997) observed an increase when space velocity is increased.

2.3. FISCHER-TROPSCH PRODUCT ANALYSIS

Knowledge of the composition of the Fischer-Tropsch synthesis product is essential for efficient utilisation of the product and for developing improvements of the process. Fischer-Tropsch synthesis product analysis can also aid with drawing relations between reaction selectivity, catalyst activity and catalyst composition (Nijs and Jacobs, 1981).

Over the years a large number of publications appeared in the field of Fischer-Tropsch chemistry, but only a few authors have described the analytical techniques they employed for product analysis in detail. Most of them have restricted themselves to the analysis of only a minor part of the product spectrum.

In the following sections (2.3.1-2.3.3) a brief overview will be given of the methods employed in the early days of Fischer-Tropsch synthesis research, how Fischer-Tropsch synthesis product analysis changed with the development of gas chromatographic techniques and what techniques are emerging that may provide exciting prospects for the future of product analysis.

2.3.1. Early Fischer-Tropsch product analysis

In the early days of Fischer-Tropsch synthesis research workers generally noted the nature of the product but did not investigate the composition of the product in detail. In the 1950s researchers started to realise that in order for them to manipulate Fischer-Tropsch synthesis and improve the process they needed information regarding the product composition.

Weitkamp et al. (1953) were amongst those who realised the importance of detailed product analysis and gave a detailed description of the analytical techniques they used to analyse product samples obtained from a Fischer-Tropsch pilot plant scale run over an iron catalyst.

In order to perform analysis on the products, the effluent of the reactors had to be separated into several product streams by successive cooling steps to produce a waxy hydrocarbon product, water and an oily hydrocarbon product. The remaining gas stream was further cooled, under reaction pressure, to -40ºC to obtain a liquid phase consisting mainly of low molecular weight hydrocarbons.

Due to the complexity of the Fischer-Tropsch synthesis product, it was impossible for Weitkamp et al. (1953) to perform analysis to identify all the individual components with the methods available at that time. They were, however, able to formulate a carbon number distribution up to C_{16} and composition of the carbon number fractions in terms of olefin, paraffin and aromatic classes up to C_6. Increasing complexity limited analysis of the C_7 fraction to identification of carbon skeletons. In higher carbon number fractions certain structural types were identified, but the picture was far from complete. Fortunately, because Fischer-Tropsch synthesis is a polymerisation reaction, knowledge of the simpler molecules enabled them to extrapolate and so obtain information of the heavier more complex molecules.

The following methods were used by Weitkamp et al. to analyse the Fischer-Tropsch synthesis products with the goal to formulate a hydrocarbon distribution as mentioned above.

The vent gas was analyzed by mass-spectrometric analysis methods whereas the liquid streams were analyzed using fractionated distillation. In order to obtain more information with regards to specific functional classes (paraffin, aromatic and olefin) within product fractions they made use of fractionated distillation to obtain narrow boiling cuts. These cuts were then further washed with water to remove oxygenated components. Isomers were determined via infrared and the rest of the components by mass spectroscopy. These methods were suitable to identify the components in the C_1 to C_5 product fractions.

Refractive index calculations, supplemented in certain cases with infrared and mass spectroscopy, were used to obtain information with regards to functional components in the C_6 product cut.

The C_7 and higher fractions were analyzed by a micropercolation technique using fluorescent dyes to mark interfaces on silica gel (Criddle and LeTourneau, 1951). The concentrations of olefins above C_5 were also

estimated from bromine numbers determined by an electrometric titration procedure (DuBois and Skoog, 1948).

Cain et al. (1953) performed analysis on the oil stream of the Fischer-Tropsch synthesis product to separate the oxygenated compounds into functional groups and Steitz and Barnes (1953) investigated the composition of the water stream.

Concerning the oil stream, the acids were determined by titration with standard sodium hydroxide to the phenolphthalein end point. Alcohols were determined by the phthalic anhydride method (Elving and Warshowsky, 1947) which is particularly suitable for oil stream analysis. Total Carbonyl content was determined by reaction between hydroxylamine hydrochloride and the carbonyl group in aldehydes and ketones. Esters were determined by a conventional saponification procedure (Siggia, 1949). The distributions of the components in the component classes were estimated by fractionated distillation.

Concerning the composition of the water stream, non-acid chemicals were separated from the water stream by fractionated distillation and the acids were separated from the aqueous residue by solvent extraction. After removal of the solvents, the acids were recovered in high purity by fractionation. Quantitative analysis of the non-acid chemicals was obtained by a combination of fractionated distillation and analysis for functional groups (Steitz and Barnes, 1953)

As reported by Weitkamp and co-workers (1953), detailed product analysis was possible but due to the complexity of the products and the analytical techniques available, quantitative information could only be obtained for the C_1 to C_{16} product fraction. Furthermore product analysis was a time consuming and labour intensive process.

2.3.2. One-dimensional Gas Chromatography

Chromatography is not a new analytical technique and was already developed in 1903 by the Russian botanist Mikhail Semyonovich Tsvet. Since then researchers have found that the principles underlying Tsvet's chromatography could be applied in many different ways, giving rise to different varieties of chromatography. One such variety is gas chromatography, developed by Martin in 1950 (Bruno, 2005). With this technique product analysis reached a whole new level, allowing the separation and analysis of complex mixtures of volatile organic and inorganic compounds.

Gas chromatography is a chemical analysis technique suitable for separating components in complex samples. This is achieved by introducing a known volume of gaseous or liquid sample via injection unto the column head. The sample molecules are then swept through the column by the carrier gas (mobile phase). The sample molecules' motion is inhibited by the adsorption of the sample molecules either onto the column walls or onto packing materials in the column. The rate at which the molecules progress along the column depends on the strength of adsorption which in turn depends on the type of molecule and on the stationary phase materials. Since each type of molecule has a different rate of progression, the various components of the sample mixture are separated as they progress along the column and reach the end of the column at different times (retention time). A detector is used to monitor the outlet stream from the column; thus, the time at which each component reaches the outlet and the amount of that component can be determined. Generally, substances are identified by the order in which they elute from the column and by the retention time of the sample in the column (Britannica Concise Encyclopedia, 2008).

As mentioned earlier it was a lengthy process for researchers working in the Fischer-Tropsch field to analyse the complex product mixtures, therefore it is no surprise that when gas chromatography was introduced to the

research world, Fischer-Tropsch researchers were quick to adopted this analytical technique.

From the 1950s researchers mainly focused on the use of gas chromatography as an analytical technique for FT product analysis. Some workers separated CO, CO_2 and hydrocarbons up to C_5 on a packed column and calculated the amount of C_{5+} products from the analysis (Elliott and Lunsford, 1979; Rosynek and Winder, 1979). Others used two or more chromatographs equipped with different columns and detectors in order to analyze the products (Everson and Woodburn, 1978). Schulz et al. (1978) used a method where gas samples were collected in evacuated glass ampoules and then analyzed on a GC system equipped with a capillary column. With this method they were able to resolve C_1-C_{10} products with a turnaround time of 100 min. In most investigations on-line injection techniques for the gaseous products followed by off-line separation of the condensates were combined to form a product spectrum (Bauer and Dyer, 1982; Feimer et al., 1981).

Although the GC methods described above delivered promising results, there were still some shortcomings. In many cases the analysis of the products was incomplete or very expensive equipment was required, or no accurate carbon balance could be made.

Aware of these shortcomings, Nijs and Jacobs (1981) developed a dual-column on-line GC system that enabled them to determine accurately and quantitatively CO, CO_2 and C_1 through C_{12} hydrocarbons in a single run of little more than 2 hours. Dictor and Bell (1984) also embarked on the same quest and developed an on-line GC system using dual-columns, temperature programming and both flame ionization and thermal conductivity detectors. With this system they were able to identify products containing up to 32 carbon atoms in a total turnaround time of 2.5 hours.

Today Fischer-Tropsch synthesis products are still mainly analyzed using gas chromatographic methods (both on-line and off-line applications), but

the set-up of the GC systems have changed. With advances in columns, inlet systems and detectors, researchers are now able to customize their GC systems by combining hardware that will give them the required separation determined by their research focus. By only using a different column combination or detector, researchers are able to detect components (such as linear and cyclic oxygenates, aromatics and other hydrocarbon isomers) in complex samples which they did not believe to be present in the sample before.

2.3.3. New Techniques

Some new analytical techniques are emerging that can be applied in Fischer-Tropsch research to analyze synthesis products. Laser-Induced Acoustic Desorption (LIAD), gas chromatography coupled to an atomic emission detector (GC-AED) and two-dimensional gas chromatography (GCxGC) are some examples.

2.3.3.1. Laser-Induced Acoustic Desorption (LIAD)

At Purdue University, West Lafayette, Indiana a method, Laser-Induced Acoustic Desorption coupled with a 3-T Fourier transform ion cyclotron resonance mass spectrometer (LIAD/FT-ICR), was developed to simultaneously analyze non-polar hydrocarbons and polar oxygenated hydrocarbon components in petroleum distillates (Crawford et al., 2005).

Crawford and his colleagues (2005) validated the method by examining model compounds representative of the various classes of polar and non-polar hydrocarbons commonly found in petroleum. LIAD successfully desorbs all the compounds as intact neutral molecules into the FT-ICR. Using this method hundreds of compounds can detected within petroleum distillate samples.

2.3.3.2. Gas Chromatography with Atomic Emission Detector (GC-AED)

Rainis and O'rear (2004) invented a method to measure oxygenate concentration using gas chromatography coupled to an atomic emission detector (GC-AED). The value of this method is that the oxygenate measurements obtained can be used to adjust and control various processes used to produce, upgrade, or finish Fischer-Tropsch products and to provide Fischer-Tropsch products with a selected oxygenate concentration.

2.3.3.3. Two-dimensional Gas Chromatography (GCxGC)

In recent years trace-level analysis of complex mixtures such as petrochemical samples, cigarette smoke, food containing a variety of flavours and organic micro-pollutants has rapidly gained increasing importance (Dallüge et. al., 2003). Conventional one-dimensional gas chromatography (1D GC) using modern capillary columns offer high peak capacities but it fails to separate all individual components present in such complex mixtures as mentioned above. The complex sample can be characterised by applying various sample preparation techniques but long analysis times and complex instrumentation make these options vary unattractive.

In 1991 Phillips and Liu introduced comprehensive two-dimensional gas chromatography (GCxGC) to the analytical world that presented a solution to restrictions posed by 1D GC (Vendeuvre et. al., 2005) and is suitable for the separation and identification of analytes in complex samples. Since then a lot of work has been published with regards to the theoretical aspects, the instrumentation and the application of this promising technique. Adahchour et al. (2008) and Dallüge et al. (2003) have published reviews regarding the principle of GCxGC and the components it consist of.

Principle of GCxGC

The resolving power of GCxGC is attributed to the fact that a sample introduced to the system is subjected to two gas chromatographic separations that are based on fundamentally different separation mechanisms to create orthogonal separation conditions (Venkatramani et. al., 1993).

The resolving power of GCxGC is achieved by first injecting the sample on a high resolution capillary GC column containing a non-polar stationary phase, and using temperature programming with a heating rate of no more than 1-5 ºC/min. A modulator, which acts as an interfacing device, is used to separate the first-column elute into a very large number of adjacent small fractions. Each individual fraction is refocused and subsequently injected into the second GC column, which is much shorter and narrower than the first column. The second-column separation generally is of a polar or shape-selective nature required to achieve orthogonal separation conditions. The separation in the second-column is extremely fast and takes only 1-10 s in comparison to the 45-120 min separation on the first-column. Consequently the second-column separation takes place at iso-thermal conditions, but in some systems the second oven is contained in a separate oven to allow more flexible and independent temperature programming.

Due to the fast separation in the second dimension, narrow peaks with widths of 100-600 ms at the base line are formed. These narrow peaks require fast detectors with a small volume and short rise time in order to reconstruct the second-dimension chromatograms properly.

The outcome of a GCxGC run is a large series of high-speed second-dimension chromatograms, which are usually grouped side by side to form a two-dimensional chromatogram with one dimension representing the retention time of the first column and the other, the retention time on the second column. This transformation into a two-dimensional matrix array is often performed by laboratory-written software. Visualisation is usually done

by displaying the peaks in the 2D plane by means of colours, shading or contour lines to indicate the signal intensity.

Orthogonality and GC column selection

In gas chromatography every separation is based on two parameters: (i) the volatility of the analytes and (ii) their interaction with the stationary phase (polarity). With GCxGC a combination of two columns are used for separation which allows the separation of compounds to take place independently on the basis of volatility and polarity. This is known as orthogonal separation (Dallüge et al., 2003) and allows compounds with similar boiling points to be separated on the basis of their functionality. To create orthogonal separation conditions in a GCxGC system, the first column has to be non-polar and the second column should be of polar nature.

In literature several GCxGC column combinations have been reported (Adahchour et. al., 2008; Dallüge et. al., 2003). Some stationary phases typically used in first-dimension columns are 100% dimethylpolysiloxane or 5% phenylene-95% dimethylpolysiloxane and for the second dimension stationary phases such as 35-50% phenylene-65-50% dimethylpolysiloxane, polyethyleneglycol (Carbowax) and carborane (HT-8) can be used. In general a GCxGC column combination should be selected that meets the requirements of orthogonality and will give optimum results with regard to the desired between-group or within-group separations.

Another issue to take in to consideration when selecting columns for GCxGC systems is the column dimensions. In general a 15-30 m x 0.25 mm I.D. conventional-size column will be selected for the first dimension separation but this may differ depending on the desired separation. The separation in the second column has to be completed in a few seconds and band broadening of the narrow pulses generated by the modulator should

be minimised, therefore short, narrow-bore columns are commonly used in the second dimension, typically 0.5-2 m x 0.1 mm I.D.

Virtually all injection techniques can be applied to the GCxGC system if a conventional first column is being used and the gas flow is similar to those applied routinely in 1D GC.

Modulation

The modulator can be considered the “heart” of a GCxGC system and must serve three functions: (i) to continuously trap small adjacent fractions of the effluent from the first column whilst the first-dimension separation proceeds; (ii) to refocus the trapped fractions either in time or space; (iii) to inject the refocused fractions as narrow pulses into the second-dimension column. In practice the modulator works in constant frequencies of typical 0.1-1.0 Hz.

Over the years various types of modulators have been developed and reported in literature (Dallüge et. al., 2003). To follow is a few examples of these modulators.

The first commercially viable modulator was the so-called “Sweeper”. A thick-film capillary was used to retain and accumulate the analytes at the end of the first column and re-injected onto the second column by heating the capillary with a moving slotted heater.

Kinghorn and Marriott (1998) developed a moving modulator, the longitudinally modulating cryogenic system (LMCS), which uses expanding liquid carbon dioxide for cryogenic trapping and focusing of the analytes in the first centimetres of the second column. Re-injection is achieved by moving the modulator away and heating the focused fraction by means of oven air.

More recently, several versions of cryogenic jet systems were introduced that is similar to LMCS, but there are no moving parts, making the jets more robust, and re-injection is achieved by either switching the modulator off or by using a pulse of hot air to refocus the fraction (Dallüge et. al., 2003).

Detectors in GCxGC

As mentioned above the GCxGC system comprise of a long first column and a very short (0.5m to 2m) second column. Every few seconds the modulator collects eluent from the first column and then focuses narrow fragments or slices of the compound peaks (widths of peaks are 100 – 600 ms) on to the second column. The narrow peaks require fast detectors with a small internal volume, short detector rise time and a high data acquisition rate to ensure a proper reconstruction of the second dimension chromatograph. The sampling rate of the signal should be at least 100 Hz (Dallüge et. al., 2003).

Initially detection in GCxGC had to be performed with a FID device which has negligible internal volumes and can acquire frequencies of 50-300 Hz (Adahchour et. al., 2008). This was a suitable detection method as most early applications in the field were focused on petrochemical analysis, but as the technology advanced and GCxGC was applied to other chemical research areas the need developed for other detection methods.

Some of the other detection methods used for GCxGC are: micro electron-capture detection (μECD), sulphur chemiluminescence detection (SCD), atomic emission detection (AED) and nitrogen chemiluminescence detection (NCD).

Data processing

It has been emphasized in many research papers that GCxGC can be used to analyse complex mixtures, consequently the chromatograms, data files and peaks lists are also extremely complex. Multivariate analysis techniques

have offered promising strategies to retrieve the essential information from these data (Adahchour et al., 2008).

Initially, peak quantification was performed by integrating all individual second-dimension peaks by means of conventional integration algorithms and then summing all the peak areas belonging to one two-dimensional peak (Adahchour et al., 2008). Today the raw data obtained from the large series of second-dimension chromatograms can be processed into usable information with the help of automated computer assisted information technologies. One of the information technologies used is GC Image, a software system developed at the University of Nebraska-Lincoln for GCxGC visualization, processing, analysis and reporting (Reichenbach et al., 2004).

GC Image is based on graphical methods and is used to create a GCxGC image from a time ordered stream of samples. In the GC Image Users' Guide the process of creating and processing a GCxGC image as well as the detection and quantification of compounds are discussed (GC Image, 2007).

According to this manual the first step in creating a GCxGC image is to apply image processing filters to correct for acquisition artefacts. One of the filters applied is the *Shift Phase* filter which shifts the phase of the image with respect to the start time of the second dimension. The second filter applied is the *Correct Baseline* filter which subtracts the baseline level from the signal. This is important because the baseline level consists primarily of the steady-state standing-current baseline in standard GC detectors and temperature-induced column-bleed which causes a rise in the signal in the later portions of the temperature-programmed runs. Accurate quantification of the chemical-related peaks requires subtractions of the baseline level from the signal.

After correcting the baseline, the separate groups of pixels associated with the separated chemicals can be detected and accurately quantified. In

image processing, each group of pixels is called a *blob* and the operation of segmenting pixels into blobs is called *blob detection*. GC Image uses a blob detection algorithm that successively attaches the largest-valued unassigned pixel to a neighbouring blob or forms its own blob if no neighbouring peaks has been established (GC Image, 2007).

With GCxGC a large number of chemicals are separated and detected. Manually analysing the data from a GCxGC analysis can be time consuming therefore GC Image provides automated tools that enable efficient processing of large GCxGC data sets (GC Image, 2007). GC Image has tools that automate much or all of the analysis process. The approach is based on pattern matching. A template is created, by making use a chemical identification process as with the case when identifying compounds with 1D GC, which described the pattern of chemicals peaks in one image (Reichenbach, 2004). This template is then matched automatically to blobs of subsequent images and accurately identifies compounds based on previously observed patterns. Standards are used to quantify the chemical compounds identified using template matching (Reichenbach, 2004).

Advantages of GCxGC

There are a few main advantages of using GCxGC over conventional 1D GC (Dallüge et. al., 2003). One of the most prominent is that it yields distinctly improved separation of analytes in a sample due to its higher peak capacity. Secondly, detectability is improved due to the refocusing process in the modulator and also improved separation of the analyte. Thirdly, if proper orthogonal conditions are used, chemically related compounds are displayed as ordered structures, which facilitate group-type analysis and the provisional classification of unknowns. With these capabilities, GCxGC appear to be a promising technique to analyse the complex products produced during the synthesis process.

CHAPTER 3

EXPERIMENTAL

To determine if two-dimensional gas chromatography (GCxGC) promises to provide better more accurate separation for Fischer-Tropsch products, GCxGC equipment, supplied by Zoex Corporation, was fixed to a micro slurry phase reactor system to provide for both on-line gas analysis as well as off-line product analysis.

A series of Fischer-Tropsch synthesis experiments were conducted at various temperatures and feed gas H_2/CO ratios (within the range of Low Temperature Fischer-Tropsch (LTFT) conditions). The gaseous, liquid and wax products collected from Fischer-Tropsch synthesis were analyzed using GCxGC and one-dimensional gas chromatography (1D GC) methods. The data collected were then processed and compared.

In the following sections an overview will be given of the reactor system used, the catalyst employed for Fischer-Tropsch product synthesis, the analytical techniques (1D GC and GCxGC) employed and the methodology followed to execute data work-up and evaluation.

3.1. REACTOR SYSTEM SET-UP

The Fischer-Tropsch synthesis reaction was conducted in a Continues Stirred Tank Reactor (CSTR). The reactor is connected to a gas supply system; on-line gas sampling system, hot trap and cold trap (see Figures 3.1 – 3.3). The set-up of the reactor and sampling systems (on-line and off-line) could have a significant impact on the integrity and the resulting interpretation of experimental results and therefore will be discussed in detail.

3.1.1. Feed gas supply and sampling

The feed supply and sampling system are illustrated in Figure 3.1.The feed gas supplied to the reactor system comprises of hydrogen (H_2: 99.999%) and carbon monoxide (CO: 99.97%). Argon (Ar: 99.999%) is also co-fed to the reactor system at approximately 10 mole % of the total feed stream and serves as an internal standard for the accurate quantification of the components in the gas analysis.

The feed gas cylinders are each equipped with an in-line pressure regulator set at a supply pressure of 40 barg. A spring loaded relief valve is provided for over pressure protection. The gas feed ranges of the system are only limited by the flow limitations of the flow controllers employed.

To protect the flow controllers from dust, each gas supply line is equipped with an in-line filter element. The H_2, CO and Ar are fed separately to the reactor (CSTR) using a Brooks mass flow controller. The flow controllers are mass flow based and make use of heat capacity measurement to measure flow.

To prevent cross contamination of gasses, the feed gas lines are each equipped with spring loaded non-return valves. The gas lines are connected and the combined feed gas stream passes through a spring loaded non-return valve that prevents wax return into the feed line. A pressure transmitter is connected to the total feed line to measure reactor pressure conditions. An on-line Gas chromatography (GC) system is also connected to the total feed gas line which allows feed gas component analysis.

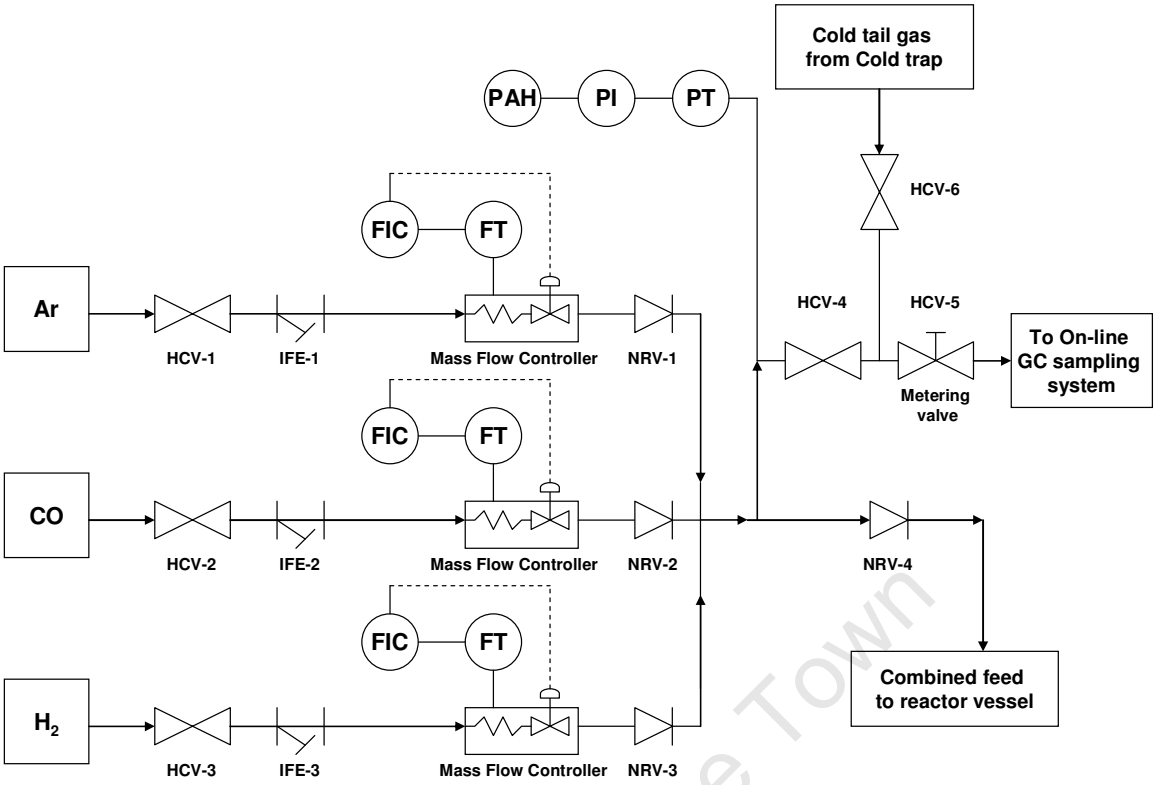

Figure 3.1: Feed gas supply and sampling system

3.1.2. Reactor

The reactor used for synthesis is a Continues Stirred Tank Reactor (CSTR) with a liquid volume of 670ml (78 mm ID). Figure 3.2 illustrates the reactor set-up used for this study and Figure 3.3 illustrates the various internal elements which a reactor consist of.

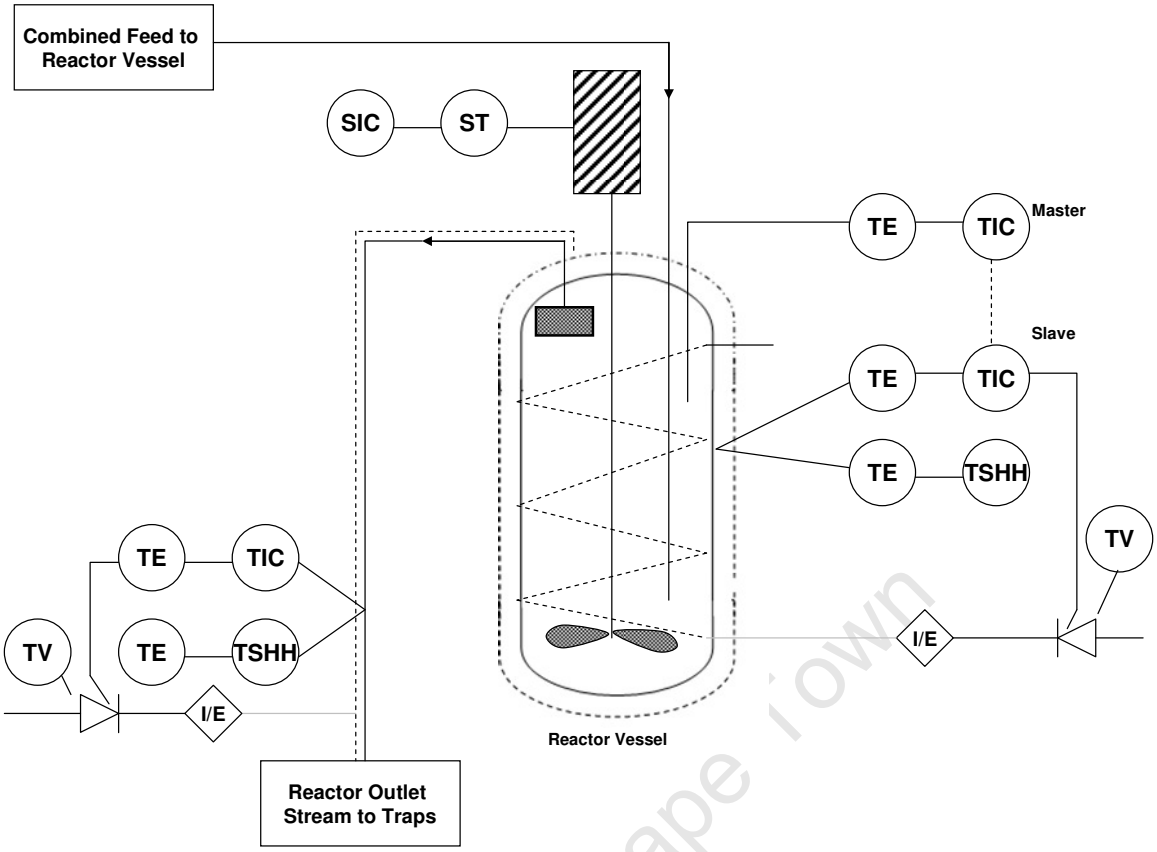

Figure 3.2: The experimental reactor system set-up

The reactor vessel is equipped with a removable electrical heating jacket and a temperature control system. The system consist of a master and slave temperature controller combination that will facilitate accurate temperature control during process changes and associated changes due to heat generated from Fischer-Tropsch synthesis reaction. This is achieved by submerging the master thermocouple halfway into the reactor vessel, ensuring direct contact with the reaction medium, and by placing the slave thermocouple between the heating jacket and the reactor vessel wall.

A mixing devise is connected through a magnetically coupled and sealed connection on the vessel flange, to an external variable speed drive motor. This mixing devise is also known as a stirrer and ensures effective mixing of the liquid and gas in the reactor vessel. The type of stirrer used is a double-blade stirrer. The first blade element (impeller) of the double-blade stirrer is located approximately in the middle of the reactor which induces a downward forcing action sufficient for adequate mixing. The second flat blade element is

located approximately 3 mm from the bottom of the reactor vessel providing additional mixing at the bottom of the reactor vessel and prevents catalyst from settling.

The gas inlet enters the reactor at the top of the reactor vessel through the flange and reaches all the way down to approximately 5 mm above the bottom stirrer element. This maximises gas dispersion and prevent gas from bypassing along the vessel walls.

The liquid and gas products exit the reactor through a 10 µm metal sintered filter at the top of the reaction vessel to ensure that the catalyst remain in the reactor. From the filter an outlet line connects to hot and cod traps where liquid products are recovered.

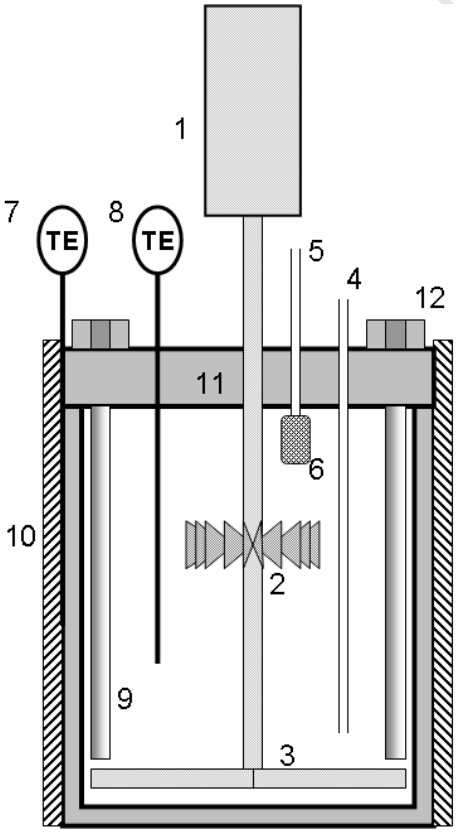

Figure 3.3: An illustration of the internals of a Continues Stirred Tank Reactor (CSTR). Note: 1. Mixer drive unit; 2. Impeller stirrer element; 3. Flat blade stirrer element; 4. Feed gas inlet; 5. Product outlet; 6. Filter element; 7. Slave thermocouple; 8. Master thermocouple; 9. Baffle; 10. Heating jacket; 11. Flange; 12. Flange Bolt

3.1.3. Liquid product recovery and sampling

Figure 3.4 is an illustration of the liquid product recovery system. From the reactor outlet a vapour stream passes through a temperature controlled (at 200˚C) product line to a hot trap vessel. The hot trap vessel is also temperature controlled at 200˚C and captures high molecular mass hydrocarbons (wax).

From the hot trap the exit line feed to a cold trap vessel. The cold trap is operated at room temperature and captures the lighter hydrocarbon products (oil) and reaction water. The hot and cold traps are drained manually on a daily basis and the products are analysed directly after sampling using off-line gas chromatographs (GC).

Part of the feed stream to the cold trap (hot gas at 200˚C) can also be diverted to an on-line GCxGC system to perform a component analysis of the hot product stream. In paragraph 3.4.2 the hot tail gas sampling system and analysis will be discussed in more detail.

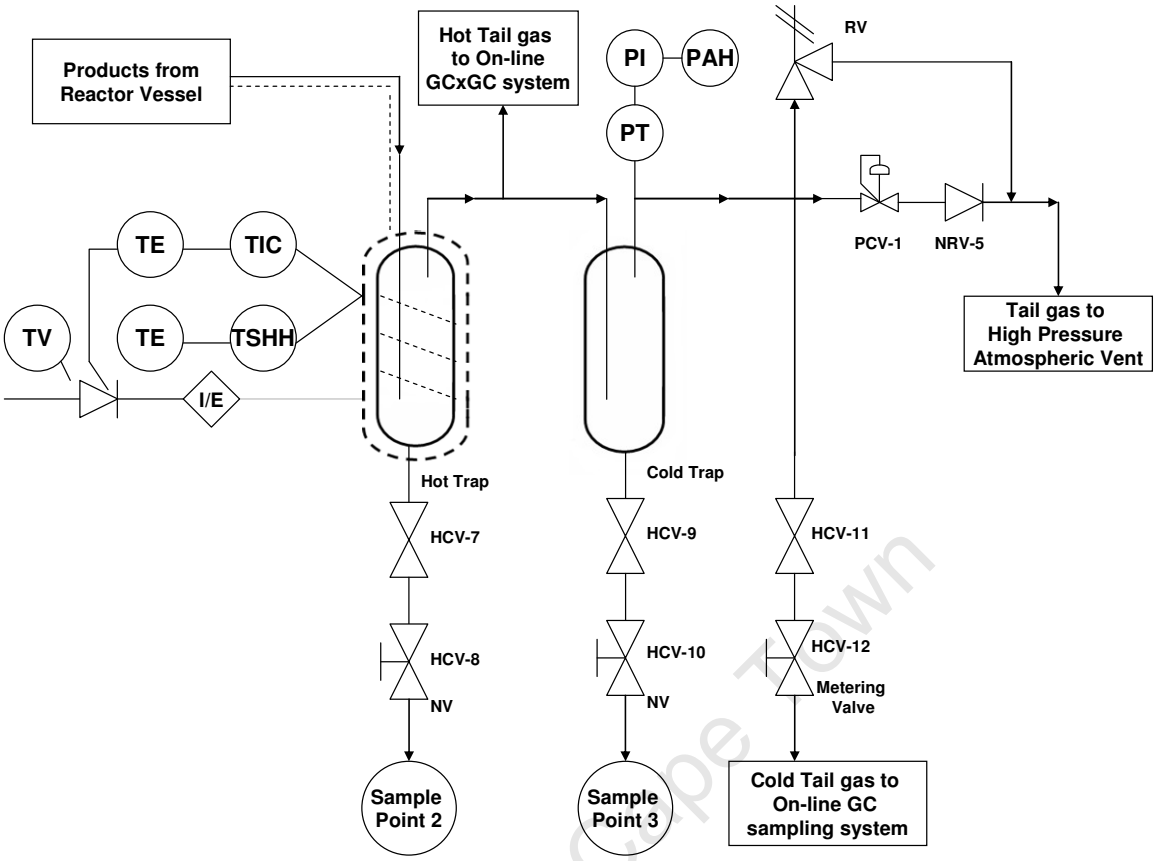

Figure 3.4: An illustration of the liquid product recovery system

3.1.4. Gas product sampling

The line that exits the cold trap is equipped with a pressure transmitter, to measure reactor exit pressure conditions, and a pressure alarm system. To protect the reactor system from over pressure, a relief valve is connected to the system. The outlet line from the cold trap is connected to an on-line GC system for gas analysis. The product gas exits the system through a pressure control valve to a vent line. The pressure control valve makes use of a back pressure regulating configuration, to maintain the reactor system at a specific set point. The typical accuracy of the pressure regulation is within 0.05 barg. Figures 3.4 and 3.5 are illustrations of the gas sampling system.

3.2. CATALYST

For the purpose of this study a model Ruhrchemie iron based catalyst was used. This type of catalyst is suitable for low temperature Fischer-Tropsch operations and is usually employed when a high molecular mass wax product is desired. The catalyst is similar to the catalyst originally developed by Ruhrchemie and is suitable for both fixed bed and slurry bed reactor operations. The catalyst preparation method is similar to the preparation used by Ruhrchemie can be described as follows (Frohning et al., 1977; Dry, 1981; Dry, 2004):

Firstly metallic iron, of suitable chemical composition, together with metallic copper is dissolved in nitric acid. The iron and copper nitrate solution (40 g/l Fe and 2 g/l Cu) is then rapidly poured into a hot solution of Na_2CO_3 whilst stirring vigorously until a pH just above 7 is reached. After this the hydrated ferric oxide is thoroughly washed with hot distilled water to remove excess sodium from the precipitate. A potassium silicate solution (known as potassium waterglass) is then added to the precipitate to give the required silica content to the catalyst (ratio of 25 g SiO_2 per 100 g Fe). Silica is then precipitated by adding a nitric solution. The precipitate is then filtered to remove excess potassium, re-slurried with water and spray-dried to obtain spherical catalyst particles.

The environment within a slurry reactor can be quite turbulent which may induce catalyst break-up. To increase the mechanical strength of the spray-dried catalyst in order to minimise the probability of catalyst break-up, the spray-dried catalyst is calcined at about 400 to 500°C.

3.3. REACTOR OPERATION

3.3.1. Start-up

During reactor start-up the reactor vessel is loaded with H1 hydrogenated hard wax (350 g) and heated to 150ºC to melt the wax and form a slurry medium. 10 g of precipitated iron catalyst is added to the slurry, the reactor is sealed, the temperature is increased and the vessel is pressurized using argon. The stirrer is set to 450 rpm. Activation gas is introduced to the system and once all the set activation conditions are at the required set points the Fischer-Tropsch synthesis run begins.

3.3.2 Catalyst activation

Before Fischer-Tropsch synthesis commence the catalyst is activated or reduced *in situ* using synthesis gas (H_2 + CO, H_2/CO = 1.5) at 255ºC and 14.5 bar (abs) for 16hrs using a gas hourly space velocity (GHSV) of 10 000 ml/g_{cat}/hr. Thereafter the knock-out pots are drained and the reactor temperature, pressures and synthesis gas flow rate are changed to synthesis conditions requirements.

3.3.3 Fischer-Tropsch synthesis

After catalyst activation the temperature was reduced to 245ºC and the pressure increased to 27 bar (abs). For this study these conditions will be referred to as the standard synthesis conditions. The reactor system, for each of the experiments performed (see Table 3.1 for experimental schedule), was kept at the standard synthesis conditions for 72hrs to allow the system to reach steady state. After this period the reactor conditions were varied as indicated by the experiment schedule by changing the GHSV. Argon (10% of total feed gas) was added to the synthesis gas to serve as an internal standard. The Fischer-Tropsch synthesis was performed for approximately 10 days at the new conditions.

Table 3.1: Schedule of experiments

Experiment	Syngas H_2/CO ratio	Temperature (ºC)	Pressure (bar absolute)
1	1.5	245	27
2	1.5	225	27
3	1.5	265	27
4	1.3	245	27
5	1.6	245	27
6	2.1	245	27

3.4. FISCHER-TROPSCH PRODUCT SAMPLING AND ANALYSIS

The Fischer-Tropsch synthesis products were sampled on a 24hr period and analyzed using gas chromatographic methods as indicated in Table 3.2.

After analysis the samples were kept in a cold store to prevent the product from evaporating and making it therefore available for re-analysis, if necessary.

Table 3.2: A summary of gas chromatography methods

Fischer-Tropsch Product	Gas chromatography (GC) method
Total Feed gas stream	On-line GC-TCD On-line GC-FID
Cold tail gas stream after wax and liquid product were condensed out (at 25 ˚C)	On-line GC-TCD On-line GC-FID
Hot tail gas stream after hot trap (at 200 ˚C)	On-line GCxGC-FID
High molecular weight hydrocarbons (wax) from hot trap	Off-line High Temperature GC-FID
Liquid hydrocarbon (oil) product from the cold trap	Off-line GC-FID
Reaction water product from the cold trap	Off-line GC-FID

To ensure representative sampling the cold tail gas and hot tail gas streams were always sampled first. Thereafter sampling and analysis of the total feed stream followed.

After gas sampling the wax and liquid products were drained from the hot and cold traps. In order to ensure that the system stays stable, the products were drained slowly from the trap vessels while monitoring the reactor pressure, ensuring that the reactor pressure did not drop more than 0.1 barg from the set point pressure. The hot trap was also drained before the cold trap to prevent wax carryover to cooler parts of the system which can result in line blockages.

The product captured in the cold trap vessel consists of oil and reaction water which needs to be separated in to two phase fractions using a separating funnel. The fractions were then analyzed off-line as indicated in Table 3.2.

To construct a mass balance and full hydrocarbon product distribution all gas flows and masses of the liquid products drained were logged as well as the reactor conditions relevant to the operation and synthesis process.

Component analyses were conducted on all the gas, liquid and wax products sampled from the Fischer-Tropsch reactor system. Because the component matrices were different for the products various on-line and off-line gas chromatography (GC) techniques were performed on these samples. The methods used will be discussed in more detail.

3.4.1. Sampling and analysis of Fischer-Tropsch synthesis feed gas and cold tail gas

The Fischer-Tropsch synthesis feed gas consists of hydrogen, carbon monoxide and argon. The tail gas consists of inorganic components such as H_2, Ar, N_2, CO, CO_2 and hydrocarbons ranging from C_1 to C_{10}. To detect and quantify these components two gas chromatography (GC) methods are used. The one method utilises a GC system fitted with a thermal conductivity detector (TCD) to detect the inorganic components and methane and the other method use a GC system fitted to a flame ionization detector (FID) to detect and quantify the hydrocarbons. Both these GC systems are connected to the reactor system making on-line sampling and analyses of the feed- and tail gas possible (see Figure 3.5).

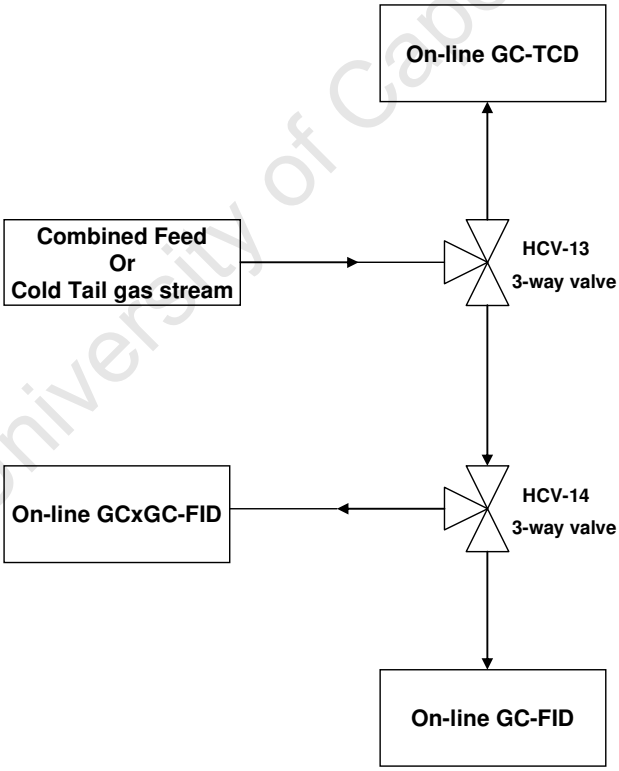

Figure 3.5: Illustration of on-line gas sampling system for combine feed gas or cold tail gas stream analysis using gas chromatography

3.4.1.1. On-line GC with TCD

An Agilent 6890N chromatograph (GC), equipped with two split/splitless injectors and two thermal conductivity detectors (TCD) were used to analyze for the inorganic compounds and methane in the gas stream. A valve-system and two packed columns were used per channel. See Table 3.3 for the columns and gas chromatographic conditions employed.

Table 3.3: Conditions for gas chromatographic analysis using TCD detection

Gas Chromatograph	**Agilent 6890N**
Detector	conductivity detector (TCD)
Front Channel	
Components detected	CO, CO_2, CH_4, Ar, N_2
Column	Restek Shin Carbon 80/100 µ, Packed 2m x 45.7mm
Carrier gas	Nitrogen
Flow rate	30 ml/min
Back Channel	
Components detected	H_2
Column	Restek PPQ Molecular Sieve 5Å, Packed 1m x 45.7mm
Carrier gas	Argon
Flow rate	30 ml/min
Oven temperature	110˚C (isothermal)
Analysis time	8 min

Helium was used as carrier gas for the one channel which was used to analyze the gas sample for CO, CO_2, CH_4, Ar, and N_2. On the other channel H_2 was analyzed and Ar was used as carrier gas. The oven was set at an isothermal temperature of 110 ˚C.

The gas samples were purged through the sample loop and injected on-line and splitless. An external standard calibration gas (containing 10.0 % CH_4, 45.0 % H_2, 2.5 % N_2, 10.0 % Ar, 22.5 % CO and 10.0 % CO_2) was used as reference to quantify the components detected. It is important, when using

external calibration, to calibrate the GC with a known gas composition and to use a sample loop with constant volume and pressure. Figure 3.6 presents a combined chromatograph (displaying detection of both channels) of a typical external standard sample analysis using on-line GC TCD.

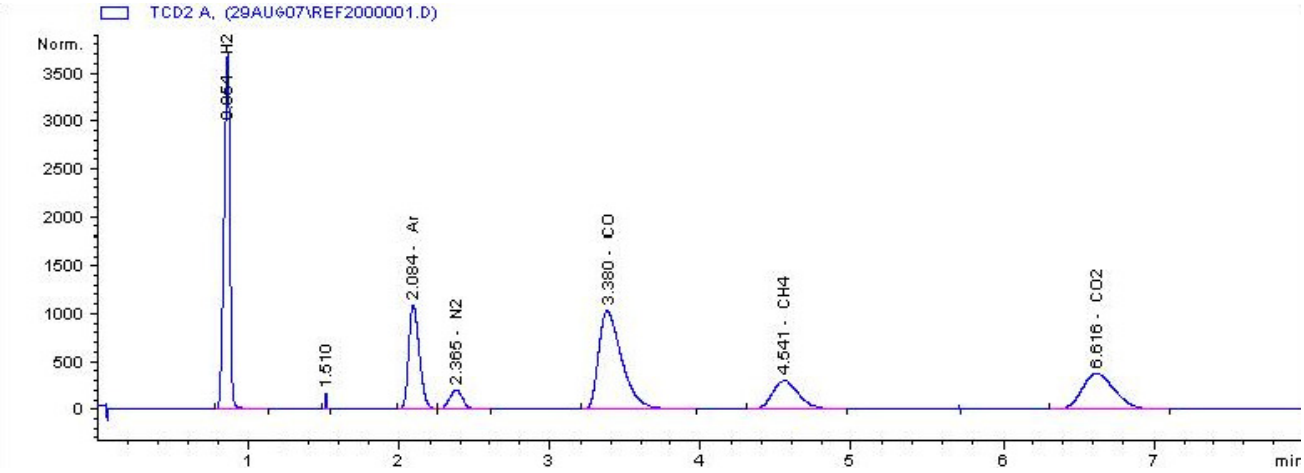

Figure 3.6: A chromatogram of a typical external standard sample analysis using on-line GC TCD.

3.4.1.2. On-line GC with FID

An Agilent 6890 GC with split/splitless injector, equipped with a flame ionization detector (FID) and a Varian WCOT silica column was used to detect the hydrocarbons (ranging from C_1 to C_{10}) present in the tail gas stream. The GC system and conditions used to achieve separation are presented in Table 3.4.

The gas samples were purged through the sample loop and injected on-line. An external standard calibration gas (containing 10.0 % CH_4, 45.0 % H_2, 2.5 % N_2, 10.0 % Ar, 22.5 % CO and 10.0 % CO_2) was used as reference to quantify the components detected with respect to methane. Part of a typical GC-FID chromatogram is shown in Figure 3.7. The components identified were quantified using methods described in paragraph 3.4.5.

Table 3.4: Conditions for gas chromatographic analysis using FID detection

Gas Chromatograph	**Agilent 6890N**
Detector	flame ionization detector (FID) Heater Temperature = 300˚C
Column	Varian CP Sil 5CB, Fused silica capillary 25m x 0.150mm x 2.0µm
Introduction gas Carrier gas Column head pressure	Hydrogen Hydrogen 2.1 bar (absolute)
Injector	split injector, T = 250˚C split ratio: 50:1
Oven Temperature program	35˚C for 2.4 min 10˚C/min to 310˚C for 5 min
Run time	34.90 min

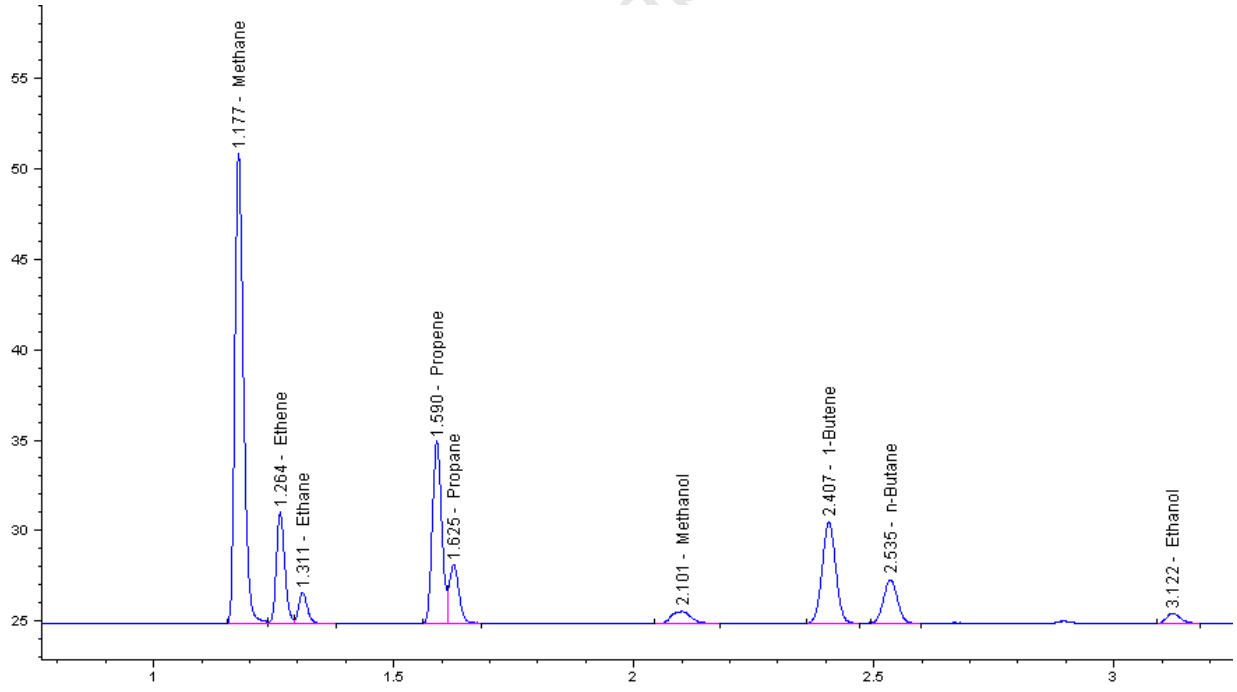

Figure 3.7: Chromatogram of cold tail gas (at 25ºC) stream analyzed on an on-line GC FID

3.4.2. Hot Tail gas sampling and analysis

Part of the gas stream feeding to the cold trap, also known as the hot tail gas stream, can be transferred directly from the reactor through a system of heated (200ºC) valves and filters to a two dimensional gas chromatography (GCxGC) system. The purpose of this is to conduct an analysis of the hot tail gas stream and gain true insight of the gaseous product composition straight out of the reactor. Figures 3.4 and 3.8 are illustrations of the sampling system.

To ensure that the sampling system stays clean and clear of heavy product the sampling system is also connected to a nitrogen source that allows for the sampling lines to be purged prior to sampling.

The hot tail gas is introduced to the GCxGC system via two heated sample loops. The samples have very similar compositions since they are sampled essentially at the same time and injected simultaneously into the GC system. The contents of each sample loop are injected through a guard column designed to protect the analytical system from heavy components (see Figure 3.9). The first sample loop's contents is injected into a thick phase non-polar column (CP Sil-5) used for the analysis of light hydrocarbons for the separation of methane through to butane since these compounds are not separated on the GCxGC column setup. See Figure 3.10 for a chromatograph of the hot tail gas injected via the first sample loop. The sample in the second loop is injected onto the first column of the GCxGC column setup.

The GCxGC system consist of two columns, a 1.5 m non-polar column (CP-Sil-5) and 50 m polar column (HP-INNOWAX) that give rise to the two dimensional separation. When the sample is introduced into the system it firstly under goes first dimension separation on the non-polar column. The interface between the two columns, called the modulator, isolates the first column eluate into a very large number of adjacent small fractions. The fractions is refocused into narrow pulses of about 0.1s width, and launched into the second-dimension column. The second-dimension column (HP-INNOWAX) is of polar nature and separation on this column is extremely fast

(7s). The fast separation results in very narrow peaks with baseline widths of 0.1-0.6 s. The peaks are then detected by a flame ionization detector. The result is a two-dimensional contour plot which indicates the various compound classes present in the sample (see Figure 3.11).

The analysis conditions used for the GCxGC system are stipulated in Table 3.5.

The GCxGC system was calibrated with the same external calibration gas as mentioned in paragraph 3.4.1.2 which consisted of 10.0 % CH_4, 45.0 % H_2, 2.5 % N_2, 10.0 % Ar, 22.5 % CO and 10.0 % CO_2 and this calibration were performed for both sample loops. The effectiveness of the calibration was then tested using a C_1-C_6 hydrocarbon mixture. Further the components were identified and quantified using methods described in paragraph 3.4.5.

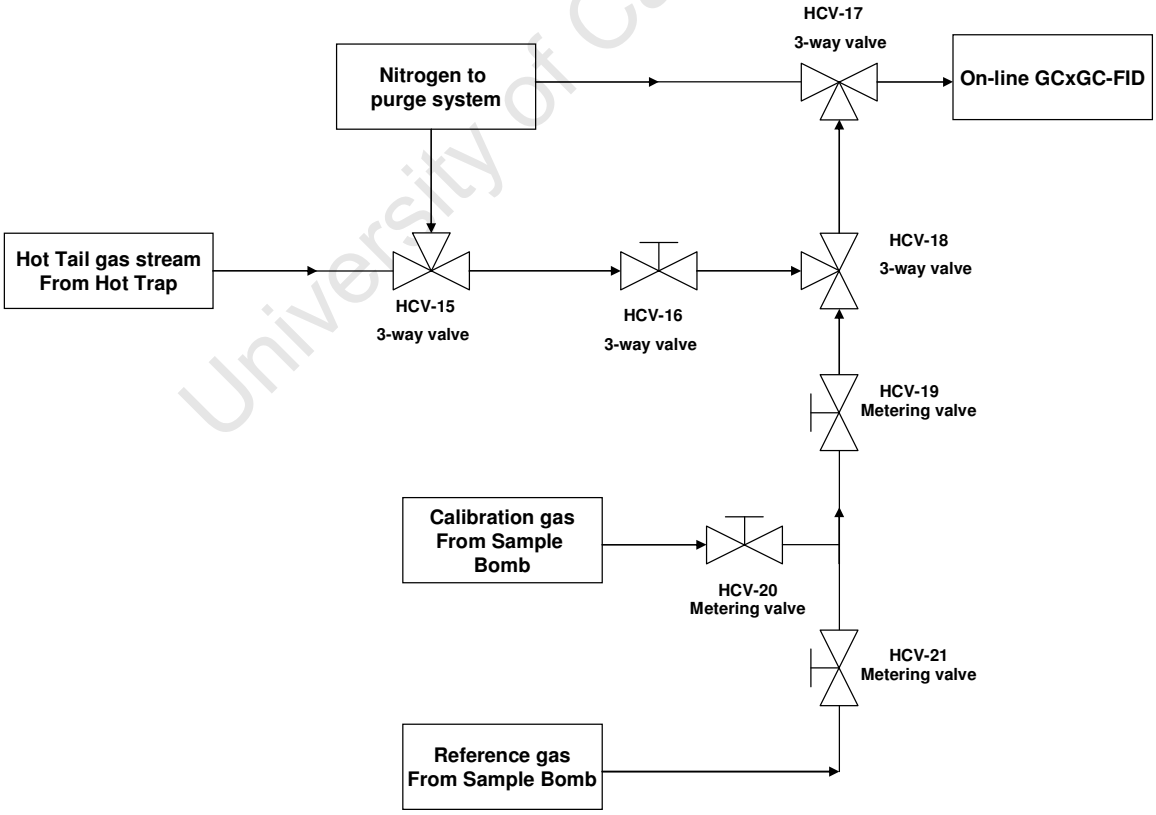

Figure 3.8: Schematic of on-line GCxGC sampling system for hot tail gas analysis.

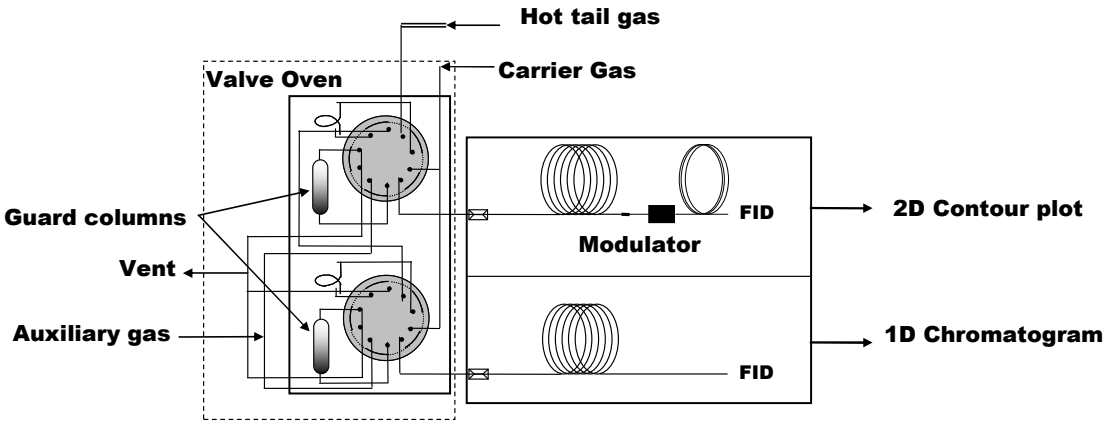

Figure 3.9: Schematic of on-line GCxGC system.

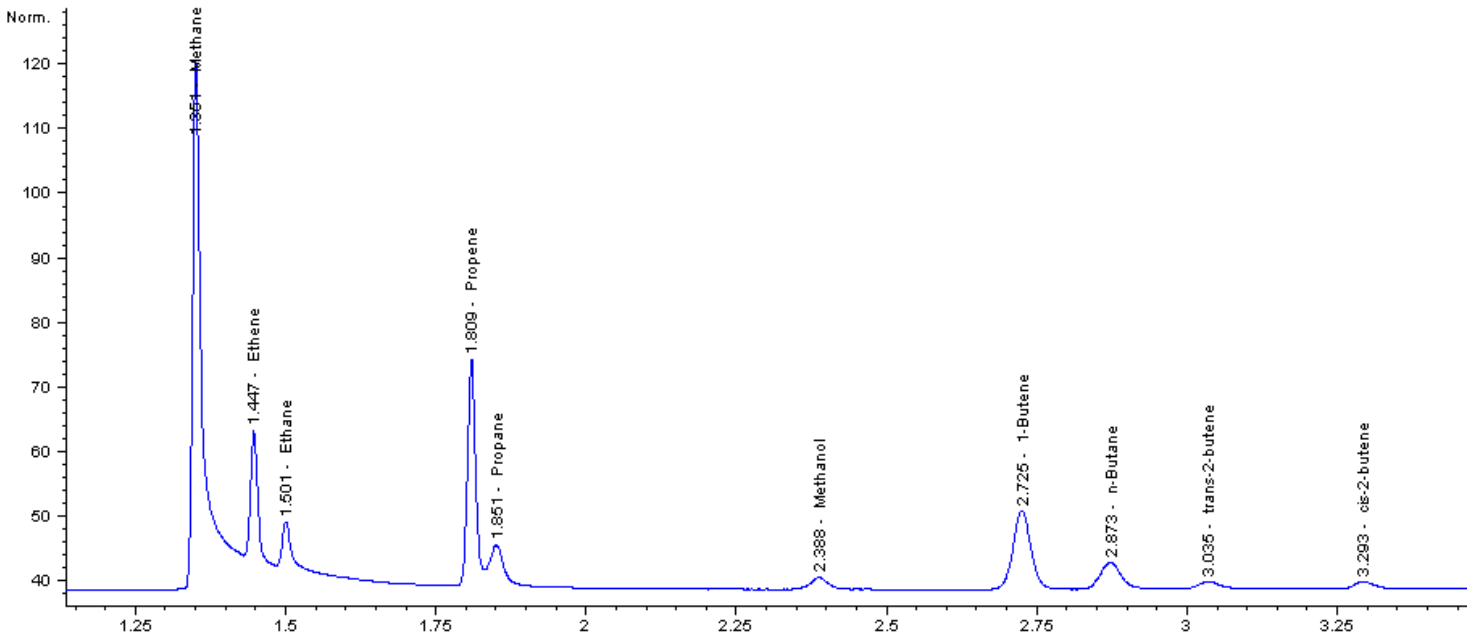

Figure 3.10: One-dimensional chromatograph of hot tail gas injected from first sample loop on GCxGC system.

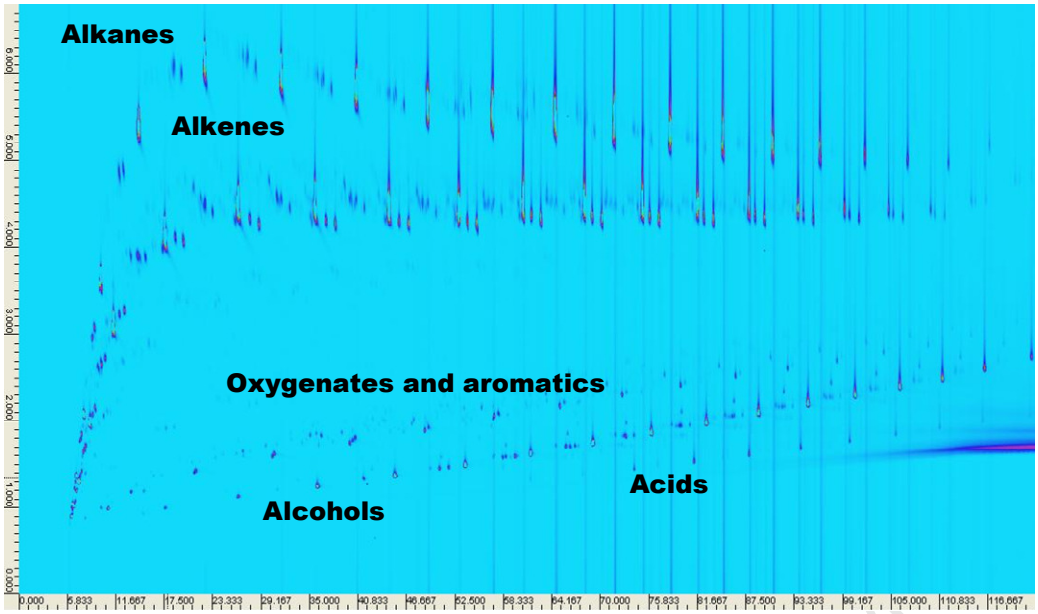

Figure 3.11: Two-dimensional chromatograph (contour plot) of hot tail gas injected from second sample loop on GCxGC system.

Table 3.5: Conditions for the two-dimensional gas chromatographic analysis using FID detection

Gas Chromatograph Agilent 6890N		
Oven	Temperature program	35 ˚C for 10 min 3 ˚C/min to 240 ˚C for 10 min
Hot jet	Temperature program	250 ˚C 1 ˚C/min to 330 ˚C
Secondary Oven	Temperature program	60˚C for 2 min 3 ˚C/min to 300 ˚C for 10min
Front Channel		
Front Inlet	Injection volume Injection Mode Introduction Gas Temperature (˚C) Pressure (kPa) Flow (ml/min) Split ratio	0.5 µl Split Hydrogen 280 142.4 43.4 50:1
Front Column	Description Pressure (kPa) Flow (ml/min)	Chrompak 7692 CP-Sil-5 25m x 150µm x 2µm 142.5 0.7
Front Detector	Heater temperature (˚C) H_2 flow (ml/min) Air flow (ml/min) Makeup gas Makeup gas flow (ml/min)	300 40 450 Nitrogen 30
Back Channel		
Back Inlet	Injection volume Injection Mode Introduction Gas Temperature (˚C) Pressure (kPa) Flow (ml/min) Split ratio	0.5 µl Split Hydrogen 250 210 21.2 5:1
Back Column	Description Pressure (kPa) Flow (ml/min)	First Column: Chrompak 7692 CP-Sil-5 1.5m x 150µm x 2µm Second Column: Agilent 19091N-205 HP-Innowax 50m x 200µm x 0.4µm 210 2.1
Back Detector	Heater temperature (˚C) H_2 flow (ml/min) Air flow (ml/min) Makeup gas Makeup gas flow (ml/min)	300 40 450 Nitrogen 25
Modulation time	7s	
Run time	88 min	

3.4.3. Analysis of liquid phase organic product

The liquid phase organic product sampled from the cold trap (at 25˚C) consists of a water fraction and an organic oil fraction. Once separated the fractions were analyzed independently using different off-line gas chromatography systems.

3.4.3.1. Analysis of water fraction

The water fraction was analyzed utilizing an Agilent 6890 GC-FID system with split/splitless injector equipped with a polar column. Table 3.6 presents more information regarding the GC system and conditions used to separate the oxygenated compounds (C_1 – C_7) in the water fraction. The compounds detected were quantified using an external standard comprising of 5.13% methanol, 5.02% ethanol, 2.59% propanol, 2.59% Acetic Acid and 2.56% propionic acid. Figure 3.12 displays a chromatogram of a water fraction analysis.

Table 3.6: Conditions for gas chromatographic analysis of the water fraction using FID detection

Gas Chromatograph	**Agilent 6890N**
Detector	flame ionization detector (FID) Heater Temperature = 50˚C
Column	HP INNOWAX Fused silica capillary 50m x 200µm x 0.40µm Stationary phase: polyethylene glycol
Introduction gas Carrier gas Column head pressure	Hydrogen Hydrogen 2.1 bar (absolute)
Injector Injection volume	auto sampler split injector, T = 250˚C split ratio: 50:1 1.0µl
Oven Temperature program	 30˚C for 10 min 4˚C/min to 240˚C for 10 min
Run Time	72 min

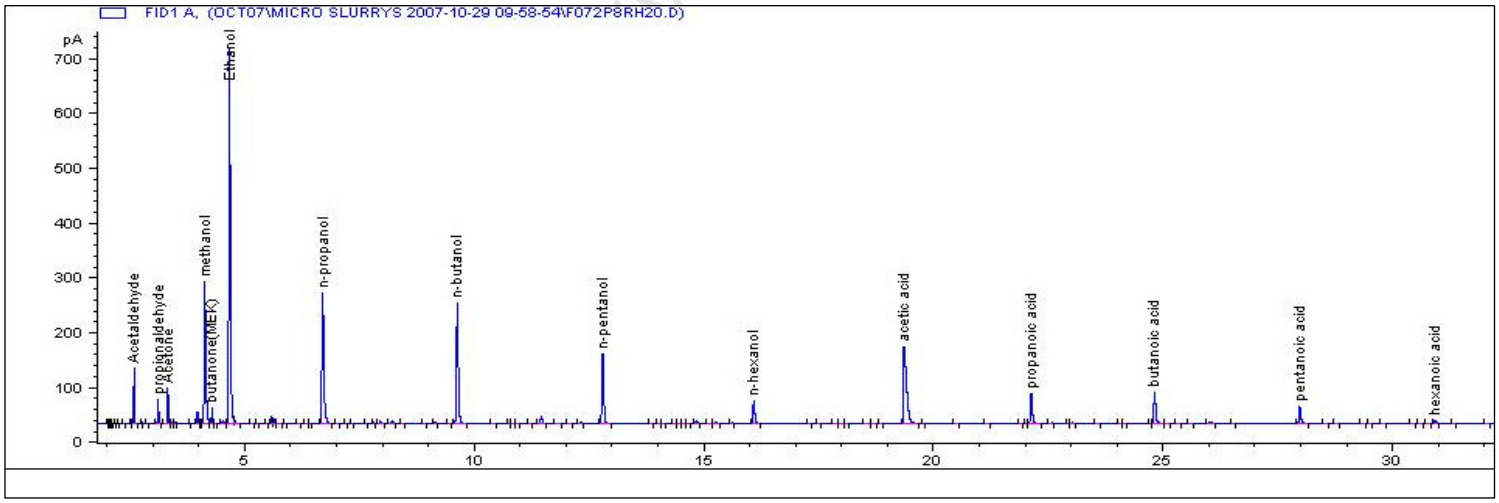

Figure 3.12: Chromatograph of aqueous phase (at 25ºC) analyzed on an off-line GC FID system.

3.4.3.2. Analysis of organic oil fraction

The organic oil fraction was analysed using both an off-line one-dimensional GC (1D GC) fitted with FID and a two-dimensional gas chromatograph (GCxGC) system.

The one-dimensional off-line GC-FID system and conditions used for the detection of C_1-C_{30} hydrocarbons in the oil fraction are listed in Table 3.7. No external or internal standard is used for quantification of the detected components but response factors were employed during quantification (see paragraph 3.4.5). Also see Figure 3.13 for a chromatograph of the oil fraction analysis performed on a 1D GC.

The same two-dimensional gas chromatographic system (as described in paragraph 3.4.2) was used to analyze the organic oil fraction. The only differences between the analysis were that the sample was injected off-line only on the back channel, bypassing the one-dimensional separation system, and the analysis conditions were different (see Table 3.8). A two-dimensional contour plot was obtained and components were identified and quantified using methods described in paragraph 3.4.5 (see Figure 3.14).

Table 3.7: Conditions for gas chromatographic analysis of the organic oil fraction using FID detection

Gas Chromatograph	**Agilent 6890N**
Detector	flame ionization detector (FID) Heater Temperature = 50˚C
Column	HP PONA Fused silica capillary 50m x 200µm x 0.50µm Stationary phase: methyl siloxane
Introduction gas Carrier gas Column head pressure	Hydrogen Hydrogen 2.5 bar (absolute)
Injector Injection volume	auto sampler split injector, T = 250˚C split ratio: 50:1 0.2µl
Oven Temperature program	 35˚C for 5min 4˚C/min to 300˚C for 14 min
Run Time	85.25 min

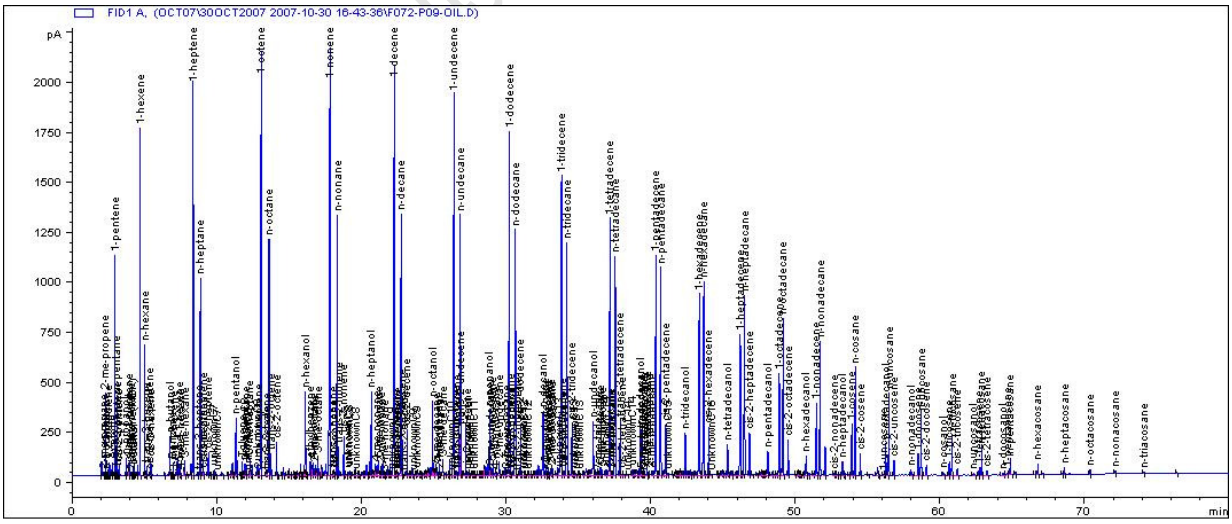

Figure 3.13: Chromatograph of organic oil fraction analyzed on an off-line one-dimensional GC FID system.

Table 3.8: Conditions for two-dimensional gas chromatographic analysis of the organic oil fraction using FID detection

Gas Chromatograph Agilent 6890N		
Oven	Temperature program	35 ˚C for 10 min 3 ˚C/min to 240 ˚C for 10 min
Hot jet	Temperature program	280 ˚C 1 ˚C/min to 360 ˚C
Secondary Oven	Temperature program	60˚C for 2 min 3 ˚C/min to 300 ˚C for 5min
Back Channel		
Back Inlet	Injection volume	0.5 µl
	Injection Mode	Split
	Introduction Gas	Hydrogen
	Temperature (˚C)	250
	Pressure (kPa)	210
	Flow (ml/min)	436
	Split ratio	200:1
Back Column	Description	First Column: Chrompak 7692 CP-Sil-5 1.5m x 150µm x 2µm Second Column: Agilent 19091N-205 HP-Innowax 50m x 200µm x 0.4µm
	Pressure (kPa)	210
	Flow (ml/min)	2.1
Back Detector	Heater temperature (˚C)	300
	H_2 flow (ml/min)	40
	Air flow (ml/min)	450
	Makeup gas	Nitrogen
	Makeup gas flow (ml/min)	25
Modulation time	7s	
Run time	88 min	

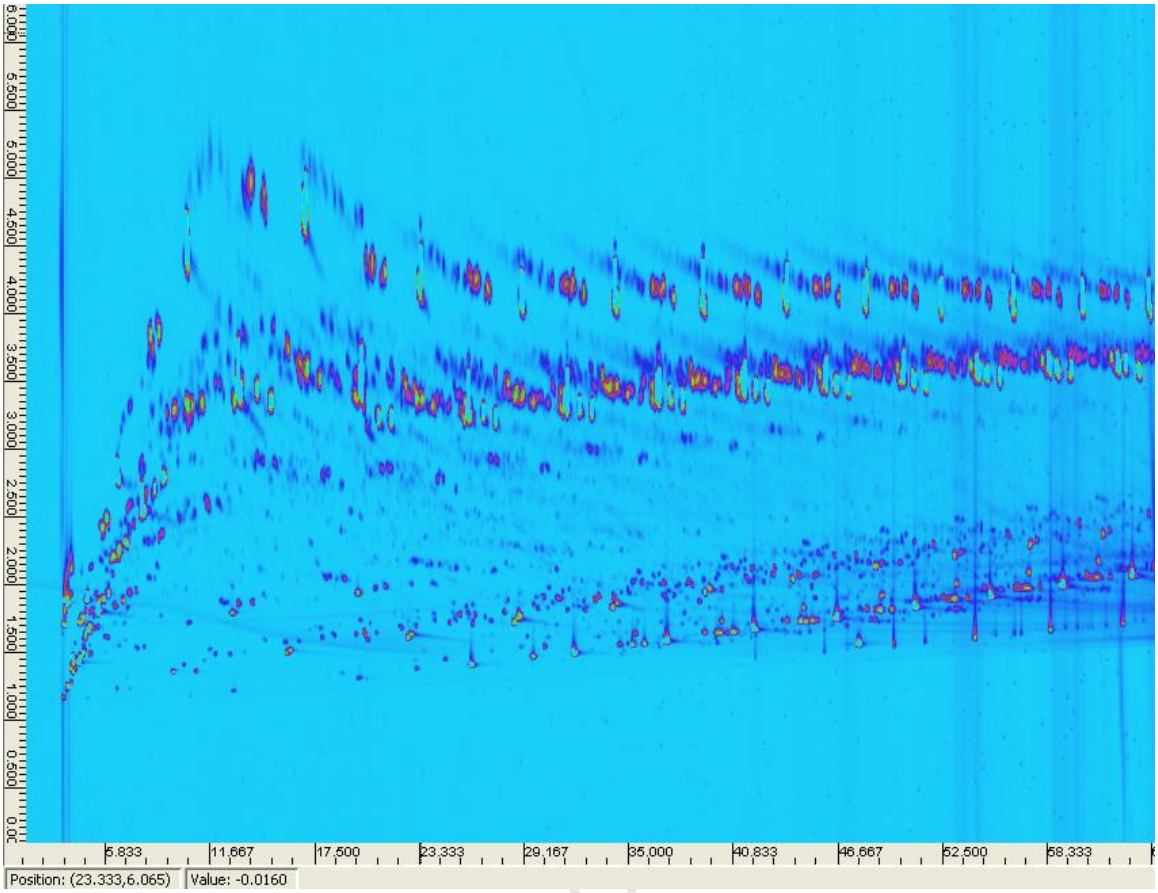

Figure 3.14: Two-dimensional contour plot of organic oil fraction.

3.4.4. Wax product analysis

The wax product collected from the hot pot at 200ºC (see Figure 3.4) is analysed using a high temperature gas chromatographic system (HTGC) consisting of a non-polar column and FID. To quantify the detected components (see Figure 3.15), an internal standard (C_{36}) is added to the product sample prior to analysis.

The C_{36} is introduced to the sample by dissolving 0.2 g of wax in 50 ml xylene and adding 2 g of C_{36} internal standard to the hot mixture. Part of the mixture is transferred to a vial and injected off-line into the HTGC system.

Refer to Table 3.9 for a summary of the analysis conditions employed.

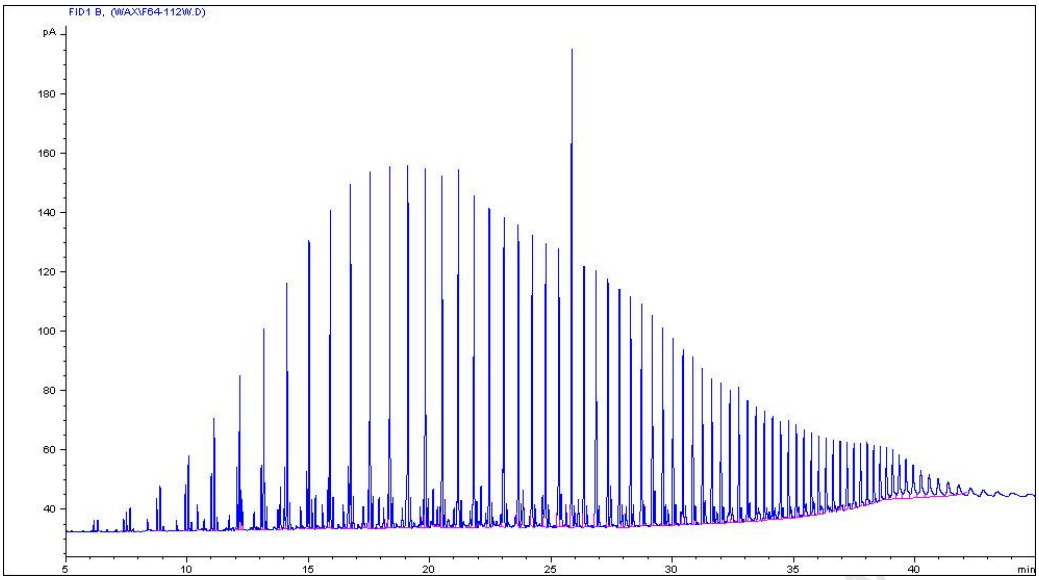

Figure 3.15: Chromatograph of wax product analyzed on an off-line HTGC FID system.

Table 3.9: Conditions for analysis of the wax product using High Temperature Gas Chromatography

Gas Chromatograph	**Agilent 6890N**
Detector	flame ionization detector (FID) Heater Temperature = 450˚C
Column	MXT-1 capillary 15m x 0.28mm x 0.15µm Stationary phase: Cross bond –dimethyl-polysiloxane
Introduction gas Carrier gas Column head pressure	Hydrogen Hydrogen 2.5 bar (absolute)
Injector	split injector split ratio: 1:0 Injection volume: 1.0µl
Oven Temperature program	420˚C for 35min
Run time	35 min

3.4.5. Data processing and analysis calculations

3.4.5.1. Calibration of gas chromatographs for gas analysis

Calibrations need to be performed on gas chromatographic systems to assist with the quantification of the compounds detected. The following calibration methods were applied for the instruments used to analyze the Fischer-Tropsch synthesis feed- and tail gas streams.

On-line GC with TCD

The on-line GC TCD was used for detecting the inorganic compounds and methane within the feed- and tail gas. Therefore a calibration mixture consisting of 10.0 % CH_4, 45.0 % H_2, 2.5 % N_2, 10.0 % Ar, 22.5 % CO and 10.0 % CO_2 were used for calibration. The instrument was calibrated on a weekly basis during which at least five samples were injected on-line to measure repeatability of the analysis.

On-line GC with FID

The on-line GC FID was used for detecting the organic compounds within the feed- and tail gas. A mixture consisting of 10.0 % CH_4, 45.0 % H_2, 2.5 % N_2, 10.0 % Ar, 22.5 % CO and 10.0 % CO_2 was used for calibration of the instrument. During the calibration, where at least five samples were injected on-line to measure repeatability, the areas of the detected methane peaks were recorded and compared with previous calibrations. An average of the methane areas were used for quantification as described in paragraph 3.4.5.2. To ensure that the calibration was effective, especially for the C_{2+} hydrocarbons present in the sample, a C_1 - C_6 test gas mixture was used to verify the calibration. See Table 3.10 for the test gas composition. The instrument was calibrated on a weekly basis.

Table 3.10: Composition of C_1-C_6 hydrocarbon test gas mixture

Compound	Vol%
Methane	15.00
Ethene	0.50
Ethane	0.50
Propene	0.50
Propane	0.10
1-Butene	0.10
n-Butane	0.25
1-Pentene	0.10
n-Pentane	0.10
1-Hexene	0.10
n-Hexane	0.10

On-line GCxGC with FID

The on-line GCxGC FID was used for detecting the organic compounds within the hot tail gas. A mixture consisting of 10.0 % CH_4, 45.0 % H_2, 2.5 % N_2, 10.0 % Ar, 22.5 % CO and 10.0 % CO_2 was used for calibration of the instrument. During the calibration at least five samples were injected on-line on both the one-dimensional channel (Channel A) and two-dimensional channel (Channel B) of the GCxGC instrument. The areas of the detected methane peaks were recorded for both channels and compared with previous calibrations. Averages of the methane areas for the respective channels were used during quantification as described in paragraph 3.4.5.7. To ensure that the calibration was effective, especially for the C_{2+} hydrocarbons present in the sample, a C_1 - C_6 test gas mixture was used to verify the calibration. See Table 3.10 for the test gas composition. The instrument was calibrated on a weekly basis.

3.4.5.2. Feed- and cold tail gas analysis obtained from GC-FID

To calculate the concentration of the components in the feed- or cold tail gas GC-FID analysis the following calculations are made:

$$C_i = RF.\frac{A_i.C_s}{A_s.i} \tag{3.1}$$

Where C_i = Concentration in mole percent of component i

RF = Response factor specific to component

A_i = Area of component i

C_s = Concentration of external standard (10 vol% of methane) in mole percent

A_s = Area of methane in external standard

i = carbon numbers 1 to n

3.4.5.3. Feed- and Cold tail gas analysis obtained from GC-TCD

To calculate the concentration of the components in the feed- or cold tail gas GC-TCD analysis the following calculations are made:

$$C_i = RF.\frac{A_i.C_s}{A_s.i} \tag{3.2}$$

Where C_i = Concentration in mole percent of component i

RF = Response factor specific to component

A_i	=	Area of component i
C_s	=	Concentration of external standard (CO, CO_2, CH_4, Ar and N_2 depending on compound) in mole percent
A_s	=	Area of component in external standard

3.4.5.4. Aqueous phase analysis

To calculate the concentration of the components in the aqueous phase the following calculations are made:

$$C_i = RF.\frac{A_i.C_s}{A_s} \tag{3.3}$$

Where	C_i	=	Concentration in mass percent of component i
	RF	=	Response factor specific to component
	A_i	=	Area of component i
	C_s	=	Concentration of external standard in mass percent
	A_s	=	Area of external standard
	i	=	carbon numbers 1 to n

3.4.5.5. Organic phase analysis

To calculate the concentration of the components in the organic (oil) phase the following calculations are made:

$$C_i = RF.\frac{A_i}{\sum_i A_i}.100 \qquad (3.4)$$

Where C_i = Concentration in mass percent of component i

RF = Response factor specific to component

A_i = Area of component i

$\sum_i A_i$ = Sum of component areas

i = carbon numbers 1 to n

3.4.5.6. Wax product analysis

To calculate the concentration of the components in the wax product the following calculations are made:

$$M_i = \frac{A_i.C_{36_{conc}}}{\left(A_{C36} - A_{C36_{calc}}\right)} \qquad (3.5)$$

Where M_i = Mass percent of component i

RF = Response factor specific to component

Ai = Area of component i

$C_{36_{conc}}$ = Concentration of internal C_{36} internal standard added to sample

A_{C36} = Area of C_{36} n-paraffin with internal

standard

$A_{C36_{calc}}$ = Calculated area of C_{36} n-paraffin = [(A_{C35} + A_{C37})/2]

i = carbon numbers 1 to n

$$C_{36_{conc}} = RF.\frac{X}{X + M_{wax}}.100 \quad (3.6)$$

Where

$C_{36_{conc}}$ = Concentration of internal C_{36}

RF = Response factor specific to component

internal standard added to sample

$C_{36_{add}}$ = C_{36} stock solution added to sample

$C_{36_{stockconc}}$ = C_{36} stock solution concentration (± 1000ppm)

M_{wax} = Mass of wax sample in sample solution

X = $([C_{36_{add}} . C_{36_{stockconc}}/1000].1000)$

3.4.5.7. Hot tail gas analysis

The hot tail gas is introduced to the GCxGC system via two heated sample loops. The samples have very similar compositions since they are sampled essentially at the same time and injected simultaneously into the GC system. Consequently the two separations can be combined to form one product distribution (see Figure 3.16).

To calculate the concentration of the components in the hot tail gas product the following calculations are made:

For the one-dimensional separation

$$C_i = RF_{1D} \cdot \frac{A_i . C_s}{A_s . i} \tag{3.7}$$

Where C_i = Concentration in mole percent of component i

RF_{1D} = Response factor specific to component detected during one-dimensional separation on GCxGC

A_i = Area of component i

C_s = Concentration of external standard (10 vol% of methane) in mole percent

A_s = Area of methane in external standard

i = carbon numbers 1 to n

For the two-dimensional separation

$$C_i = RF_{2D} \cdot \frac{A_i . C_s}{A_s . i} \tag{3.8}$$

Where C_i = Concentration in mole percent of component i

RF_{2D} = Response factor specific to component detected during two-dimensional separation on GCxGC

A_i = Area of component i

C_s = Concentration of external standard (10 vol% of methane) in mole percent

A_s = Area of methane in external standard

i = carbon numbers 1 to n

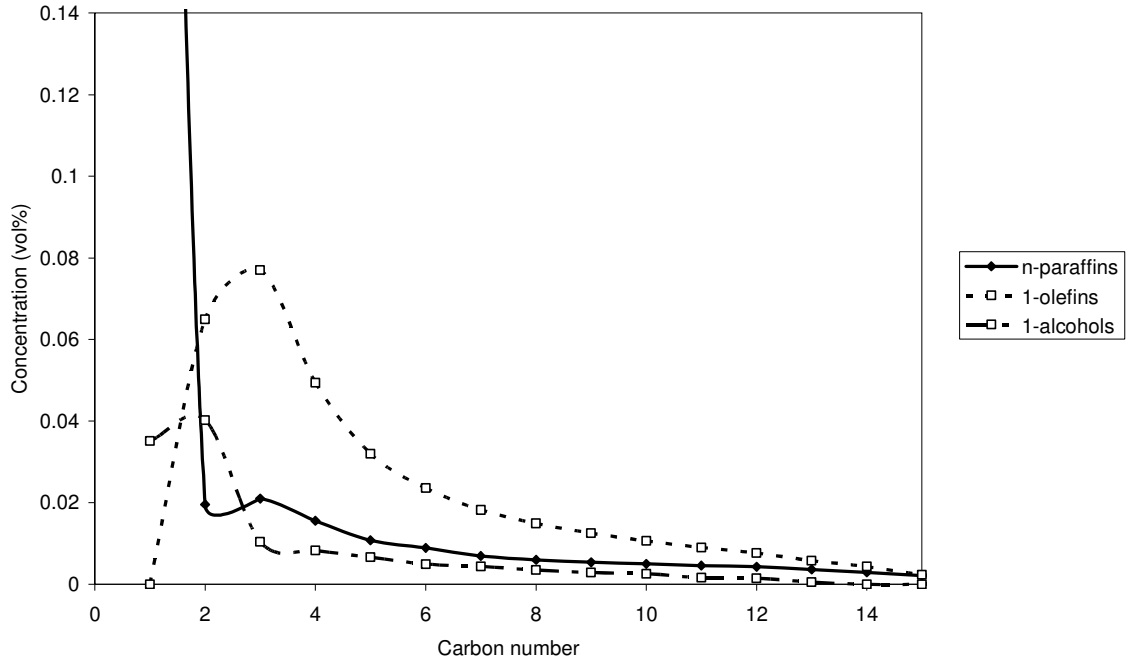

Figure 3.16: The one-dimensional separation is combined with the two-dimensional separation of the hot tail on the GCxGC system to form one product distribution.

3.5 DATA EVALUATION

During a Fischer-Tropsch synthesis experiment a lot of data is captured. The data include:

- Reaction conditions such as temperatures and pressures
- Feed gas and tail gas flow rates
- Amount of liquid and wax product drained
- Concentrations of compounds present in feed gas, tail gas, liquid products and wax product

The data is of little value on its own but by combining it; the data is converted to valuable information which allows for the evaluation of the synthesis

process. Typical information that can be extracted from the data is reaction rates, reactant conversion percentages and component selectivities. The following sections will discuss how the data is processed for evaluation purposes.

3.5.1. Calculating flow rates of various compound from GC analysis

The first step in data evaluation is to determine the flow rates of the various compounds from gas chromatographic analysis. To make the quantification process easier, Argon was added to the fresh feed at a known flow rate, which is used as a basis for all flow rate calculations. The flow rates of the inorganic compounds (hydrogen, carbon monoxide and carbon dioxide) and methane can be calculated using the concentrations (in mole percent) of the compounds obtained in the GC TCD trace analysis (see paragraph 3.4.5.3).

$$F_i = \frac{C_i}{C_{Ar}}.F_{Ar} \tag{3.9}$$

Where F_i = flow rate of compound i in mole/hr

F_{Ar} = flow rate of internal standard, Argon, in ml_n/min

C_i = compound i concentration in mole percent

C_{Ar} = internal standard, argon, concentration in mole %

The flow rate of water is calculated from an oxygen balance, i.e. the flow rates of CO and CO_2 in the feed and the reactor outlet streams.

$$F_{H_2O} = F_{CO,feed} - F_{CO,tail} + 2.F_{CO_2,feed} - 2.F_{CO_2,tail} \tag{3.10}$$

The flow rate of organic product compounds in the tail gas can be determined by relating it to the tail gas flow rate, which can be linked to the flow rate of argon, and using the concentrations of the compounds detected by GC-FID (see paragraph 3.4.5.1 and 3.4.5.6).

$$F_i = \frac{F_{TG} C_i}{100A} \tag{3.11}$$

Where F_i = flow rate of compound i in mole/hr
F_{TG} = flow rate of tail gas in litre/hr
C_i = compound i concentration in mole percent
A = Avogadro's constant (22.44litre at STP)
i = carbon numbers 1 to n

The flow rate of organic product compounds in the liquid and wax products can be determined by relating the concentrations of the compounds detected by the various GC-FID methods (see paragraph 3.4.5.2 to 3.4.5.5) with the amount of product drained from the hot and cold traps over a period of time.

$$F_i = \frac{M_P C_i}{100Mr} \tag{3.12}$$

Where F_i = flow rate of compound i in mole/hr
M_P = mass of product drained in g/hr
C_i = compound i concentration in mass percent
Mr = molecular weight of compound (g/mole)
i = carbon numbers 1 to n

3.5.2. Calculation of partial pressure in the reactor

If the reactor is well mixed, the assumption can be made that the composition of the reactor outlet stream is similar to the composition of the reactor contents. Therefore the partial pressure of each component (p_i) in the reactor

is calculated using the flow rates of the components detected in the tail gas (outlet stream).

$$p_i = \frac{F_i}{\sum_i F_{TG}} . p_{reactor} \tag{3.13}$$

Where F_i = flow rate of compound i at reactor outlet (tail gas)

F_{TG} = total flow rate of outlet gas (tail gas)

$p_{reactor}$ = total reactor pressure

3.5.3. Calculation of conversion and reaction rate

The overall conversion of component i (X_i) is calculated from the flow rate of a component i in the tail gas (TG) using the fresh feed gas (FF) flow rate minus the tail gas flow rate.

$$X_{i,overall} = \frac{F_{i,FF} - F_{i,TG}}{F_{i,FF}} \tag{3.14}$$

The rate of formation of organic Fischer-Tropsch products can be calculated from the amount of CO consumed minus the amount of CO_2 formed in relation to the mass of unreduced catalyst present in the reactor (m_{cat}).

$$r_{FT} = \frac{\left(F_{CO,feed} - F_{CO_2,feed}\right) - \left(F_{CO,tail} - F_{CO_2,tail}\right)}{m_{cat}} \tag{3.15}$$

The rate of the water gas shift reaction is determined from the amount of CO_2 formed.

$$r_{WGS} = r_{CO_2} = \frac{\left(F_{CO_2,feed} - F_{CO_2,tail}\right)}{m_{cat}} \quad (3.16)$$

3.5.4. Calculation of selectivity

The selectivity of component i is calculated relative to the amount of carbon converted. The amount of carbon is determined from the amount of CO converted to FT products, which is (CO + CO_2) conversion.

$$S_i = \frac{F_i}{\left(F_{CO,FF} + F_{CO_2,FF}\right) + \left(F_{CO,TG} + F_{CO_2,TG}\right)} \quad (3.17)$$

3.5.5. Constructing a total hydrocarbon distribution

A total hydrocarbon distribution for the complex Fischer-Tropsch synthesis product can be obtained using two methods.

The one method use the flow rates of compounds detected in the cold tail gas, feed gas, oil, water and wax product to construct a distribution. The second method use flow rates of compounds from the hot tail gas, oil and wax product to construct a total hydrocarbon distribution. The flow rates of the compounds were combined as displayed in Table 3.11 and Figures 3.17 and 3.18.

Table 3.11: Equations for combining the flow rates of compounds detected in various products to form a total hydrocarbon distribution of the Fischer-Tropsch synthesis product

Product Range	Equation
	Method 1
C_1 - C_9	$C_i = C_{cold\ tail} - C_{feed} + C_{water} + C_{oil}$
C_{10} - C_{25}	$C_i = C_{oil} + C_{wax}$
C_{26+}	$C_i = C_{wax}$
	Method 2
C_1 - C_9	$C_i = C_{hot\ tail} - C_{feed}$
C_{10} - C_{25}	$C_i = C_{oil} + C_{wax}$
C_{26+}	$C_i = C_{wax}$

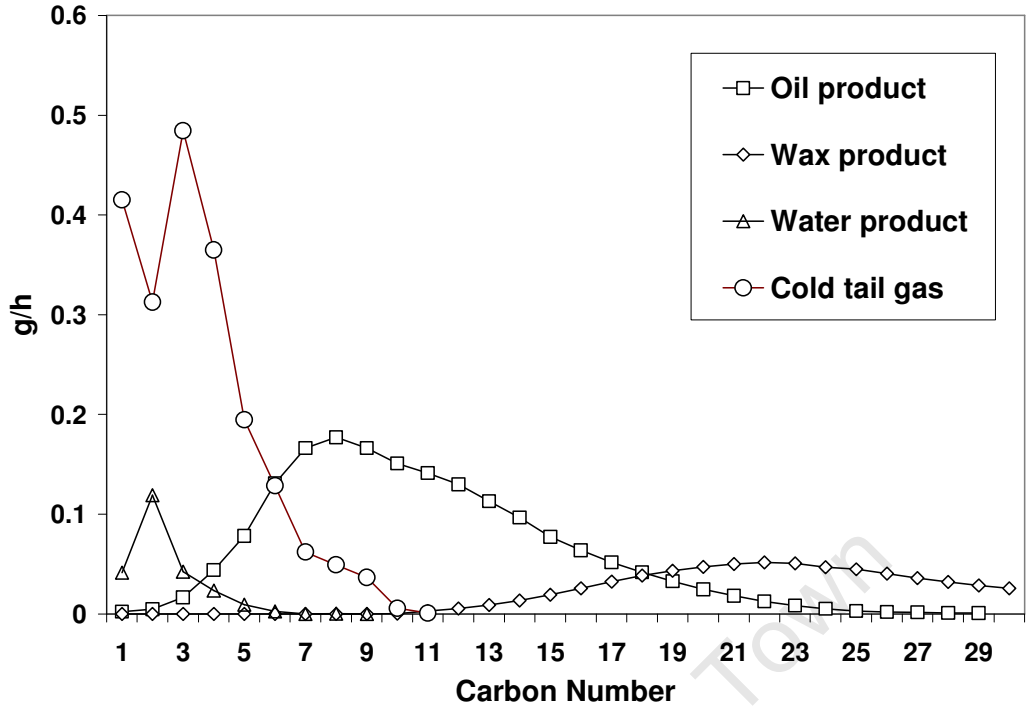

Figure 3.17: A visual representation of how the compounds detected in the product analysis are combined using method 1 (see Table 3.11) to form a total hydrocarbon distribution of the Fischer-Tropsch product

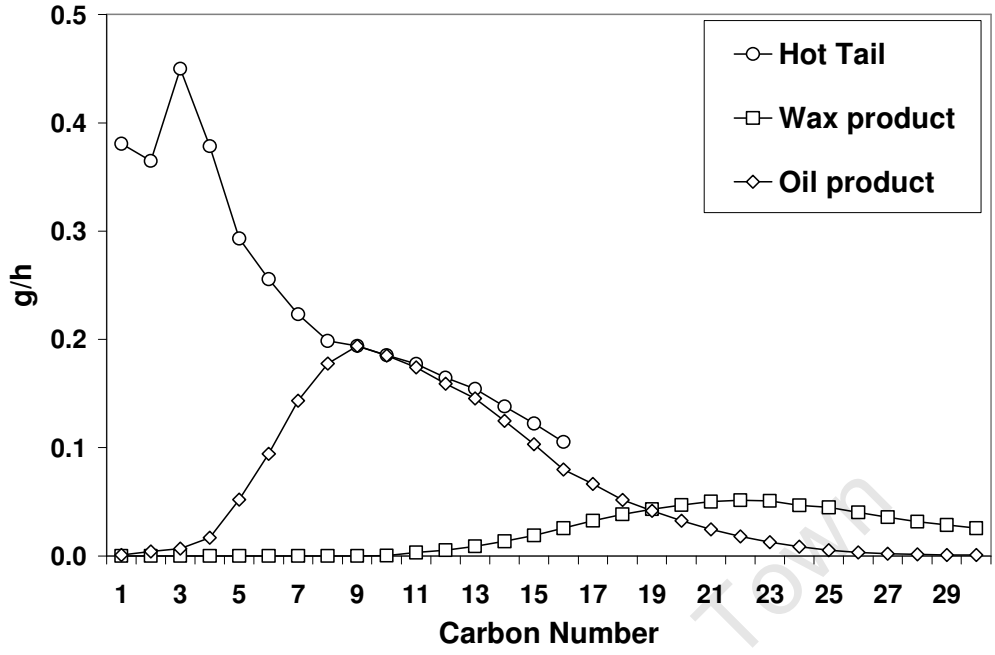

Figure 3.18: A visual representation of how the compounds detected in the product analysis are combined using method 2 (see Table 3.11) to form a total hydrocarbon distribution of the Fischer-Tropsch product

CHAPTER 4

RESULTS

4.1 CALIBRATION OF 1D GC AND GCXGC

The Fischer-Tropsch tail gas stream consists of H_2, N_2, Ar, CO, CO_2 and a range of organic product compounds. These organic product compounds in the stream are detected using both on-line one-dimensional GC (1D GC) and two-dimensional GCxGC systems. In order to quantify the hydrocarbons an external calibration method is used where a constant volume of a known gas mixture is injected into the GC system and the detected peak areas are recorded.

For this study the gas chromatographs were calibrated before each of the Fischer-Tropsch experiments were started. The systems were also checked on a weekly basis and if the calibration values deviated from the initial values the calibration values, used for quantification, were adjusted.

The same test gas mixture was used for calibration on channel A of the one-dimensional GC and channels A and B of the two-dimensional GCxGC system and consisted of: 10.0 % CH_4, 45.0 % H_2, 2.5 % N_2, 10.0 % Ar, 22.5 % CO and 10.0 % CO_2.

For the calibration of channel A, on the one-dimensional GC, a sample of the test gas mixture was injected via a sample loop on the GC at a split ratio of 50:1. After 2 minutes when the methane peak has eluted from the system the run was stopped and another sample was bubbled through the sampling system for at least 5 minutes. Thereafter the sample was injected into the system. This was repeated four times to create a calibration set. If the %RSD of the calibration set was below 1% the calibration was accepted and the average calibration value was used for quantification. If the average calibration value deviated from the previous calibration value, which is used for quantification, the calibration value was adjusted.

In Table 4.1 the methane peak areas of 4 calibration sets which were recorded on channel A of the one-dimensional GC are presented. Each of the calibration sets (1 to 4) were performed on different days usually after routine maintenance was performed on the 1D GC. This explains the difference in average peak areas detected for the 4 different calibration sets. Although the split ratio stayed constant (50:1) the sample loops were also replaced and therefore a slight variation in sample loop volume might have occurred thus explaining the variation in peak areas.

Table 4.1: Peak areas detected for methane on Channel A of the one-dimensional GC separated out of a gas mixture containing 10.0 % CH_4, 45.0 % H_2, 2.5 % N_2, 10.0 % Ar, 22.5 % CO and 10.0 % CO_2

Calibration	Injection 1	Injection 2	Injection 3	Injection 4	Average	Standard Deviation	RSD, %
	Detected Area for 10% Methane						
1	1554.5	1551.9	1557.4	1556.4	1555.1	2.4	0.16
2	1542.8	1543.5	1542.3	1546.2	1543.7	1.7	0.11
3	1526.3	1524.6	1525.6	1523.6	1525.0	1.2	0.08
4	1529.5	1525.6	1529.5	1527.6	1528.1	1.9	0.12

Tables 4.2 and 4.3 present some of the methane peak areas recorded on channels A and B of the two-dimensional GCxGC system. Channel A on the GCxGC system is connected to the first sample loop (see chapter 3 section 3.4.2) which injects contents into a thick phase non-polar column (CP Sil-5) used for the analysis of light hydrocarbons, methane through to butane, since these compounds are not separated on the GCxGC column setup. Channel B of the GCxGC system is connected to the second sample loop and injects the sample onto the first column of the GCxGC column setup. The sampling and injection of the sample onto both channels happen simultaneously.

For the calibration of channels A and B, of the two-dimensional GC, a sample of the test gas mixture was injected via two sample loops on the GCxGC system at a split ratio of 50:1 for channel A and 5:1 for channel B. The methane peak elutes from both channels after 8 minutes at which point the run was stopped. Before a new sample is injected onto the system, the sample was bubbled through the sampling system for at least 10 minutes.

This was repeated four times to create a calibration set. Similar to the calibration of the 1D GC the calibration set was accepted if the %RSD was below 1% for both channels. If the average calibration value deviated from the previous calibration value, which is used for quantification, the calibration value was adjusted.

The calibration sets (1 to 4) for both channels A and B on the GCxGC were performed on different days usually after routine maintenance was performed on the GCxGC (see Tables 4.2 and 4.3). Routine maintenance includes replacing columns, sample loops, injector liners, sampling valves, etc. Therefore the difference in the average peak areas detected for the 4 different calibration sets can be explained by the replacement of sample loops, which might have slightly different sample volumes.

Table 4.2: Peak areas detected for methane on Channel A of the two-dimensional GCxGC separated out of a gas mixture containing 10.0 % CH_4, 45.0 % H_2, 2.5 % N_2, 10.0 % Ar, 22.5 % CO and 10.0 % CO_2

Calibration	Injection 1	Injection 2	Injection 3	Injection 4	Average	Standard Deviation	RSD, %
	Detected Area for 10% Methane						
1	1262.8	1262.7	1264.6	1266.7	1264.2	1.9	0.15
2	1253.5	1256.5	1253.4	1254.4	1254.5	1.4	0.11
3	1654.6	1658.3	1656.3	1657.4	1656.7	1.6	0.10
4	1352.8	1348.0	1347.2	1348.0	1349.0	2.6	0.19

Table 4.3: Peak areas detected for methane on Channel B of the two-dimensional GCxGC separated out of a gas mixture containing 10.0 % CH_4, 45.0 % H_2, 2.5 % N_2, 10.0 % Ar, 22.5 % CO and 10.0 % CO_2

Calibration	Injection 1	Injection 2	Injection 3	Injection 4	Average	Standard Deviation	RSD, %
	Detected Area for 10% Methane						
1	3120.5	3120.6	3123.3	3119.8	3121.1	1.5	0.05
2	2865.6	2864.2	2862.1	2864.0	2864.0	1.4	0.05
3	2865.6	2863.2	2865.1	2861.0	2863.7	2.1	0.07
4	2864.1	2862.5	2860.0	2865.5	2863.0	2.4	0.08

In general the observed deviations between the calibration data sets presented in Tables 4.1 to 4.3 have a RSD <1% which is well within precision estimates and is thus acceptable for calibration purposes.

After calibration of the one-dimensional GC (1D GC) and the two-dimensional GCxGC systems a $C_1 – C_6$ test gas mixture was injected into the systems to verify the effectiveness of the calibration especially for the C_{2+} hydrocarbons present in the gas sample (see Tables 4.4 and 4.5).

The Association of Analytical Communities (AOAC) (see Appendix C, Tables C1 and C2) stipulated that for a 95% confidence limit the RSD for the data should be < 5.3% and the recovery should be between 90% and 107%.

As shown in Table 4.4, the methane concentrations recorded on the GCxGC system had a RSD < 2.7% and a recovery of 99%. The rest of the hydrocarbons had a RSD < 5.3% and recovery between 94% and 105%. The balance of the test mixture was also 97%.

For the 1D GC system the RSD for methane concentrations was less than 2.7% and the recovery was 99%. For the C_2 to C_6 hydrocarbons the RSD was below 5.3% and the recovery varied between 66% and 101%. The balance of the test mixture was 92%.

All the components in the test mixture, obtained from the GCxGC system fall within the RSD range stipulated by the Association of Analytical Communities (AOAC). Although all the recoveries are within range, a slightly lower recovery was recorded for ethene and a slightly higher recovery was recorded for ethane. This can be attributed to peak overlap of ethane and ethane. From C_4 onwards the olefin/paraffin separation is considered to be perfect.

Therefore it can be concluded that the external calibration method was sufficient for the GCxGC system. For the 1D GC system the RSD for 1-hexene and n-hexane were out of range and the recovery for n-pentane were lower than 80%. An explanation for this odd behaviour may be that the sample

lines that transfer sample to the GCxGC system are heated (200ºC) and therefore ensures that the C_5 and C_6 compounds are in the gas phase and are transferred to the GCxGC system. The gas sample fed to the 1D GC is transferred to the 1D GC system via sample lines at ambient temperature. It may be possible that the C_5 and C_6 compounds start to condense out of the sample matrix into the sample lines which leads to poor recovery and under reporting of these compounds. In general it can be concluded that for the 1D GC system the external calibration is suitable for the determination of the C_1 to C_4 fraction but not necessarily for the C_{5+} compounds.

Table 4.4: Results for C_1 - C_6 test gas mixture injected in to GCxGC system to verify suitability of GCxGC calibration (Balance is 97% recovery)

Compound	Calibration True value	Calibration 1	Calibration 2	Calibration 3	Calibration 4	Average	Standard Deviation	RSD, %	Recovery, %	95% Confidence limit (±)
	Vol%									
Methane	**15.00**	14.689	14.879	15.052	15.050	14.918	0.173	1.160	99	0.55
Ethene	**0.50**	0.483	0.484	0.482	0.452	0.475	0.015	3.249	95	0.05
Ethane	**0.50**	0.510	0.519	0.513	0.513	0.514	0.003	0.664	103	0.01
Propene	**0.50**	0.485	0.498	0.480	0.480	0.485	0.009	1.761	97	0.03
Propane	**0.10**	0.100	0.104	0.104	0.104	0.103	0.002	2.018	103	0.01
1-Butene	**0.10**	0.096	0.094	0.093	0.093	0.094	0.001	1.479	94	0.00
n-Butane	**0.25**	0.251	0.233	0.242	0.252	0.244	0.009	3.641	98	0.03
1-Pentene	**0.10**	0.099	0.091	0.098	0.098	0.096	0.004	3.764	96	0.01
n-Pentane	**0.10**	0.086	0.086	0.089	0.089	0.087	0.002	2.234	87	0.01
1-Hexene	**0.10**	0.097	0.096	0.095	0.099	0.097	0.002	1.872	97	0.01
n-Hexane	**0.10**	0.098	0.095	0.100	0.100	0.098	0.002	2.365	98	0.01

Table 4.5: Results for C_1 - C_6 test gas mixture injected in to one-dimensional GC system to verify suitability of calibration (Balance is 92% recovery)

Compound	Calibration True value	Calibration 1	Calibration 2	Calibration 3	Calibration 4	Average	Standard Deviation	RSD, %	Recovery, %	95% Confidence limit (±)
	Vol%									
Methane	**15.00**	14.963	14.689	14.853	14.981	14.871	0.134	0.903	99	0.43
Ethene	**0.50**	0.452	0.465	0.473	0.474	0.466	0.010	2.125	93	0.03
Ethane	**0.50**	0.505	0.528	0.493	0.494	0.505	0.016	3.240	101	0.05
Propene	**0.50**	0.480	0.501	0.467	0.468	0.479	0.016	3.318	96	0.05
Propane	**0.10**	0.090	0.094	0.088	0.088	0.090	0.003	2.996	90	0.01
1-Butene	**0.10**	0.093	0.096	0.089	0.090	0.092	0.003	3.389	92	0.01
n-Butane	**0.25**	0.254	0.260	0.243	0.243	0.250	0.008	3.394	100	0.03
1-Pentene	**0.10**	0.091	0.090	0.084	0.084	0.087	0.004	4.254	87	0.01
n-Pentane	**0.10**	0.070	0.068	0.064	0.064	0.066	0.003	4.426	66	0.01
1-Hexene	**0.10**	0.101	0.091	0.086	0.086	0.091	0.007	7.860	91	0.02
n-Hexane	**0.10**	0.109	0.098	0.092	0.092	0.098	0.008	8.435	98	0.03

4.2 BENEFITS OF GCXGC FOR ANALYSIS OF FISCHER-TROPSCH PRODUCTS

The Fischer-Tropsch synthesis product is a complex mixture that consist of a wide range of major compounds present in high concentrations such as linear olefins, paraffins and alcohols and a range of minor products present in low concentrations such as internal olefins, branched olefins, branched paraffins, branched alcohols, secondary alcohols, acids, branched acids, aldehydes and ketones.

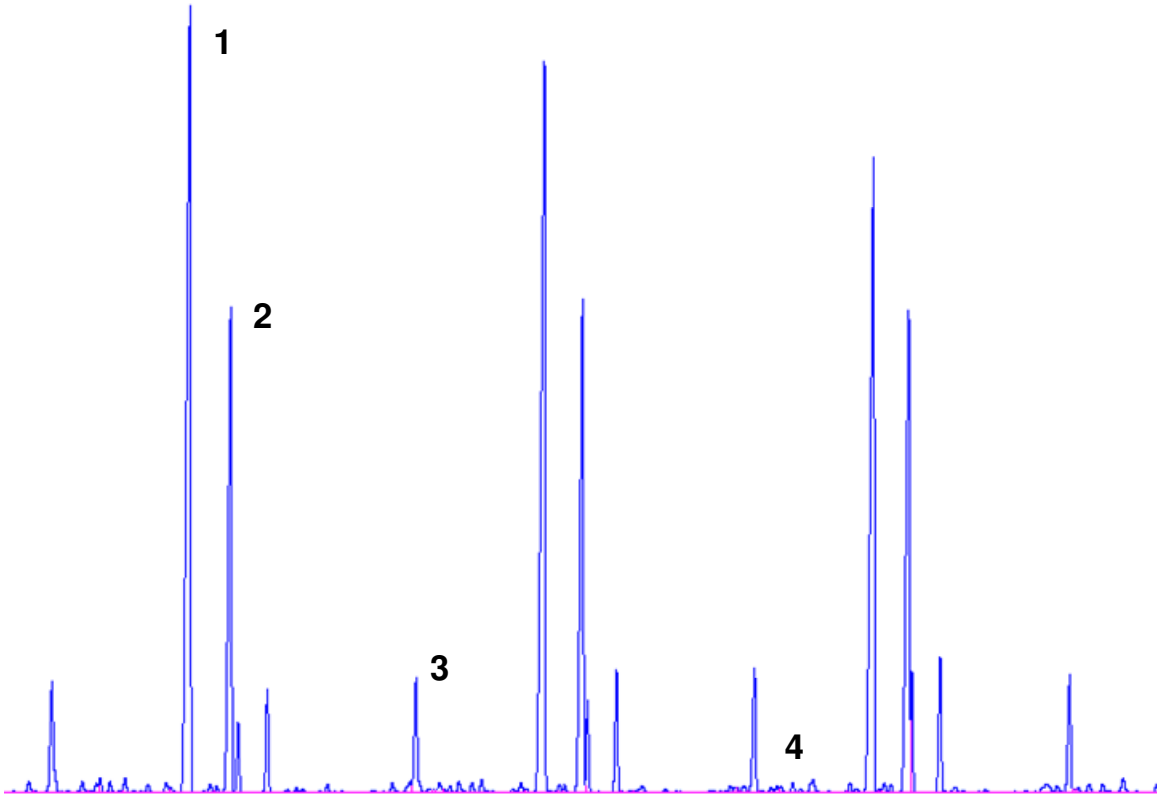

Figure 4.1: A section of a 1D GC chromatogram for the analysis of a Fischer-Tropsch synthesis oil product. Note: (1) 1-olefin; (2) n-paraffin; (3) n-alcohol-(1) and (4) branched olefins, branched paraffins and oxygenates

These compounds are usually separated and quantified using a one-dimensional gas chromatographic (1D GC) method (see Figure 4.1). The principle of separation in gas chromatography is based on two parameters: (1) the volatility of the analytes (compounds) and (2) their interaction with

the stationary phase by means of e.g. hydrogen bonding, $\pi - \pi$ interaction, steric effects, etc. These factors cause the compounds to move through the column at different velocities and results in a retention time profile (Dallüge et al., 2003).

The biggest challenge with separating compounds in the product distribution of the Fischer-Tropsch synthesis lies with the analysis of the so-called oil products (C_6 to C_{30} product range). The oil product contains compounds which move through the column at similar velocities which cause the compounds to co-elute making individual quantification of these compounds difficult (see Figure 4.2).

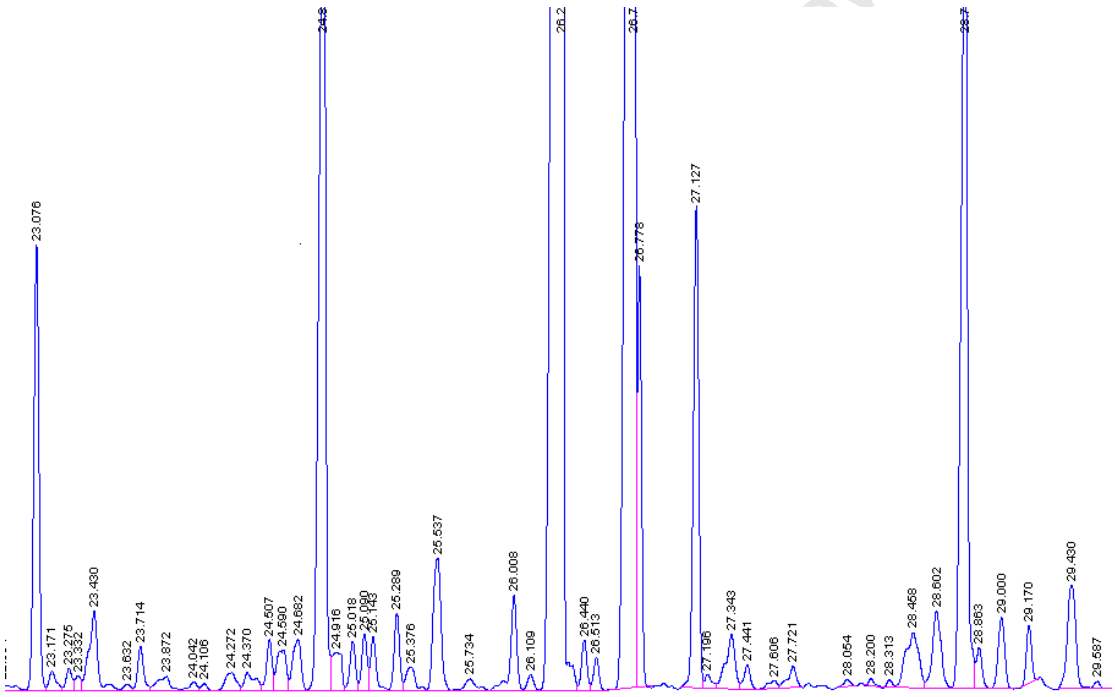

Figure 4.2: An enlarged section of a 1D GC chromatogram for the analysis of a Fischer-Tropsch synthesis oil product

To illustrate the limitations of the 1D GC to separate compounds in the oil product one can evaluate the peak separation by determining the resolution of separation. Resolution is a characteristic of the separation of two adjacent peaks and can be expressed by the following equation:

$$R_{AB} = 2\frac{\left|d_R(B) - d_r(A)\right|}{\left|w(B) + w(A)\right|} \quad (4.1)$$

where R_{AB} is the resolution, $d_R(A)$ and $d_R(B)$ are the retention times of each eluted compound A and B and $w(A)$ and $w(B)$ are the respective widths of each peak at its base (McNaught and Wilkinson, 1997).

Good separation of compounds in a mixture is achieved when there is a baseline between the peaks therefore a resolution above 1.50. If the resolution is below 1.50 co-elution of compounds is observed (Labhouse, 2003)

In Figure 4.2 the GC-trace of an oil product of the Fischer-Tropsch synthesis, eluting between retention times of 23.076 and 26.298 minutes, are displayed. These peaks represent minor Fischer-Tropsch compounds such as the branched compounds and oxygenates. Very few of the adjacent peaks are separated by the baseline and therefore have resolutions less than 1.50.

Another issue regarding the use of 1D GC to analyze the Fischer-Tropsch synthesis oil product is the low detectability and the accurate determination of the minor compounds. The minor compounds have much lower concentrations than the major compounds and have peak heights very similar in magnitude to the noise of the flame ionization detector (signal-to-noise ratio < 2). Therefore the minor compounds can not be accurately detected.

The GCxGC technique is an attractive alternative for the analysis of products of the Fischer-Tropsch synthesis, especially the oil product, since it provides solutions for the limitations of the 1D GC method. The use of a combination of two columns in the GCxGC technique allows the separation of compounds to take place independently on the basis of two separation characteristics, e.g. volatility and polarity. This is known as orthogonal

separation (Dallüge et al., 2003). It allows compounds with similar boiling points in a mixture with a boiling point range to be first separated out based on their volatility and subsequently on the basis of their functionality. Thus, chemical related compounds in the oil product of the Fischer-Tropsch synthesis can now be separated into functional groups and distinctions can be made between the various compounds within the functional group (see Figure 4.3).

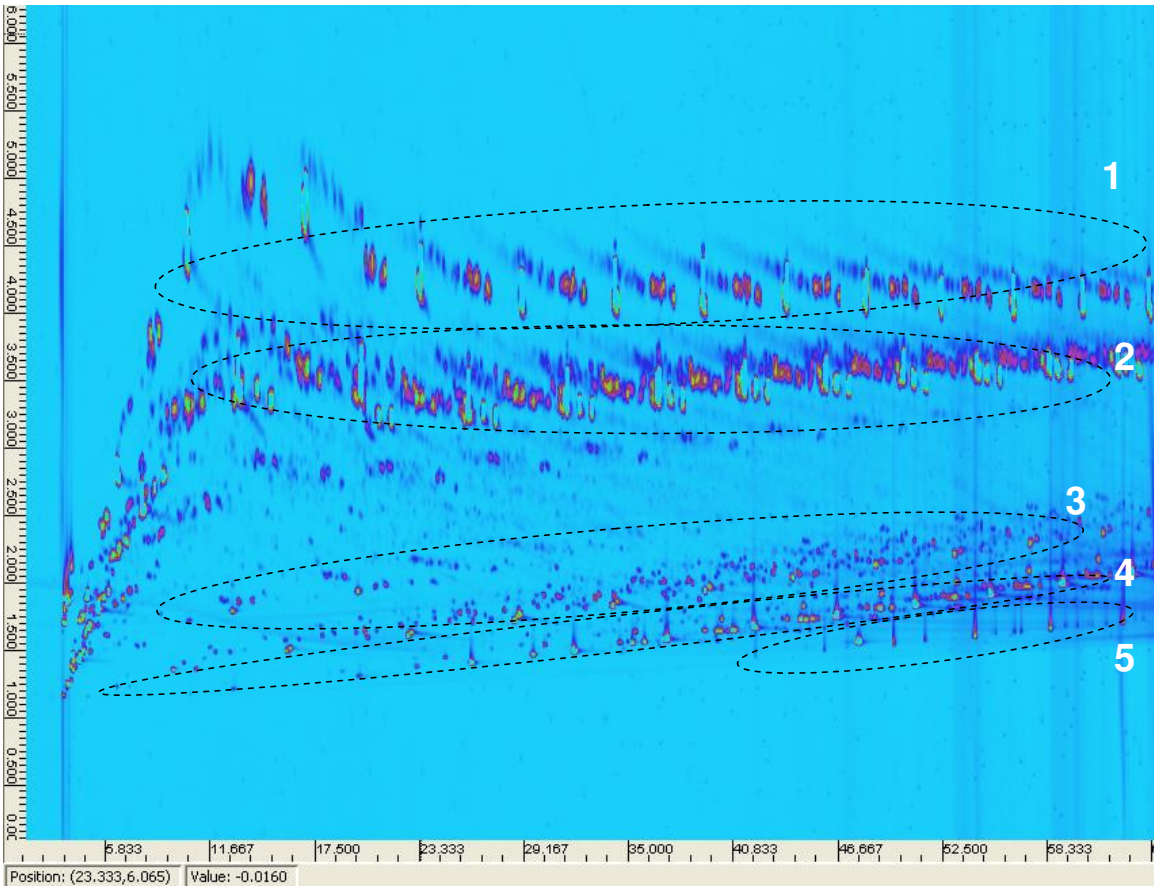

Figure 4.3: Two-dimensional chromatograph (contour plot) of Fischer-Tropsch synthesis oil product injected off-line on to the GCxGC system (1. Paraffins; 2. Olefins; 3. Aldehydes, ketones and aromatics; 4. Alcohols; 5. Acids)

Furthermore, minor compounds such as oxygenates can be detected with improved accuracy using the GCxGC technique (see Figure 4.4). This is achieved by making use of modulation (Dallüge et al., 2003). The modulator is the interface between the two coupled columns and is responsible for the quantitative transfer and refocusing of the compounds. Compounds eluting

from the first (e.g. non-polar) column are trapped by the modulator, resulting in very sharp, narrow peaks, with increased height (modulation is a mass conservative process which causes the peak height to increase to accommodate for the reduction of peak width). These compounds are then rapidly released onto the second (e.g. polar), much shorter column. Once detected the narrow peak areas of a specific compound can be summed together to form a single peak area for that compound. Due to the modulation process the sensitivity (signal-to-noise ratio) of the minor peaks increases allowing for better accuracy and unambiguous detection.

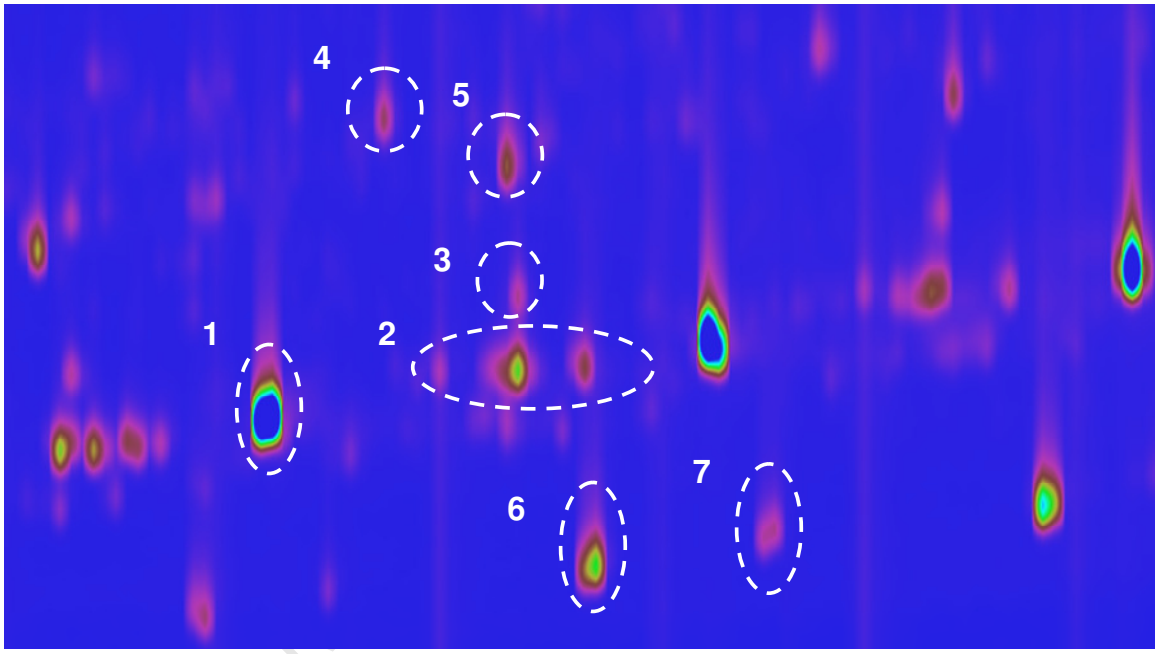

Figure 4.4: Enlargement of a GCxGC-trace (contour plot) of the oil product of the Fischer-Tropsch synthesis focussing on the detected oxygenates (1: n-alcohol-(1); 2: branched alcohols; 3: n-alcohol-(2); 4: aldehyde; 5: ketone; 6: acid; 7: branched acid)

It is thus expected, that more compounds will be detected when using the GCxGC-technique to analyze the product stream of the Fischer-Tropsch synthesis. Especially low level oxygenates formed during Fischer-Tropsch synthesis can be detected with increased accuracy, which will lead to a more complete picture of the product formation in the Fischer-Tropsch synthesis.

To test the above assumptions, oil product from the Fischer-Tropsch synthesis process was injected into both the off-line 1D GC and GCxGC systems and the results were compared. Figures 4.5 to 4.10 graphically compares the results obtained for some of the compounds detected by the 1D GC and the GCxGC.

The major product compounds, n-paraffins (see Figure 4.5), 1-olefins (see Figure 4.6) and n-alcohols-(1) (see Figure 4.7) are equally well determined using 1D GC and GCxGC.

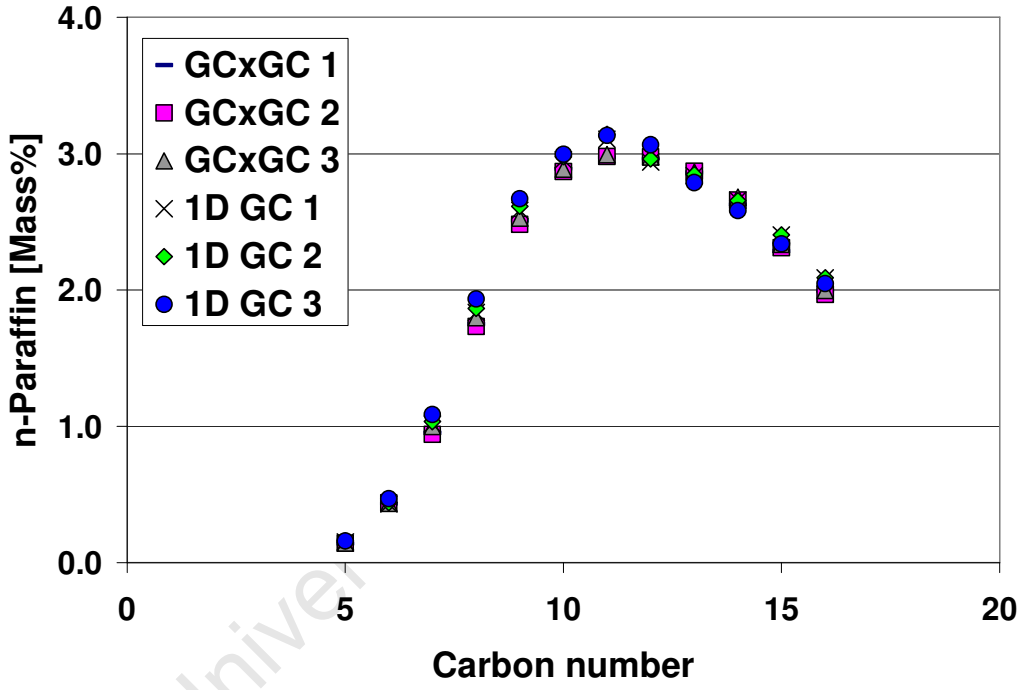

Figure 4.5: Comparing the quantification of n-paraffins in the oil product of the Fischer-Tropsch synthesis (range C_5 to C_{16}) using 1D GC and GCxGC

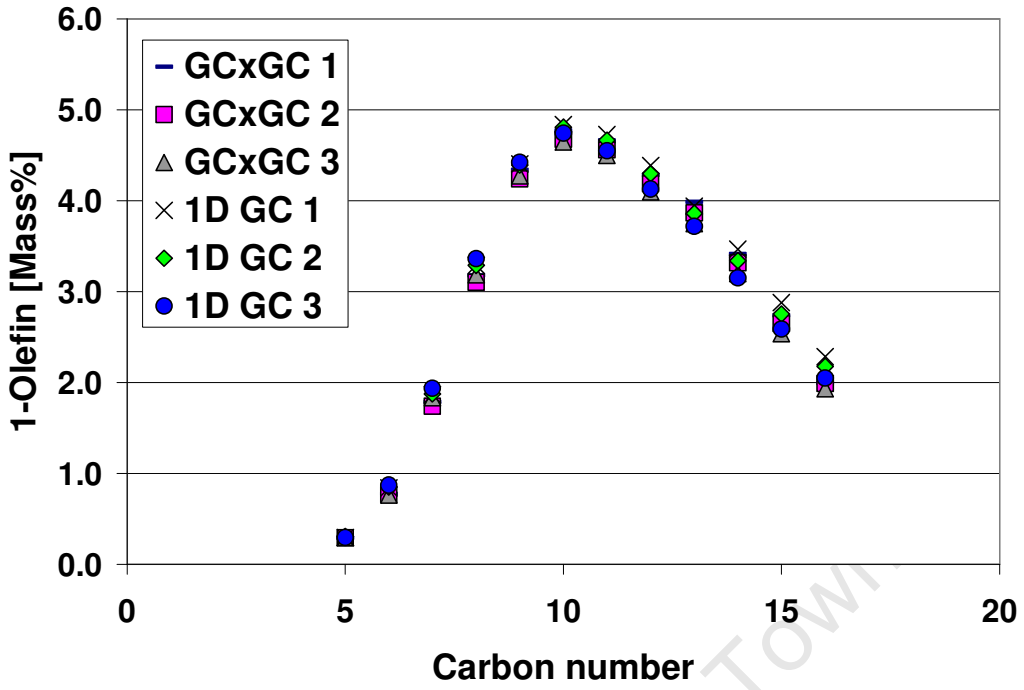

Figure 4.6: Comparing the quantification of 1-olefins in the oil product of the Fischer-Tropsch synthesis (range C_5 to C_{16}) using 1D GC and GCxGC

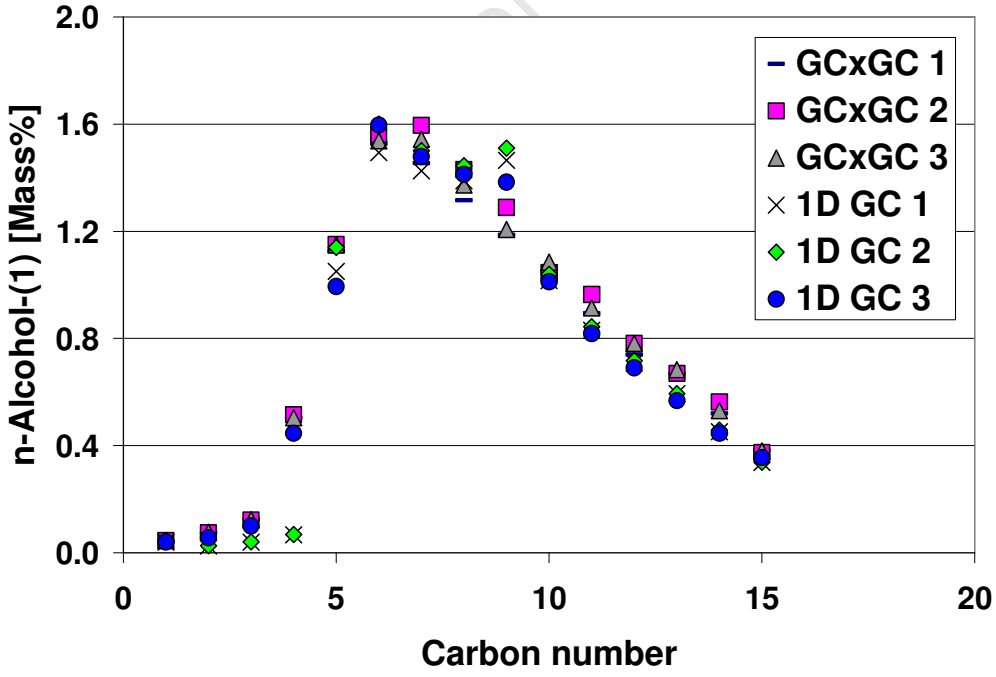

Figure 4.7: Comparing the quantification of n-alcohols-(1) in the oil product of the Fischer-Tropsch synthesis (range C_1 to C_{15}) using 1D GC and GCxGC

Linear carboxylic acids in the oil product of the Fischer-Tropsch synthesis are not separated on the 1D GC, and hence the amount of linear carboxylic acids in the oil products could not be evaluated using this technique. These compounds could be separated from the other compounds in the mixture and quantified using the GCxGC. Therefore only the GCxGC results are displayed in Figure 4.8.

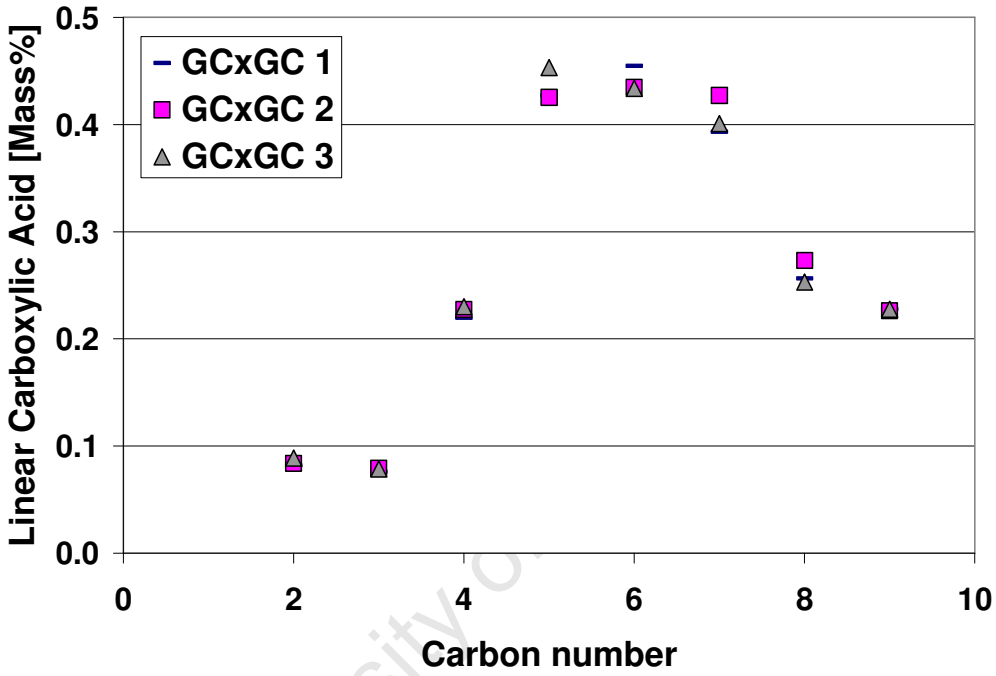

Figure 4.8: Quantification of linear carboxylic acids in the oil product of the Fischer-Tropsch synthesis using GCxGC

Ketones ranging from C_3 – C_9 were separated and detected on the GCxGC but on the 1D GC only the C_3 and C_4 ketones were detected (see Figure 4.9). In Figure 4.10 the detection of the aldehydes on the GCxGC are displayed. On the 1D GC aldehydes were not detected.

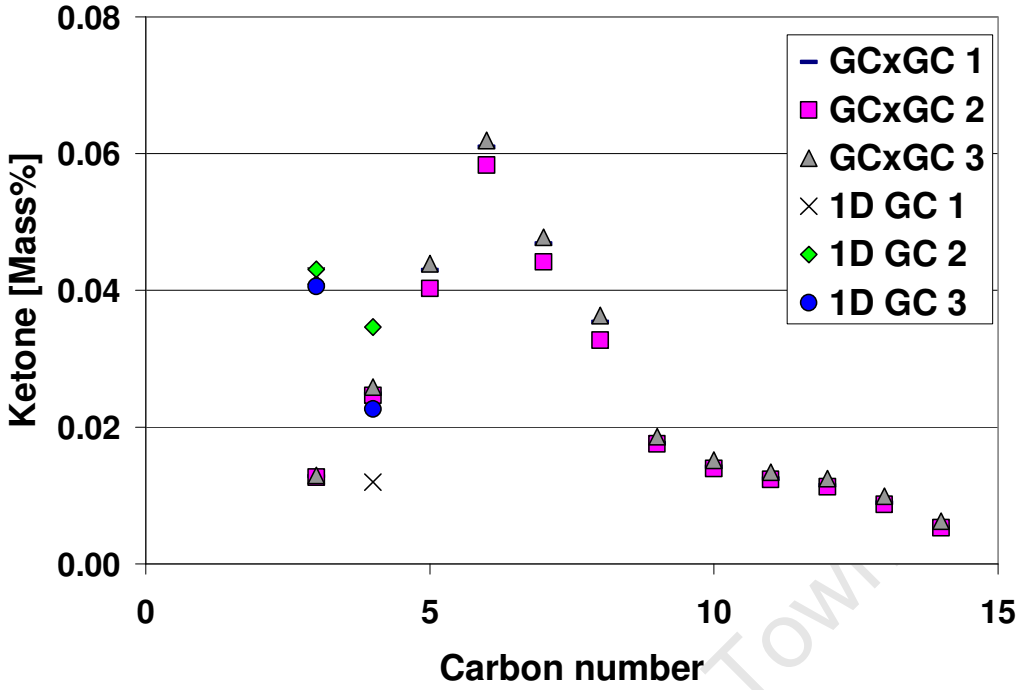

Figure 4.9: Comparing the quantification of ketones in the oil product of the Fischer-Tropsch synthesis using 1D GC and GCxGC

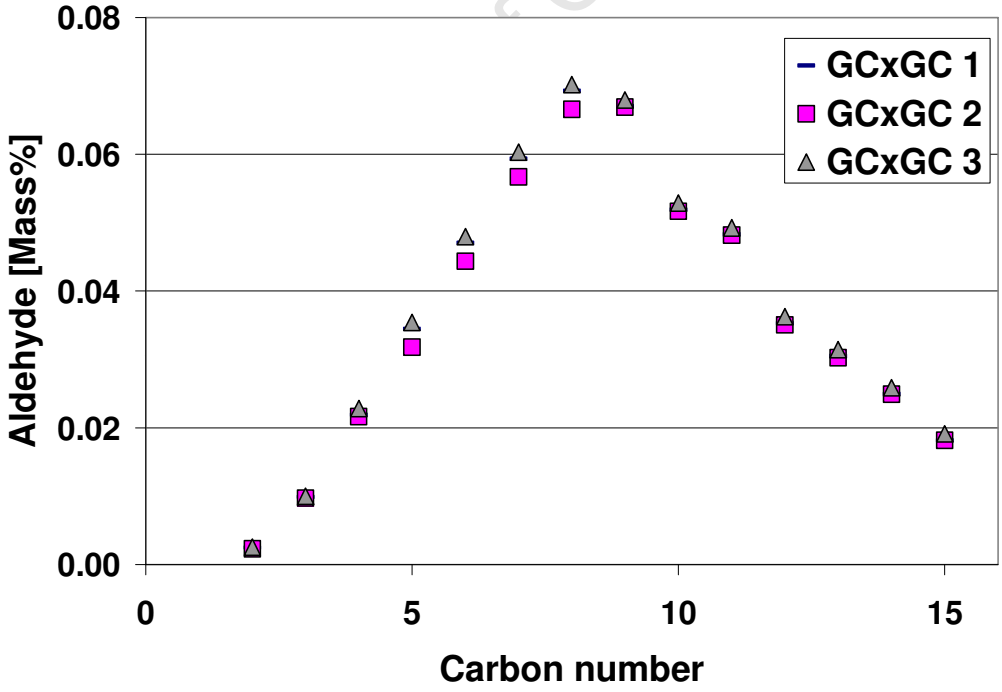

Figure 4.10: Quantification of aldehydes in the oil product of the Fischer-Tropsch synthesis using GCxGC

Other minor compounds such as n-alcohols-(2), branched alcohols, branched acids, internal olefins, branched olefins and branched paraffins

were also detected using the GCxGC. Sufficient separation could not be achieved on the 1D GC for some of these compounds. Table 4.6 presents the total concentration of the hydrocarbons (ranging between C_1 – C_{16}), detected using 1D GC and GCxGC. The accuracy level with which the 1D GC and GCxGC methods can determine these compounds is also indicated in this table.

It is evident from the above results that when comparing the total product distribution obtained from GCxGC and 1D GC methods, one can expect to get a more complete picture of the product distributions for the aldehydes, ketones, acids, branched compounds, etc. when using GCxGC methods.

Table 4.6: Accuracy of 1D GC and GCxGC systems with the analyses of compounds within the oil product of the Fischer-Tropsch synthesis (*Note these selectivities are fractions of the oil product which ranges from C_1 to C_{30} and will not count up to a 100% for only the C_1 to C_{16} range of this product are used for the discussion)*

Compound classes	GCxGC [Mass%]	1D GC [Mass%]
n-Paraffins (C_5 - C_{16})	25 ± 0.48	25 ± 0.42
Branched Paraffins (C_6 - C_{16})	2 ± 0.25	-
1-Olefins (C_5 - C_{16})	36 ± 1.98	36 ± 2.23
Internal Olefins (C_6 - C_{16})	2 ± 0.15	2 ± 0.34
Branched Olefins (C_6 - C_{16})	2 ± 0.22	-
Branched olefins and paraffins (C_6 - C_{16})	4 ± 0.37	3 ± 0.75
n-Alcohols-(1) (C_1 - C_{15})	12 ± 0.90	11 ± 0.83
n-Alcohols-(2) (C_3 - C_{13})	0.2 ± 0.05	-
Branched Alcohols (C_4 - C_{15})	2 ± 0.21	-
Ketones (C_3 - C_{14})	0.3 ± 0.04	-
Aldehydes (C_3 - C_{16})	0.5 ± 0.04	-
Linear Carboxylic Acids (C_2 - C_9)	2 ± 0.07	-
Branched acids (C_4 - C_9)	1 ± 0.04	-

4.3 ANALYSIS OF FISCHER-TROPSCH PRODUCT DISTRIBUTIONS USING GCXGC

4.3.1. Overview of experiments

4.3.1.1. Overview of Fischer-Tropsch synthesis at different operating temperature

In Table 4.7 the performance data, after ca. 225 hours on stream, for the Fischer-Tropsch synthesis runs performed at different temperatures are displayed. During all the runs the H_2/CO feed ratios and total pressure were kept constant through out the runs. The CO + CO_2 conversion was kept constant by changing the space velocity. The reactor temperature was changed to 225ºC, 245 ºC and 265 ºC after ca. 100 hours.

Table 4.7: Quantitative comparison of results obtained from Fischer-Tropsch synthesis runs at 225ºC, 245ºC and 265ºC after ca. 225 hours on stream

Temperature	**225ºC**	**245ºC**	**265ºC**
Fischer-Tropsch Reaction rate [µmol CO/g-cat/s]	5.5	10	24
Water Gas Shift Reaction rate [µmol CO_2/g-cat/s]	1.4	2.3	7.2
GHSV syngas [ml(STP)/g-cat/h]	4797	9800	18843
CH_4 Selectivity [% C atom]	2.21	4.01	5.23
C_{10+} Selectivity [% C atom]	81.91	65.43	55.7

4.3.1.2. Overview of Fischer-Tropsch synthesis runs at different H_2/CO feed ratios

In Table 4.8 the performance data, after ca. 190 hours on stream, for the Fischer-Tropsch synthesis runs performed at different H_2/CO feed ratios are displayed. During all the runs the reactor temperature and total pressure

were kept constant through out the runs. The CO + CO_2 conversion was kept constant by changing the space velocity. Only the H_2/CO feed ratio was changed to 1.3, 1.6 and 2.1 after ca. 100 hours on line. In the sections to follow data collected after 190 hours on stream will be used for discussion.

Table 4.8: Quantitative comparison of results obtained from Fischer-Tropsch synthesis runs at H_2/CO feed ratios of 1.3, 1.6 and 2.1 after ca. 190 hours on stream

H_2/CO feed ratio	**1.3**	**1.6**	**2.1**
Fischer-Tropsch Reaction rate [µmol CO/g-cat/s]	6.3	10	12
Water Gas Shift Reaction rate [µmol CO_2/g-cat/s]	3.0	2.7	2.2
GHSV syngas [ml (STP)/g-cat/h]	4107	9800	14519
CH_4 Selectivity [% C atom]	2.98	4.01	6.20
C_{10+} Selectivity [% C atom]	79.40	65.43	68.69

4.3.2. Overall product distribution as a function of carbon number

The product formed during Fischer-Tropsch product synthesis consist of a variety of products of different chain length and functionality. The composition of the product distribution depends on many reaction variables such as reactor conditions, the reactor system used as well as the type of catalyst and the physical properties thereof (Claeys and Van Steen, 2004). The Fischer-Tropsch synthesis product consists mainly of 1-olefins, n-paraffins, n-alcohols-(1) and minor concentrations of other oxygenated and branched compounds.

For this study Fischer-Tropsch runs were performed at different temperatures and H_2/CO feed ratios. On a daily basis Fischer-Tropsch products were sampled and analyzed. Flow rates of compounds from the hot tail gas, oil and wax product were determined and combined using equations as described in Table 4.9. Small errors in the mass of the

products collected or in the flow rates of the gasses may account for larger deviations in the product distributions especially at $C_8 – C_{11}$ and $C_{23} – C_{27}$ where the products are calculated (merged) together to form a total distribution.

Table 4.9: Equations for combining the flow rates of compounds detected in various products to form a total hydrocarbon distribution of the Fischer-Tropsch synthesis product

Product Range	Equation
$C_1 – C_9$	$\mathbf{C_i = C_{hot\ tail} – C_{feed}}$
$C_{10} – C_{25}$	$\mathbf{C_i = C_{oil} + C_{wax}}$
C_{26+}	$\mathbf{C_i = C_{wax}}$

In order to characterize the Fischer-Tropsch product distributions, formulated using the above method, Anderson-Schulz-Flory (ASF) plots were constructed of the product distributions (see Figures 4.11 and 4.12). A negative deviation for the C_2 fraction of the product is observed. This is consistent with the deviations observed by Schulz and Claeys (1999). In contrast with the typical observed model deviations, a positive C_1 deviation is not observed. However when evaluating only the n-paraffin functionality of the Fischer-Tropsch product (see Figures 4.13 and 4.14), the positive C_1 deviation is evident and in apparent agreement with the proposal by Schulz et al. (2002) that methane is specifically responsible for the observed deviation.

The ASF plots for the 1-olefin functionality is also shown in Figures 4.13 and 4.14 which clearly indicate that the source of the C_2 model deviation may be attributed to the high reactivity of ethylene, as described by Schulz and Claeys (1999).

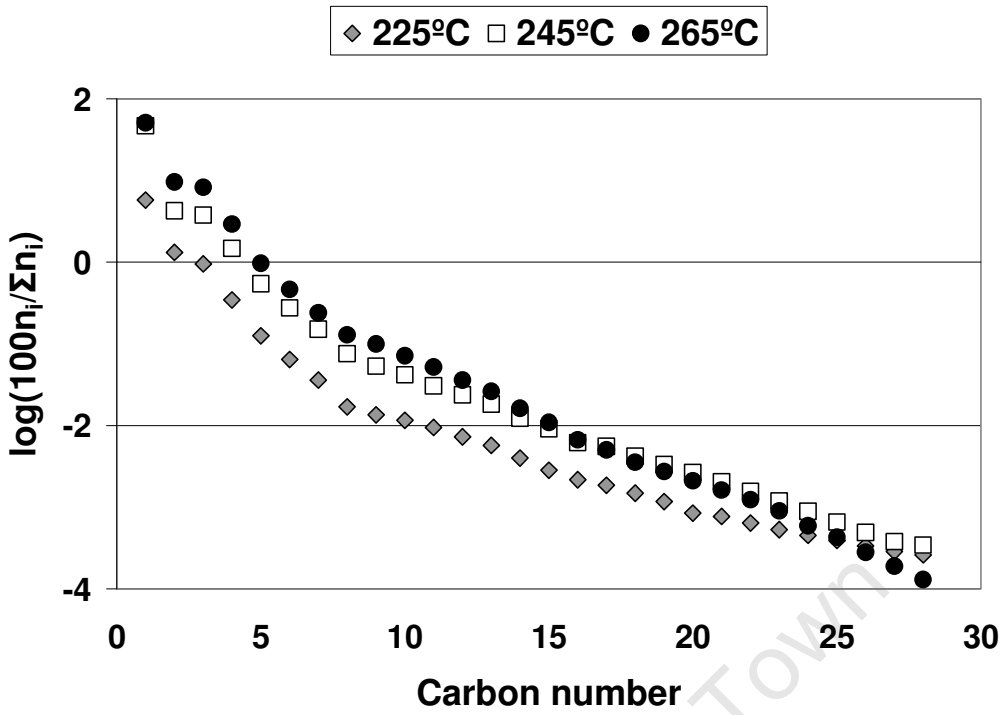

Figure 4.11: Anderson-Schulz-Flory plots of the product of the Fischer-Tropsch synthesis from C_1 to C_{28} for the experiments performed at 225ºC, 245ºC and 265ºC

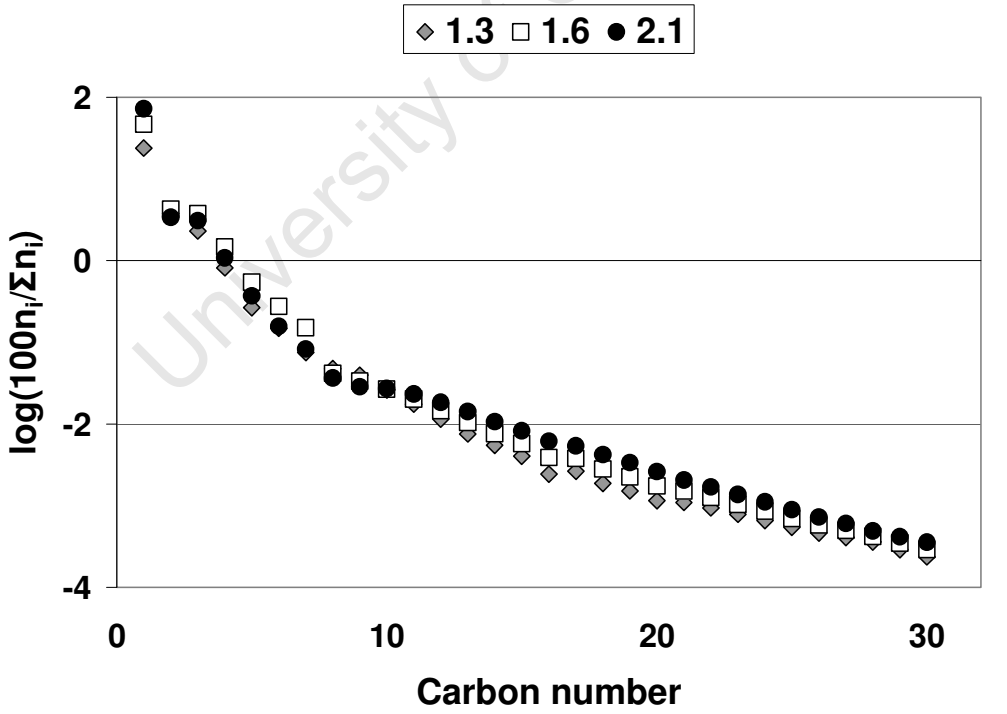

Figure 4.12: Anderson-Schulz-Flory plots of the product of the Fischer-Tropsch synthesis from C_1 to C_{30} for the experiments performed at H_2/CO feed ratios of 1.3, 1.6 and 2.1

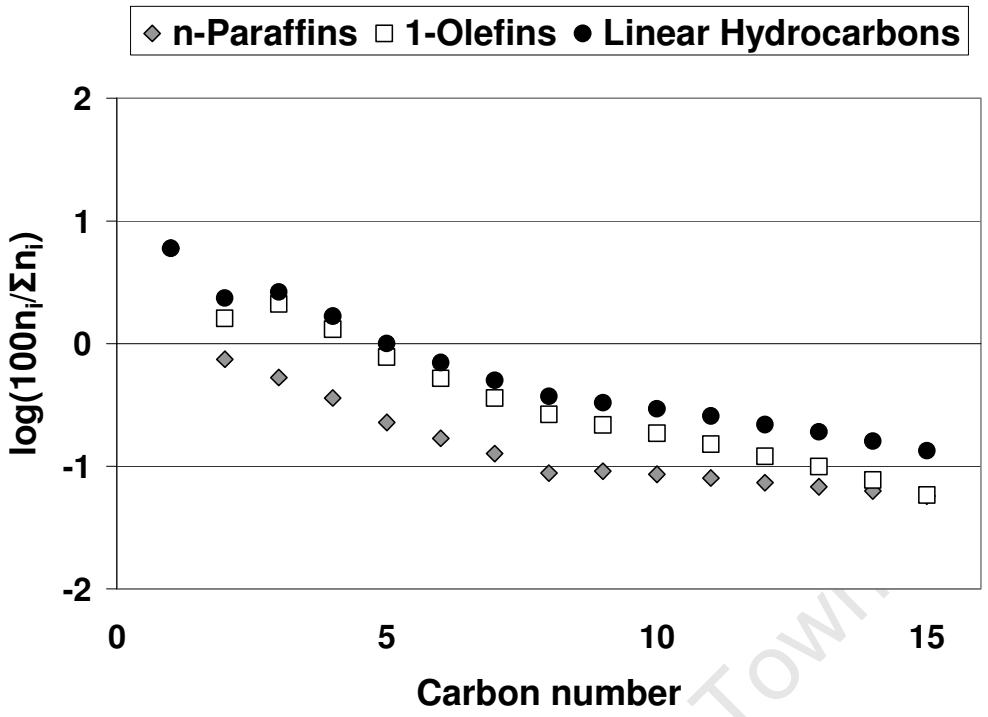

Figure 4.13: Anderson-Schulz-Flory plots for the C_1 to C_{15} n-paraffins, 1-olefins and linear hydrocarbons (T = 265ºC)

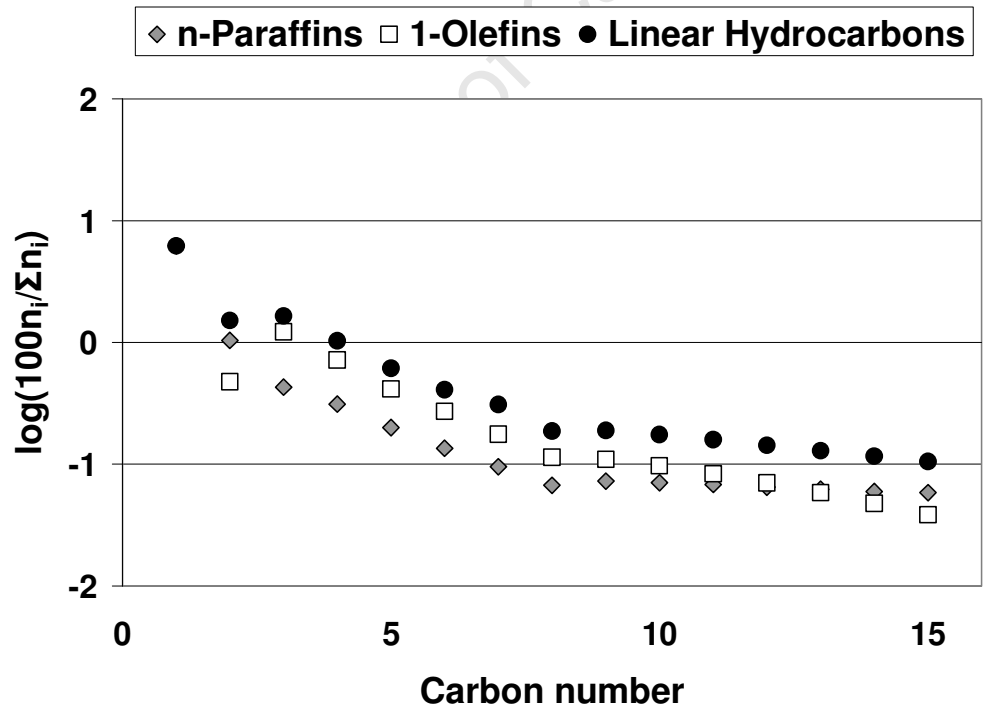

Figure 4.14: Anderson-Schulz-Flory plots for the C_1 to C_{15} n-paraffins, 1-olefins and linear hydrocarbons (H_2/CO feed ratio = 2.1)

If one assumes that an ideal polymerisation mechanism is responsible for the formation of the Fischer-Tropsch products, a single value can be

obtained from the ASF plots which is known as the chain growth probability or α. The significance of the α-value is that the entire product spectrum can be calculated from this value.

In Table 4.10 and 4.11 the chain growth probabilities (α- values) are displayed for the product cuts obtained from Fischer-Tropsch synthesis at different temperatures (225ºC, 245ºC and 265ºC) and different H_2/CO feed ratios (1.3, 1.6 and 2.1). In Table 4.10 the α-values for the 265ºC Fischer-Tropsch synthesis run appear to be lower. This is in accordance with observations in literature (Dry, 2004), that at higher temperatures the α-values of the product distribution would we lower. One explanation for this observation is that at higher synthesis temperatures, the rate of desorption increases thus restraining surface species growth and producing light products (Dry, 2004).

Table 4.10: Chain growth probabilities (α- values) for the total hydrocarbon product calculated over various product cuts for the Fischer-Tropsch synthesis runs performed at different temperatures

Temperature	C_3-C_7	C_{10}-C_{20}	C_{20}-C_{28}
225ºC	0.70	0.89	0.94
245ºC	0.70	0.89	0.89
265ºC	0.68	0.85	0.86

According to literature (Dry, 2004) at higher H_2/CO feed ratios the probability of chain termination is higher which should lead to a lighter product spectrum. Therefore one would expect lower α-values for the product distributions of Fischer-Tropsch synthesis runs at higher H_2/CO feed ratios. In Table 4.11 the α-values for the C_3 to C_7 product cut appears to decrease but for the rest of the product cuts the α- values appear to stay the same as H_2/CO feed ratio varies.

Table 4.11: Chain growth probabilities (α- values) for the total hydrocarbon product calculated over various product cuts for the Fischer-Tropsch synthesis runs performed at different H_2/CO feed ratios

H_2/CO feed ratio	C_3-C_7	C_{10}-C_{20}	C_{20}-C_{28}
1.3	0.75	0.88	0.94
1.6	0.70	0.88	0.93
2.1	0.67	0.89	0.94

4.3.3. Olefin Formation

Linear 1-olefins and linear paraffins are the main primary products produced in the Fischer-Tropsch synthesis. These compounds are believed to be formed by desorption of a terminally bonded surface alkyl species either via β-hydrogen abstraction to form the olefin or via associative hydrogen addition to form the paraffin (Claeys and Van Steen, 2004; see Scheme 4.1).

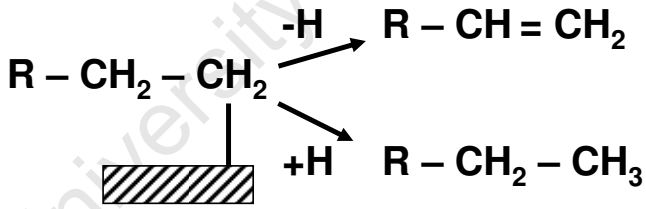

Scheme 4.1: Kinetic scheme of the desorption of a alkyl surface species for the primary formation of 1-olefins and n-paraffins (Claeys and Van Steen, 2004)

The olefin content in the fraction of linear hydrocarbons (see Figures 4.15 and 4.16) is above 60% for the range C_2-C_8 in the products collected during the runs at different temperatures and H_2/CO feed ratios. The olefin content in the fraction of linear hydrocarbons decreases with increasing carbon number (from C_3 onwards). Such high olefin selectivities were also observed by Schulz and Gökcebay (1984). This may be an indication that

the rate of desorption to form an olefin is faster than the rate of desorption to from a paraffin. 1-Olefins may also undergo secondary reactions such as: hydrogenation to form an n-paraffin, incorporation into growing chains or the formation of olefins with internal double bonds via double bond shift (Iglesia et al., 1993; Schulz and Claeys, 1999), which can explain the decrease in linear olefin selectivity as the carbon number increases. See Scheme 4.2 for a graphical presentation of the secondary reactions.

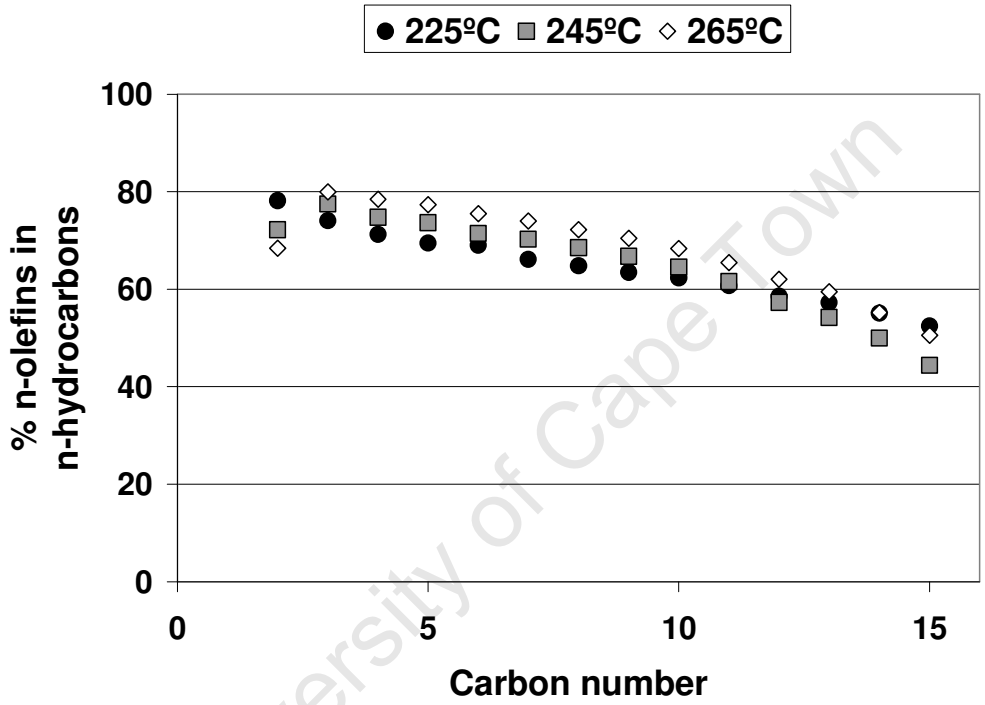

Figure 4.15: Olefin content in the fraction of linear hydrocarbons (C_2 to C_{15}) for the experiments performed at 225ºC, 245ºC and 265ºC

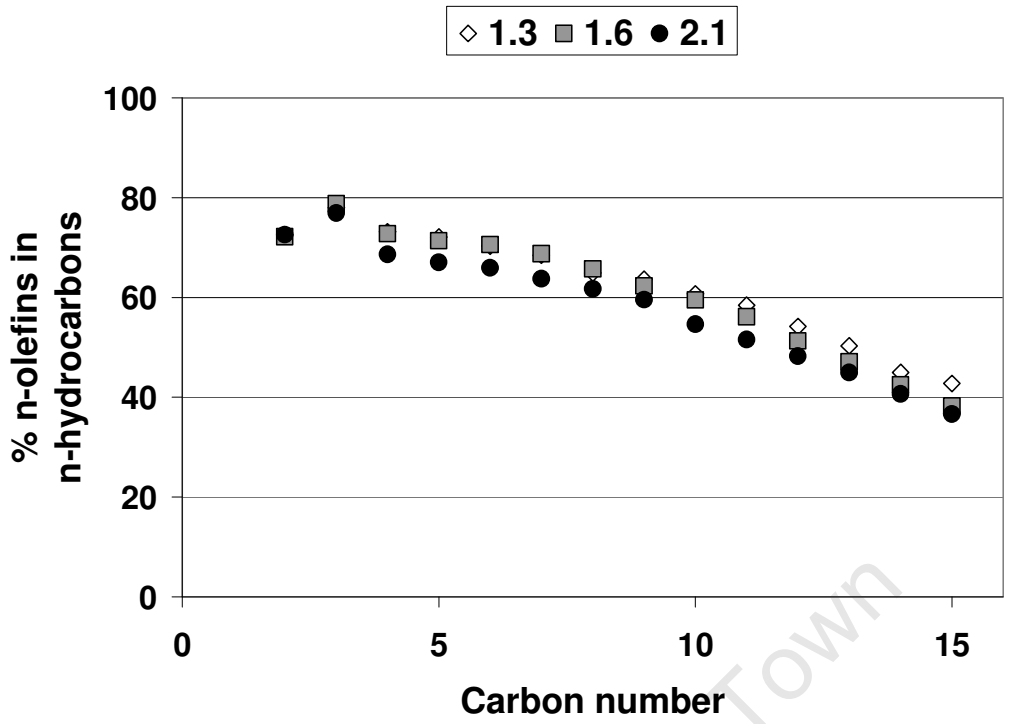

Figure 4.16: Olefin content in the fraction of linear hydrocarbons (C_2 to C_{15}) for experiments performed at H_2/CO feed ratios of 1.3, 1.6 and 2.1

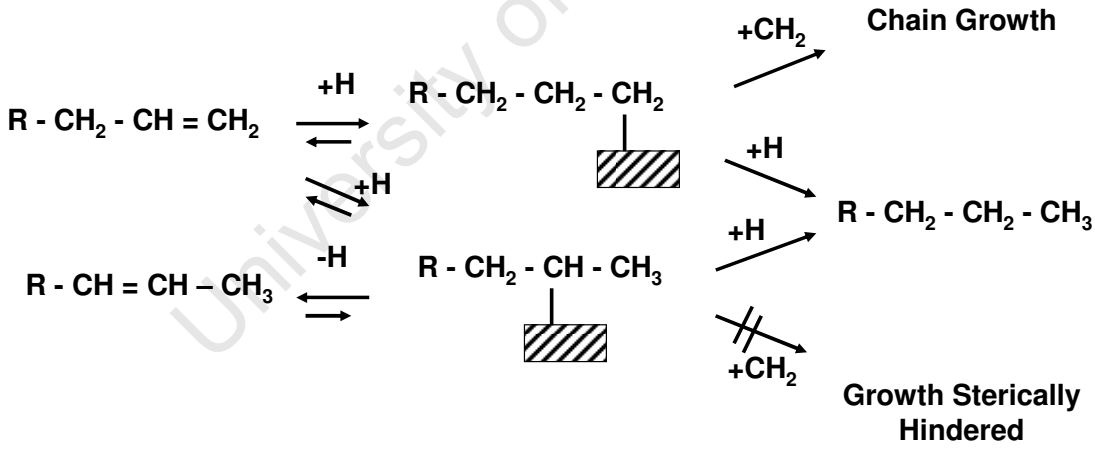

Scheme 4.2: Kinetic scheme of main secondary reactions that olefins may undergo during the Fischer-Tropsch synthesis (Claeys and Van Steen, 2004)

In Figures 4.17 and 4.18 the 1-olefin content in the fraction of linear olefins as a function of carbon number is displayed for the various runs. The 1-olefin content decreases with increasing carbon number, thus showing the

carbon number dependency of the formation of 1-olefins and internal olefins.

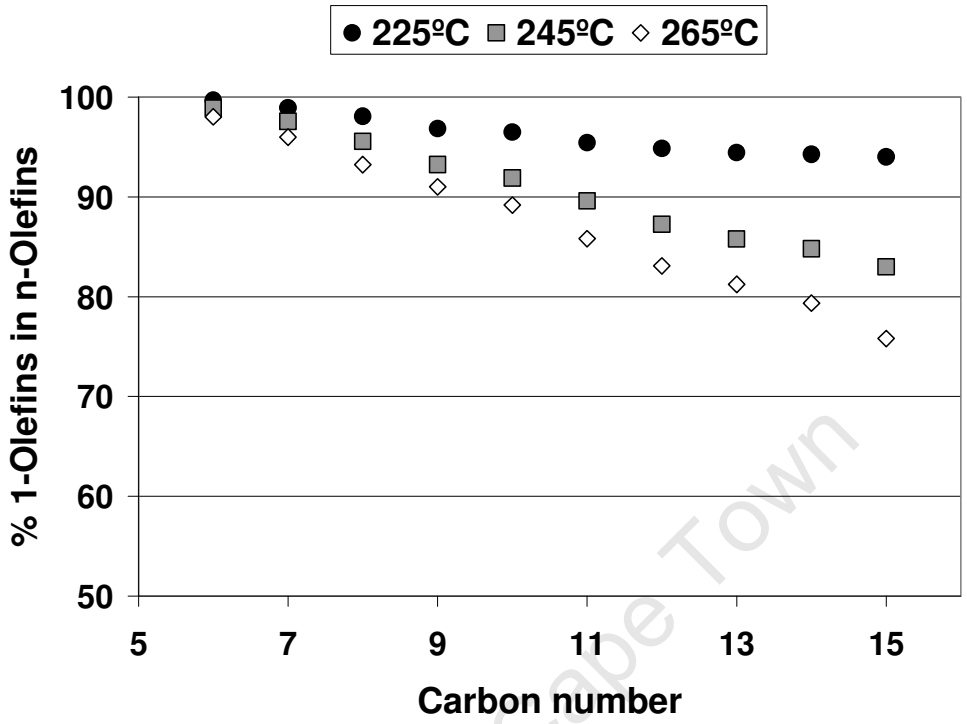

Figure 4.17: 1-Olefin content in the fraction of linear olefins as a function of carbon number (C_6 to C_{15}) for experiments performed at 225ºC, 245ºC and 265ºC

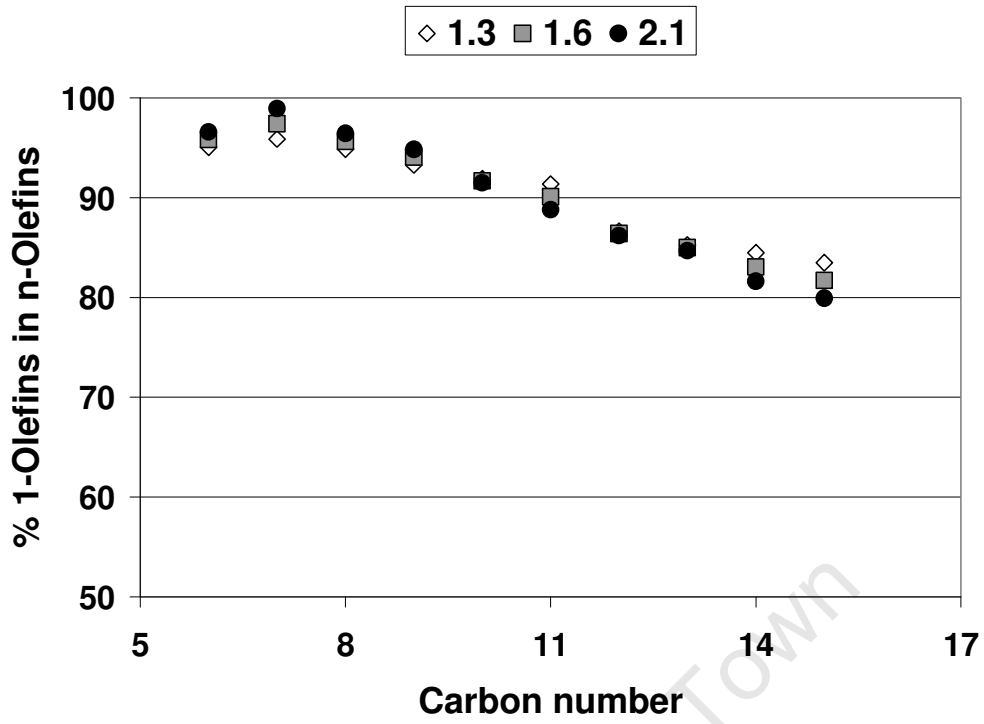

Figure 4.18: 1-Olefin content in the fraction of linear olefins as a function of carbon number (C_6 to C_{15}) for experiments performed with H_2/CO feed ratios of 1.3, 1.6 and 2.1

4.3.4. Formation of Oxygenates

Oxygenates formed in the Fischer-Tropsch synthesis are mainly n-alcohols-(1) and to a smaller extent aldehydes, acids, ketones, secondary alcohols and branched oxygenated products. Little is know about the primary and secondary formation routes of these compounds but some researchers have proposed mechanisms that may account for their formation.

Pichler and Schulz (1970) proposed that the primary formation of alcohols and aldehydes may originate from oxygen containing surface species, formed via CO insertion into an alkyl-metal bond (see section 2.1.4.4). Johnston and Joyner (1993) postulated that the same oxygen containing surface species might be formed via the addition of a hydroxyl group to an alkylidene species (see Scheme 4.3). The desorption would then result in the formation of alcohols or aldehydes.

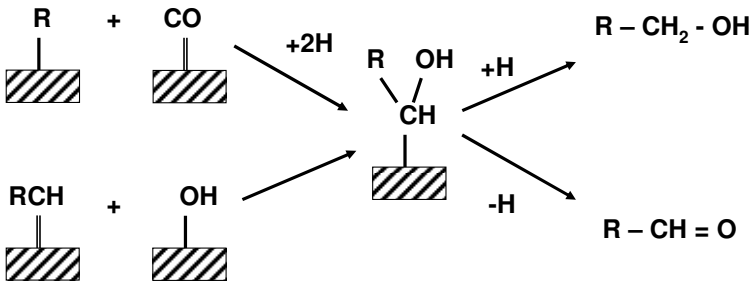

Scheme 4.3: Proposed formation routes of oxygenates in Fischer-Tropsch synthesis (Johnston and Joyner, 1993)

.

Schulz et al. (1990) noted the primary character of linear alcohols and aldehydes by comparison of the ASF plots of the hydrocarbons with the ASF plots of the alcohols and aldehydes. The observed parallel lines suggested that these components were also formed via a primary product formation route and not via secondary reactions.

Oxygenates can just like olefins re-adsorb on a catalyst surface and undergo further secondary reactions (Davis et al.,1990) which might, in addition to olefins, also impact on the deviation from ideal ASF distributions

For this study, ASF plots were constructed of the linear products, linear hydrocarbons and linear oxygenates (n-alcohols-(1), aldehydes and linear carboxylic acids). Figure 4.19 presents the ASF plots of product collected from the Fischer-Tropsch synthesis performed at 265ºC and Figure 4.20 presents the ASF plots of product collected from the Fischer-Tropsch synthesis performed with a H_2/CO feed ratio of 2.1.

In both figures the ASF plots for the linear oxygenates and the linear hydrocarbons appear to be parallel, indicating that the n-alcohols-(1), linear carboxylic acids and aldehydes possibly also form via a primary route as suggested above and may even form via the same route as the olefins and paraffins. It should however be noted that ASF distributions are semi-logarithmic plots and although it is in principle correct to draw these

conclusions on the parallel behaviour of the plots, it should be noted that these ASF plots may hide some details.

A deviation form the linear oxygenate ASF distribution is noted at C_2. This may be an indication that the rate of desorption to form a C_2 oxygenate is must faster than the rate of propagation to form C_{3+} oxygenates (see Scheme 4.4; Claeys and Van Steen, 2004).

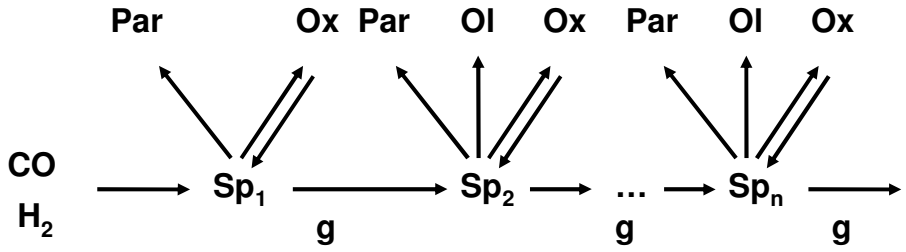

Scheme 4.4: Proposed kinetic scheme accounting for the formation of paraffins, olefins and oxygenates and their re-adsorption (Claeys and Van Steen, 2004)

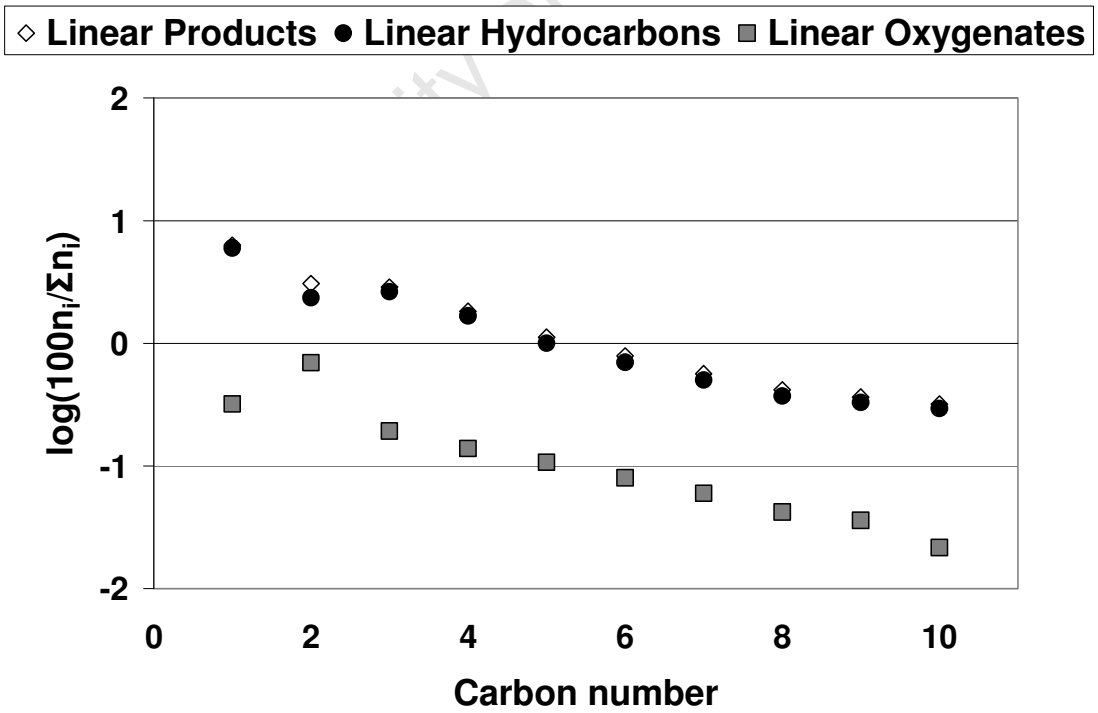

Figure 4.19: Anderson-Schulz-Flory plots for the C_1 to C_{10} linear products, linear hydrocarbons and linear oxygenates (T = 265ºC)

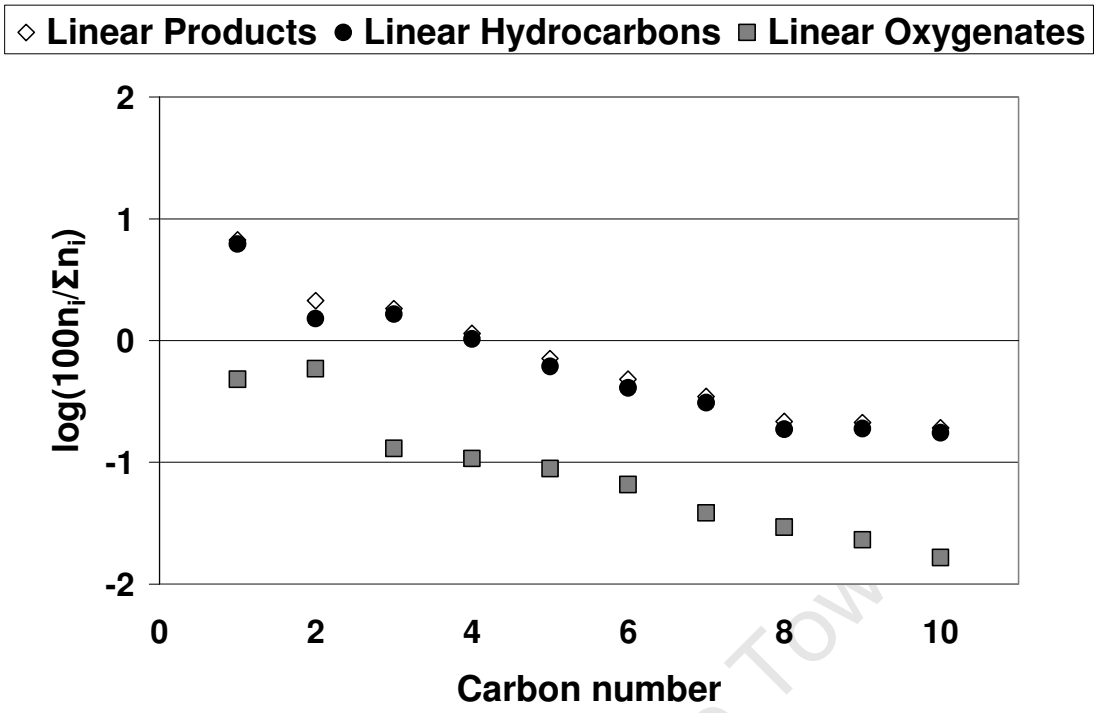

Figure 4.20: Anderson-Schulz-Flory plots for the C_1 to C_{10} linear products, linear hydrocarbons and linear oxygenates (H_2/CO feed ratio = 2.1)

ASF plots were also constructed for the linear products, linear hydrocarbons and the ketones plus n-alcohol-(2) products. Figure 4.21 presents the ASF plots of product collected from a Fischer-Tropsch synthesis run at 265ºC and Figure 4.22 presents the ASF plots of product collected from a synthesis run at a H_2/CO feed ratio of 2.1.

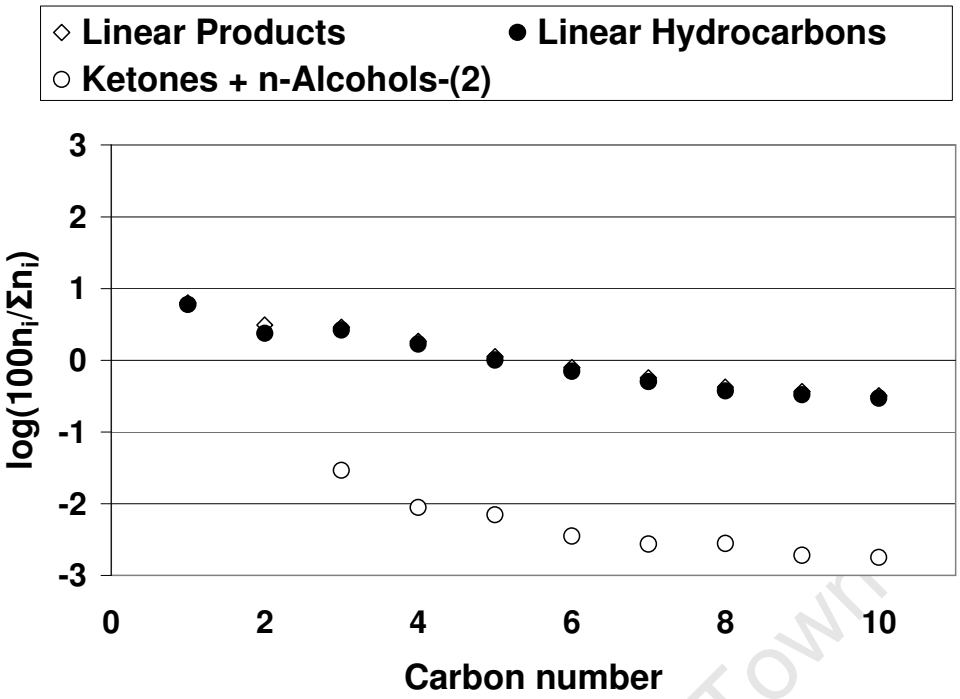

Figure 4.21: Anderson-Schulz-Flory plots for the C_1 to C_{10} linear products, linear hydrocarbons and ketones + n-alcohols-(2) (T = 265ºC)

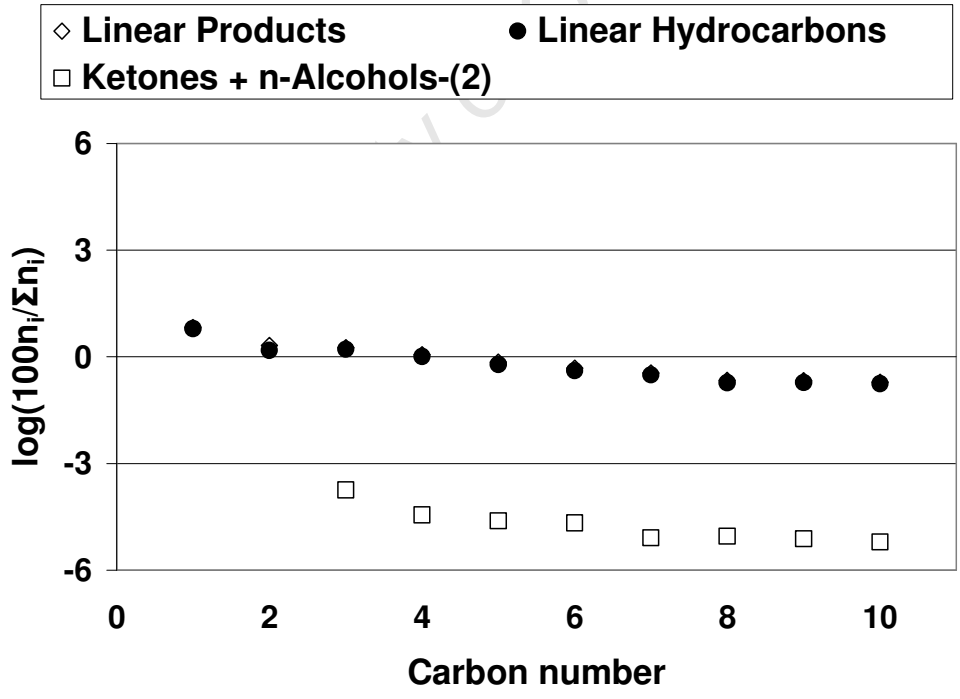

Figure 4.22: Anderson-Schulz-Flory plots for the C_1 to C_{10} linear products, linear hydrocarbons and ketones + n-alcohols-(2) (H_2/CO feed ratio = 2.1)

The ASF plot for the ketones + n-alcohols-(2) appears to be parallel to the linear product and linear hydrocarbon ASF plots, except for the C_3-product. This may indicate that ketones too may form via a primary route but at a very slow rate in comparison to the other products. Ketones can also form via a secondary route, namely ketonisation, as presented in equation 4.1. This is especially viable at high process temperatures for the Fischer-Tropsch synthesis (Dry, 2004).

$$acid \leftrightarrow ketone + CO_2 + H_2O \quad (4.1)$$

Ketones can also undergoing secondary reactions to form secondary alcohols (Dry, 2004; see equation 4.2). This will be discussed further in Chapter 5 section 5.2.

4.3.5. Formation of Branched products

The amount of branched compounds produced during low temperature Fischer-Tropsch synthesis is very low. Mainly mono-methyl branched compounds are formed (Claeys and Van Steen, 2004).

It is believed that the formation of branched products occur when a surface alkyl species bonds to the catalyst surface with the second last carbon atom as displayed in Scheme 4.5 (Schulz, 1990). This may proceed via both primary and secondary routes. The secondary route includes olefin re-adsorption and has been proven experimentally (Schulz et al., 1970).

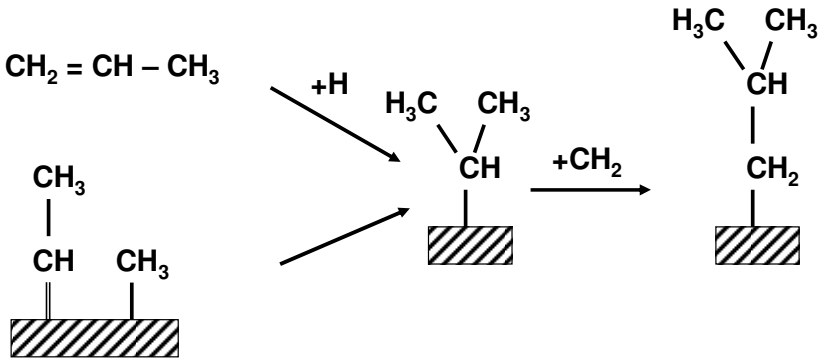

Scheme 4.5: Proposed reaction pathways for the formation of branched hydrocarbons in the Fischer-Tropsch synthesis according to Schulz et al. (1990)

ASF plots of the n-paraffins, 1-olefins, n-alcohols-(1) and their branched counterparts were constructed for the product collected from a Fischer-Tropsch synthesis run performed at 265ºC and a run at a H_2/CO feed ratio of 2.1 respectively (Figures 4.23 to 4.28). The ASF plot lines for the branched products are parallel to their linear counterparts indicating that branched products may also be formed via a primary reaction, but the Fischer-Tropsch mechanism favours the formation of linear products over the formation of branched products therefore resulting in low concentrations of branched products present in the Fischer-Tropsch product.

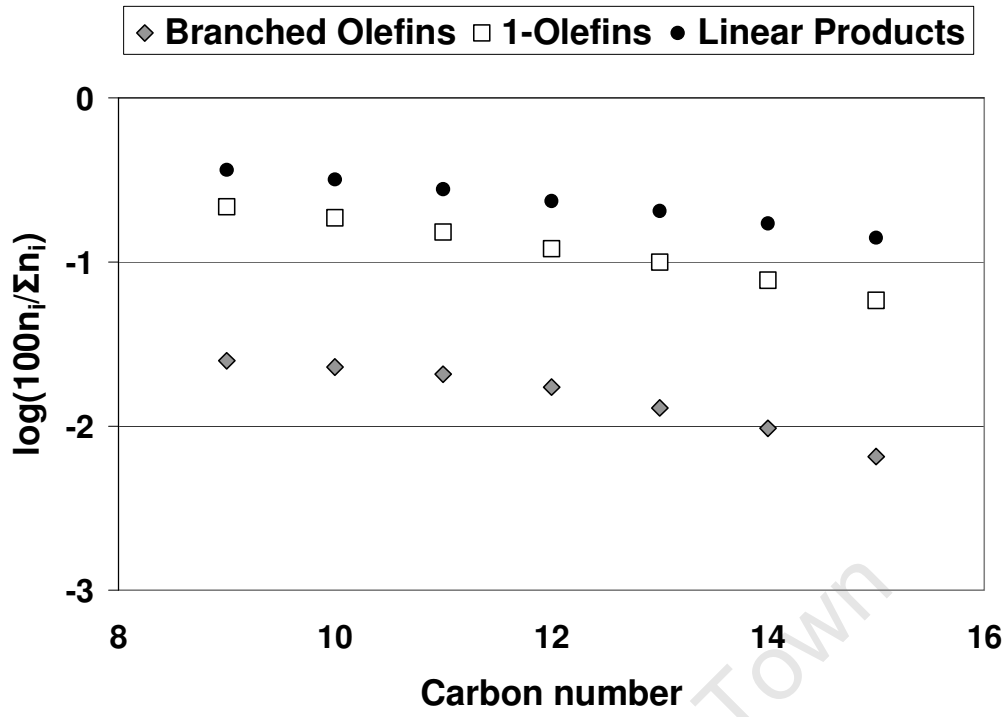

Figure 4.23: ASF plots for the 1-olefins and branched olefins (C_9 to C_{15} product range) for the product distribution obtained from a Fischer-Tropsch run at 265ºC

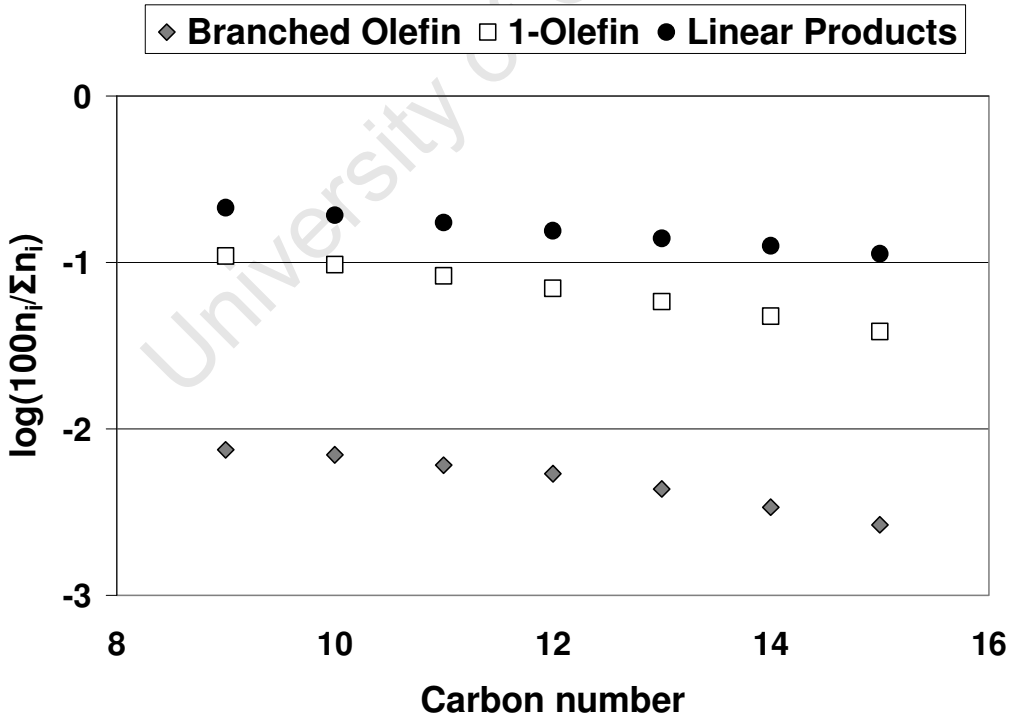

Figure 4.24: ASF plots for the 1-olefins and branched olefins (C_9 to C_{15} product range) for the product distribution obtained from a run at 2.1 H_2/CO feed ratio

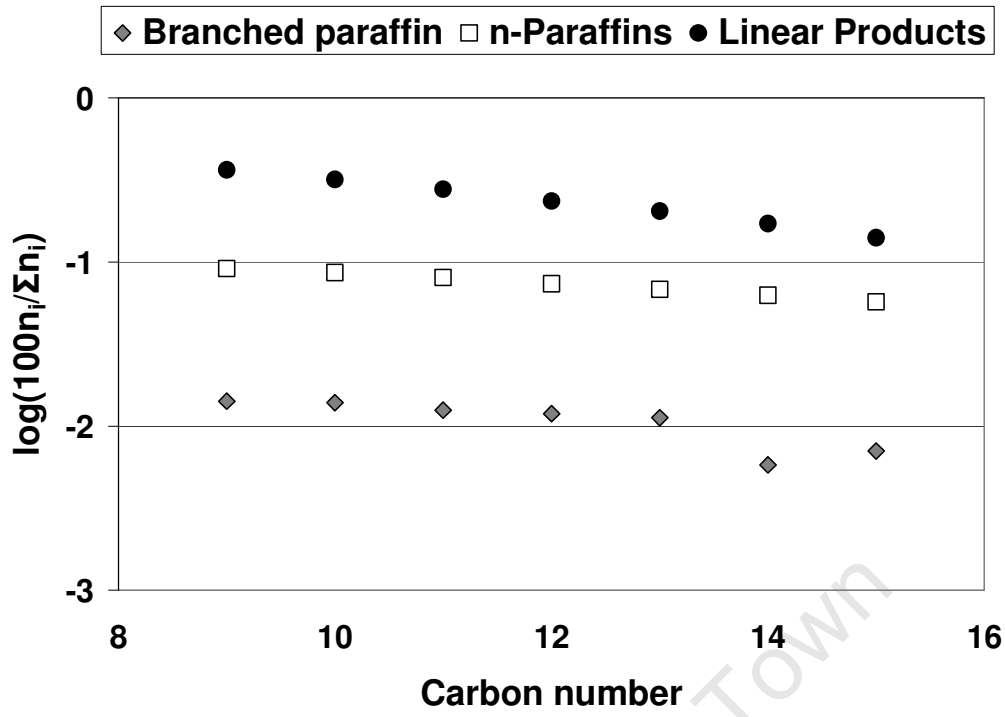

Figure 4.25: ASF plots for the n-paraffins and branched paraffins (C_9 to C_{15} product range) for the product distribution obtained from a run at 265ºC

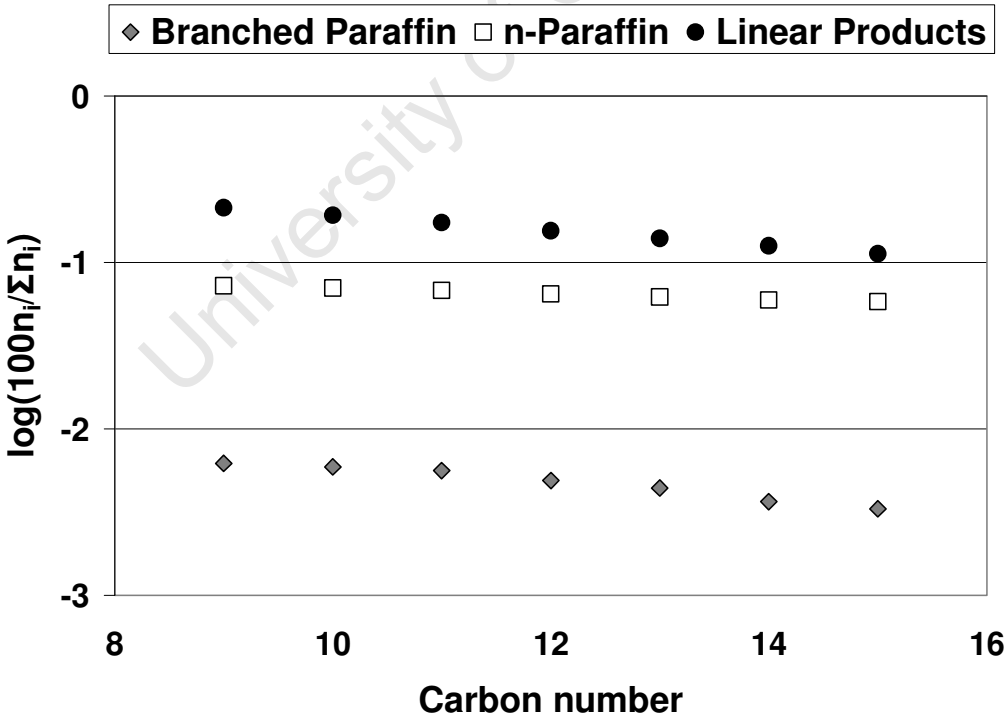

Figure 4.26: ASF plots for the n-paraffins and branched paraffins (C_9 to C_{15} product range) for the product distribution obtained from a Fischer-Tropsch synthesis run at 2.1 H_2/CO feed

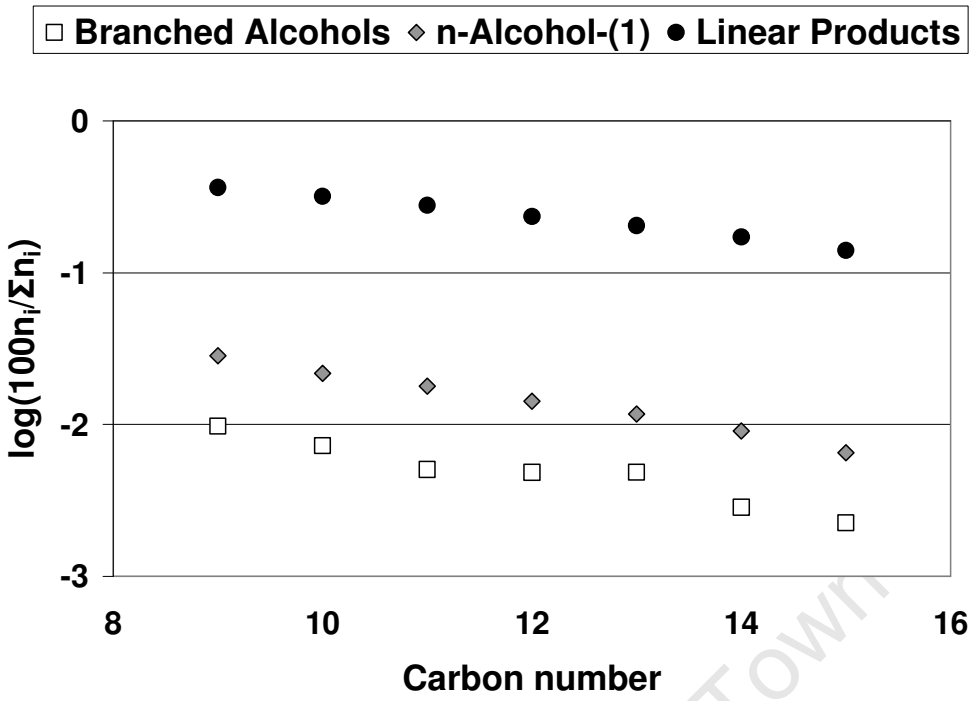

Figure 4.27: ASF plots for the n-alcohols-(1) and branched alcohols (C_9 to C_{15} product range) for the product distribution obtained from a run at 265ºC

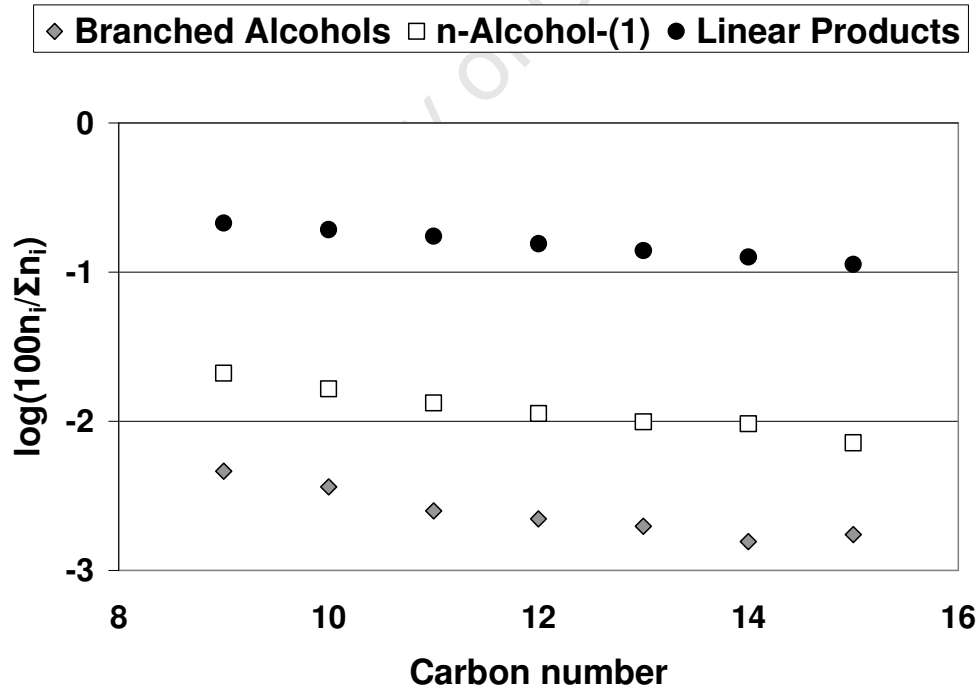

Figure 4.28: ASF plots for the n-alcohols-(1) and branched alcohols (C_9 to C_{15} product range) for the product distribution obtained from a Fischer-Tropsch run at 2.1 H_2/CO feed ratio

CHAPTER 5

DISCUSSION

The Fischer-Tropsch synthesis (FTS) process produces a huge variety of products of different chain lengths and different functionality. Although these products can be processed further to produce fuel and high value chemicals, it is known to be an expensive technology (Dry, 2002). Therefore it is necessary to optimize the Fischer-Tropsch synthesis process in such a way that as much as possible of the desired products are formed. This can be achieved by selecting the most suitable catalyst, reactor and operational conditions.

Over the years many researchers have researched the factors playing a role in the formation of certain products and compound functionality (Dry et al., 1981; Schulz, 1985; Liu et al., 2007). Many of them also tried to describe the full product spectrum (e.g. Donnelly and Satterfield, 1981; Friedel and Anderson, 1950). This however is not such a trivial task due to the complexity of the products. A true understanding of the product formation can only be obtained if the formation of all product compounds can be understood, also the trace compounds.

In the early years of Fischer-Tropsch research, scientists used various distillation and extraction methods (Weitkamp, et al., 1953) to divide the Fischer-Tropsch product up in fractions to define the individual functionalities. These methods in general were labour intensive, time consuming and usually only delivered information regarding major functionalities such as linear olefins, paraffins and alcohols ranging from C_1 to C_5, which were then extrapolated to get information regarding the product distribution of the heavier Fischer-Tropsch synthesis product. Some also reported information regarding the minor compounds such as acids, aldehydes and ketones, but most of the times these compounds were grouped together and reported as oxygenates (Weitkamp, et al., 1953; Dry, 2004).

Later when gas chromatography was introduced to the science world and the application potential thereof was realised, researchers used gas chromatography to separate the compounds in the Fischer-Tropsch synthesis product (Nijs and Jacobs, 1981; Dictor and Bell, 1984). Once again the detection and quantification of olefins, alcohols and paraffins was quite easy, but the separation of the oxygenated compounds, which normally co-elute with the major compounds, was not a trivial task. In many cases the reported oxygenated contents reflected only the selectivity obtained from the water fraction of the liquid product.

In recent years a new analytical technique, two-dimensional gas chromatography (GCxGC), has emerged which claims to provide improved separation and quantification of trace compounds within complex mixtures such as petrochemical samples (Dallüge et. al., 2003; Vendeuvre et. al., 2005). In some of the literature it also claims to present improved separation of minor compounds within the complex Fischer-Tropsch synthesis product (Vendeuvre et. al., 2004). If this is true then it may be possible to separate and quantify the oxygenated compounds from the rest of the product, especially within the complex oil product, and a more complete description of the Fischer-Tropsch product distribution may be achieved.

The aim of this study was to investigate if two-dimensional gas chromatography (GCxGC) really presents improved separation and identification of compounds in the complex Fischer-Tropsch product and will lead to a more complete product distribution especially of the minor compounds such as branched hydrocarbons, ketones, aldehydes and acids.

In order to test this hypothesis the following approach was followed. Firstly GCxGC methods were developed and the system was calibrated as discussed in Chapters 3 and 4. Thereafter a test sample (oil product from Fischer-Tropsch synthesis process) was injected several times into both the GCxGC and 1D GC systems. The purpose of this was to compare the detection ability and accuracy of the two instruments (see Chapter 4). From

these results it is clear that both GCxGC and 1D GC are suitable methods for the detection and quantification of n-paraffins, 1-olefins and n-alcohols-(1), but for the separation and detection of the minor compounds such as the acids, ketones, aldehydes, secondary alcohols and branched compounds, the performance of the GCxGC is far more superior.

5.1 THE BENEFITS OF GCXGC AS A TOOL FOR FT RESEARCH

To illustrate the benefits of GCxGC in relation to 1D GC for the analyses of Fischer-Tropsch products, Fischer-Tropsch synthesis experiments were conducted at various temperatures (225˚C, 245˚C and 265˚C) and H_2/CO feed ratios (1.3, 1.6 and 2.1). The products of these experiments were analyzed using both GCxGC and 1D GC and the results of all the Fischer-Tropsch products, including the tail gas, oil, water and wax products and the inlet gas (or fresh feed gas) were merged together as discussed in section 3.5.5 to determine the selectivity of the compounds (see equation 3.17 in section 3.5.4). It should be noted that the compounds detected, using gas chromatography, ranges from C_1 to approximately C_{80} and the selectivity of these compounds are expressed as a fraction of the total product produced during Fischer-Tropsch synthesis.

For the purpose of this discussion results from Fischer-Tropsch product samples (3 sets of product samples drained consecutively at stable conditions) from one of the Fischer-Tropsch synthesis runs at 225˚C will be used to illustrate the benefits of GCxGC in comparison to 1D GC. Also note that from the total products produced (C_1 to C_{80}), which adds up to a 100%; only the C_1 to C_{15} fraction was used for the discussion. Thus when adding up all the compound selectivities for the C_1 to C_{15} fraction it will not add up to a 100% but to approximately 30% because at least 70% of the low temperature Fischer-Tropsch product are high molecular weight product (product from C_{30+}).

The n-paraffin selectivity was determined by summing the linear paraffins detected in the Fischer-Tropsch gas product (C_1 to C_8) and the oil product (C_6 to C_{30}) together. In general the n-paraffin selectivity showed a good correlation between those obtained with the GCxGC and with the 1D GC techniques, except for the C_5 to C_8 product fraction (Figure 5.1). This is likely not associated with the capabilities of the two techniques to quantify the formation of n-paraffins, but with the calibration and the sampling technique (and thus the need to combine two different analyses to obtain the value for the n-paraffin selectivity for a certain carbon number). It was noted that the method used to calibrate the 1D GC and quantify the compounds in the gas sample was not sufficient for the C_{5+} compounds (see Table 4.5 in Chapter 4). Large deviations between the various calibration data sets for pentane and hexane on the 1D GC were noted. This may explain the under reporting of the C_5 to C_8 compounds when 1D GC is used. Furthermore, the hot tail gas (at 200˚C) was fed to the GCxGC system through heated lines. Therefore one can assume that all the compounds from C_1 to C_8 were definitely in the gas phase. The gas stream fed to the 1D GC was cold tail gas at ambient temperature. It may be possible that some of the C_5 to C_8 product condensed out of the gas and was retained in the sample line, therefore all the compounds in the gas was not transferred onto the GC leading to the under reporting of these compounds. To improve the noted deviation for the 1D GC analyses, the oil product results were added to the gas analyses results but it did not improve the C_5 to C_8 product selectivity. Therefore it is recommended that the sample lines for the cold tail product should also be heated to ensure that all the compounds in the gas matrix are in the gas phase.

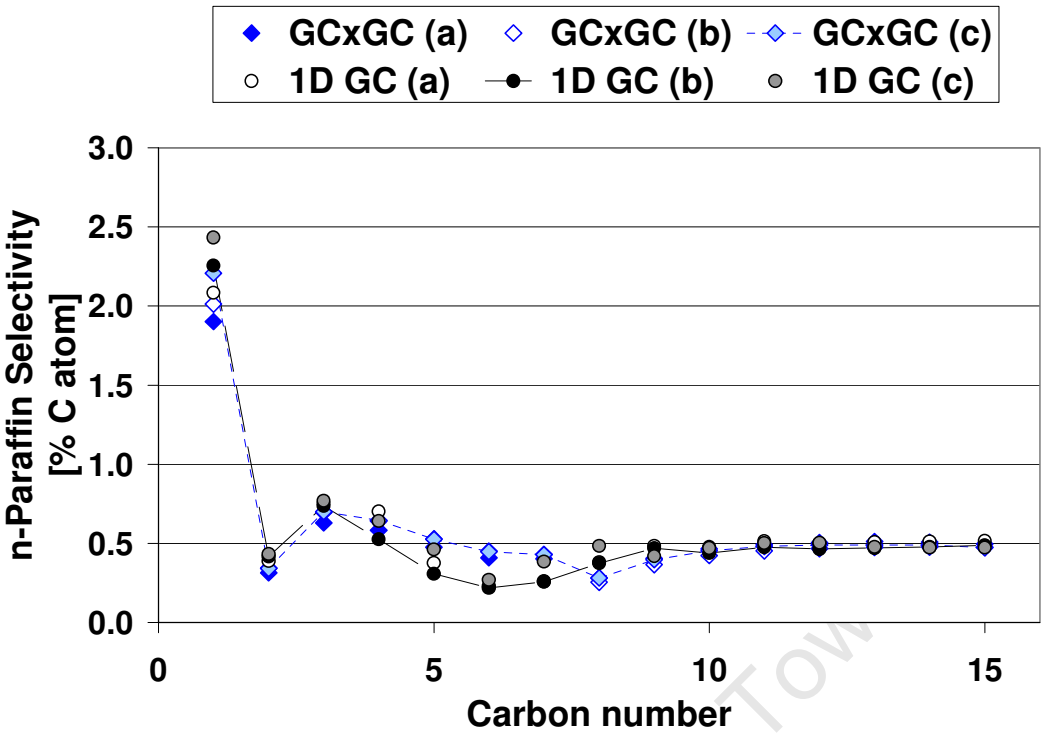

Figure 5.1: n-Paraffin selectivity in the product range from C_1 to C_{15} as a function of carbon number obtained by GCxGC and 1D GC technique

The deviations observed in the n-paraffin selectivity as a function of carbon number between the GCxGC and 1D GC technique are also observed in the 1-olefin selectivity as a function of carbon number (see Figure 5.2) and therefore the explanations given above are also relevant explanations for the 1-olefin deviations.

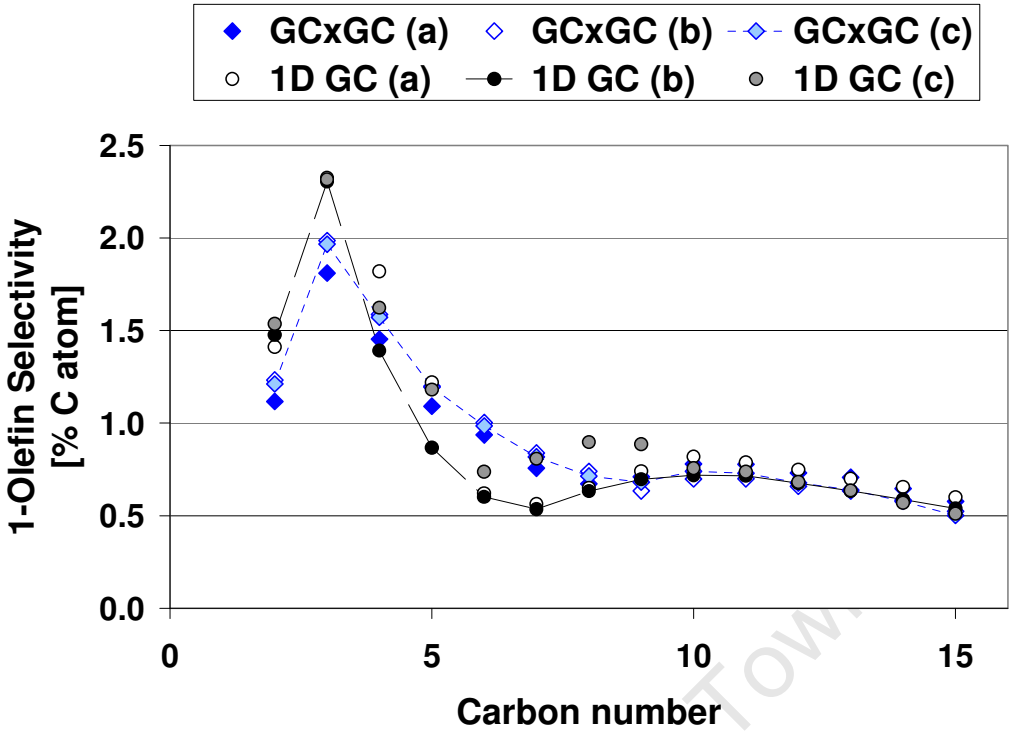

Figure 5.2: 1-Olefin selectivity in the product range from C_2 to C_{15} as a function of carbon number obtained by GCxGC and 1D GC technique

Figure 5.3 shows the comparison of the total internal linear olefin selectivity. According to the figure a lot of scatter occurs in the 1D GC data. For the 1D GC the C_{12+} internal olefin selectivity is also higher than the GCxGC data. These observations are attributed to the fact that peak overlap of the internal linear olefins and n-paraffins occur. For the C_1 to C_{12} compounds the minor compound, which in this case is the linear internal olefin, sits on the tail of the major compound, n-paraffin, and therefore accurate quantification of the linear internal olefin is difficult thus leading to scatter in the data. Beyond C_{12} the separation between trans-2-olefin and n-paraffin is normally very difficult and it is no longer separated, i.e. the area is added to that of the n-paraffin thus leading to over reporting of the linear internal olefins. This is especially observed in the Fischer-Tropsch oil product (C_6 to C_{30} product fraction) analysis. See Figure 5.4.

The internal olefin selectivity trends obtained from the GCxGC methods (Figure 5.3) are much more consistent and no deviations are observed thus indicating that the separation of internal olefins on GCxGC is much more

efficient. The efficiency of the GCxGC technique to separate compounds which are likely to co-elute with other compounds, as seen in the above discussion on the deviations observed for the 1D GC methods, is attributed to the enhanced separation ability due to orthogonal separation (see section 2.3.3.3), where compounds are not just separated on the basis of volatility but also on their functionality. Another factor that attributes to enhanced separation is the enhanced resolution provided by the use of modulation (see section 2.3.3.3).Therefore the trans-2-olefin peak is not absorbed by the n-paraffin peak and is separated effectively.

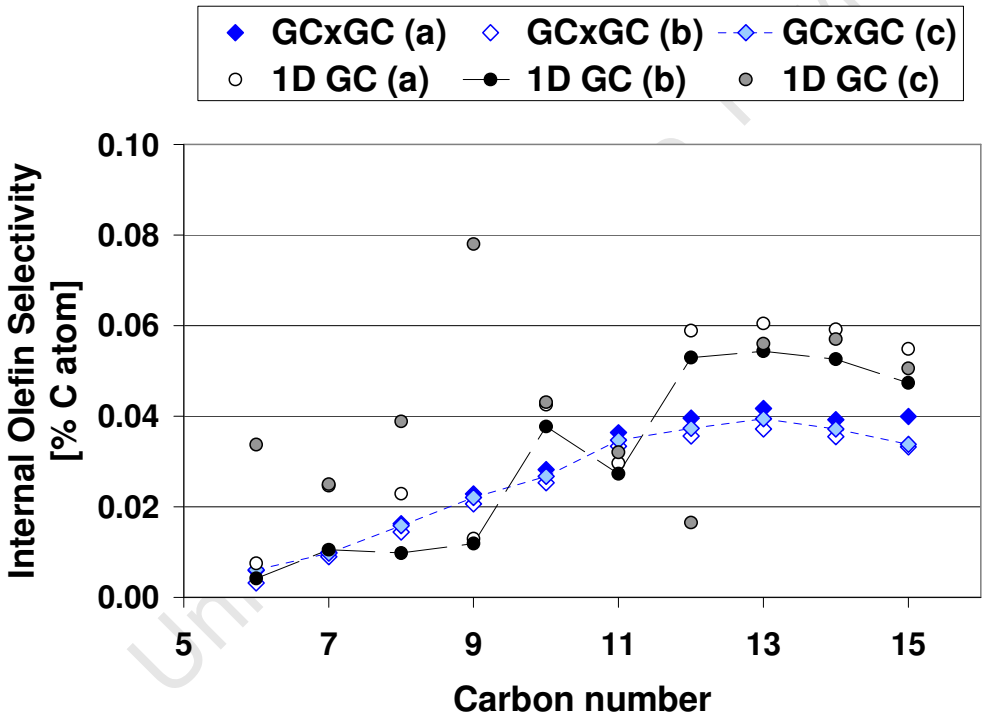

Figure 5.3: Internal linear olefin selectivity in the product range C_6 to C_{15} as a function of carbon number obtained with the GCxGC and 1D GC techniques

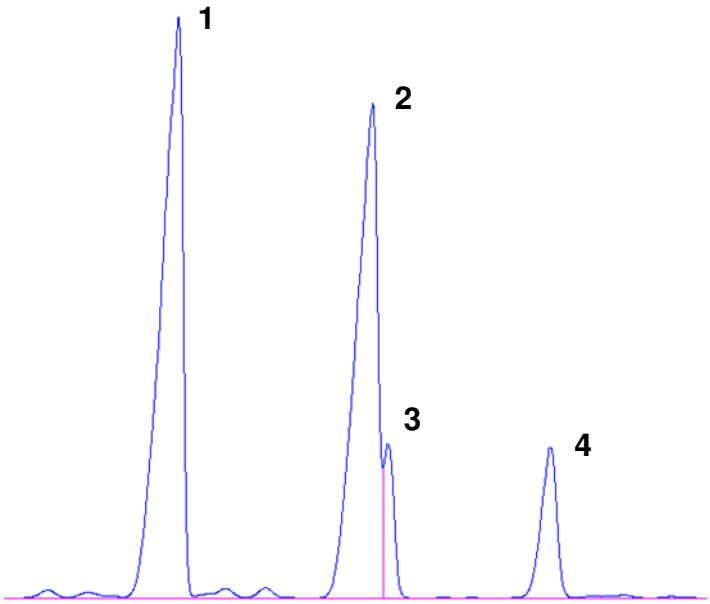

Figure 5.4: Enlargement of a 1D GC chromatograph of Fischer-Tropsch synthesis oil product in the C_{11} range focussing on the paraffins and olefins ((1) 1-olefin; (2) n-paraffin; (3) trans-2-olefin; (4) cis-2-olefin)

Comparing the total n-alcohol-(1) selectivity obtained with GCxGC and 1D GC analyses (Figure 5.5), variations are observed at the C_1, C_3, C_4 and C_9 alcohols. Not only does the selectivity data for the two methods differ but significant variation exists between the 1D GC data points. On the 1D GC instrument alcohols often co-elute with some of the other compounds especially when analyzing the oil and water Fischer-Tropsch products. This is due to the temperature program and the type of columns used for separation (see section 3.4.3 in Chapter 3 for GC methods). When performing the 1D GC oil product analyses, using a HP Pona column with a methyl siloxane stationary phase, propanol co-elutes with some of the branched olefinic C_6 hydrocarbons (3-methyl-1-pentene or 4-methyl-1-pentene). When analysing the water product on a HP Innowax column with a polyethylene glycol stationary phase, heptanol co-elutes with acetic acid and nonanol with butanoic acid. No significant variations are observed for the selectivity obtained using the GCxGC technique except for a minimum at C_3, but this can not be explained due to co-elution of compounds when

separated on the GCxGC columns for propanol is well separated from other compounds due to the orthogonal separation employed by GCxGC. Dry (2004) reported that at low Fischer-Tropsch temperatures (236ºC), alcohols can undergo de-hydration to form olefins, therefore a possible explanation for the minimum at C_3 is that the n-propanol could have been subjected to secondary reaction to form propene, therefore one would expect a maximum for the olefin selectivity at C_3 as seen in Figure 5.2.

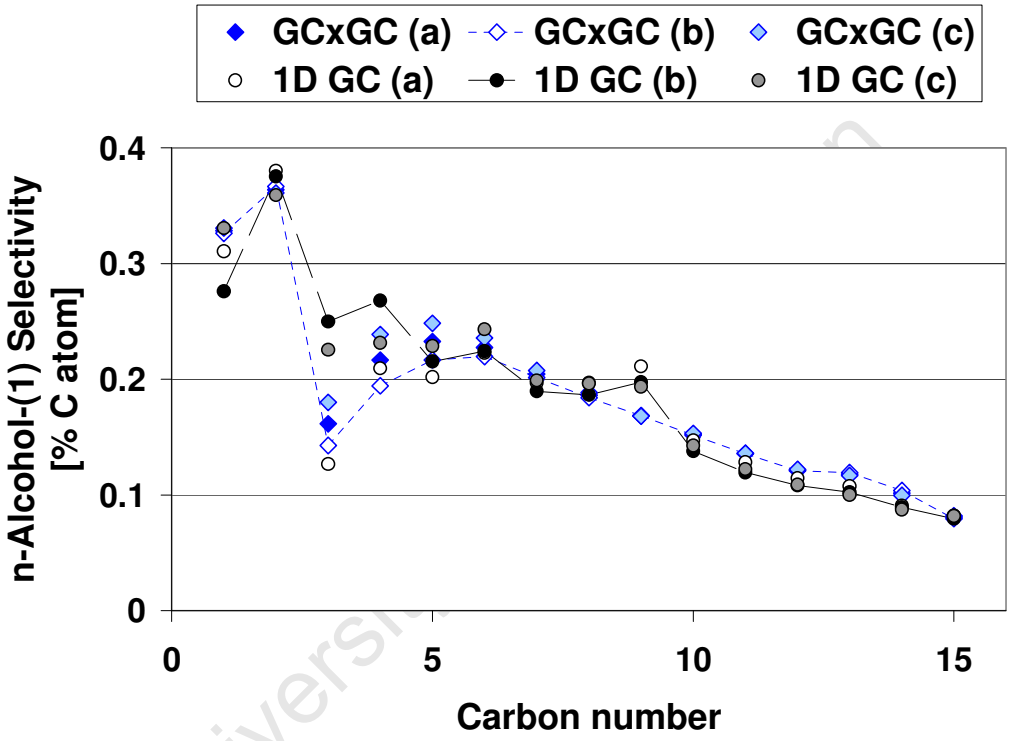

Figure 5.5: n-Alcohol-(1) selectivity in the product range from C_1 to C_{15} as a function of carbon number obtained by GCxGC and 1D GC technique

The benefit of using GCxGC as an analytical technique to identify and quantify compounds present in the Fischer-Tropsch products becomes more apparent when looking at the selectivities of the minor compounds such as the oxygenates. In Figures 5.6 to 5.8 the selectivity of n-alcohol-(2), branched alcohol and branched acid compounds are displayed. As noted from the figures only selectivity calculated from GCxGC analyses are displayed. The reason for this is that these compounds could not be

separated using the 1D GC system. The ability of GCxGC and inability of 1D GC to separate these compounds can be ascribed to two things. Firstly, as mentioned earlier, GCxGC is based on the concept of orthogonal separation where a short non-polar column (CP-Sil-5), ca. 1.5 m, and a 50 m polar HP-Innowax column combination are used to effectively separate compounds with similar volatilities on the basis of volatility and functionality. Secondly GCxGC makes use of a modulator that traps compounds separated on a first non-polar column and refocuses fractions of these compounds as narrow pulses onto the second polar column. This enhances sensitivity and the resolution of the eluting peaks and therefore leads to the separation of minor compounds that are sometimes absorbed by other major peaks (see section 2.3.3.3) especially when using 1D GC.

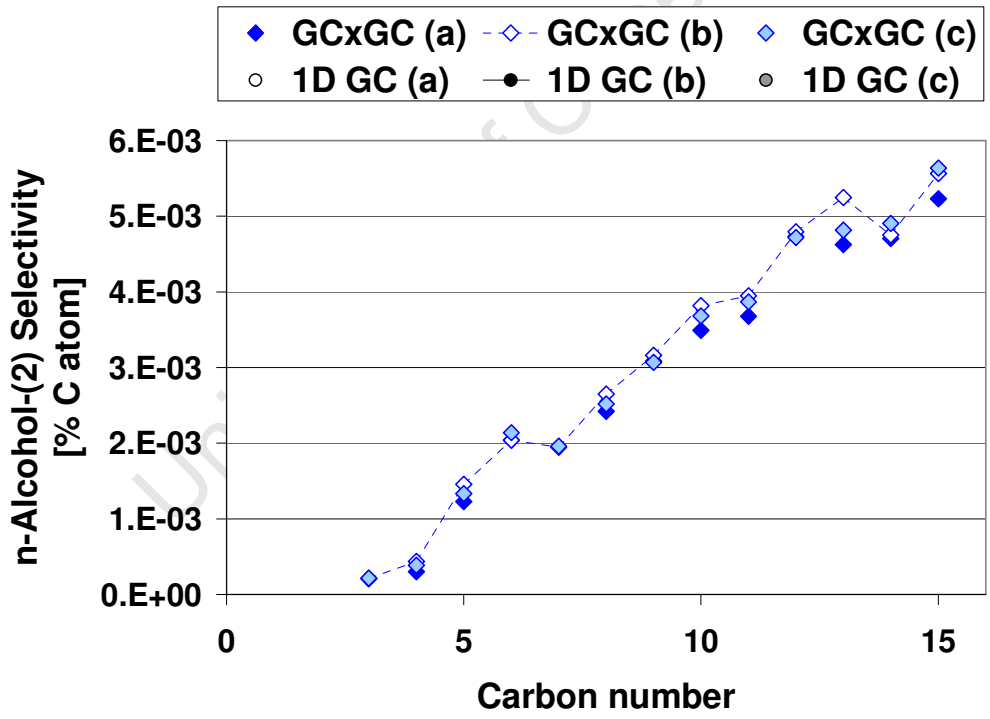

Figure 5.6: n-Alcohol-(2) selectivity in the C_3 to C_{15} product range as a function of carbon number obtained by the GCxGC technique

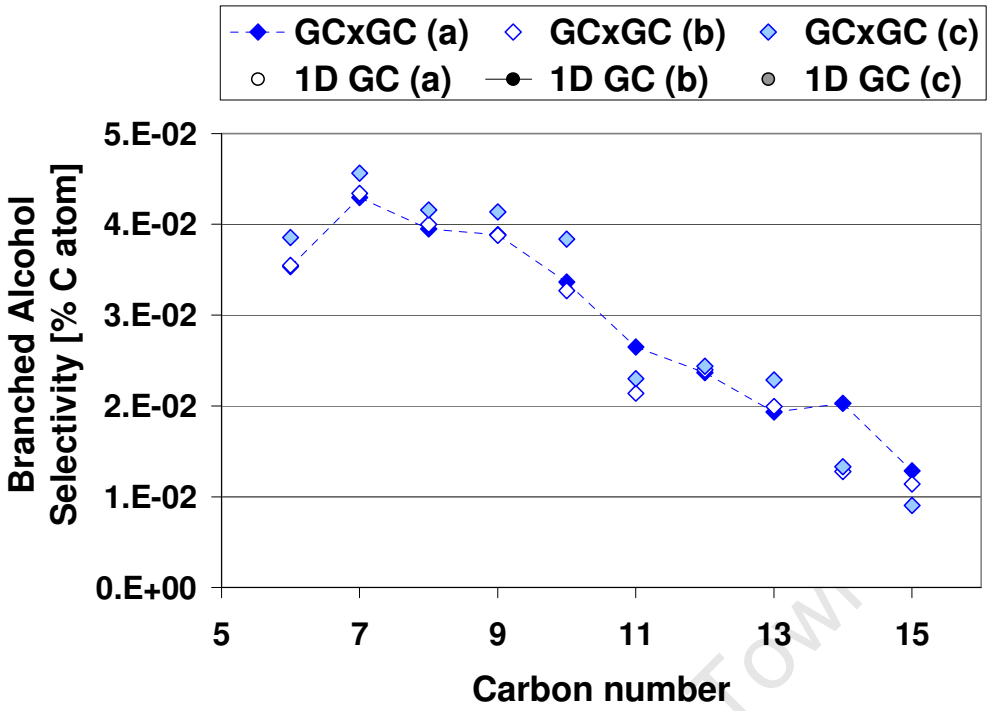

Figure 5.7: Selectivity for branched alcohols in the product range C_6 to C_{15} as a function of carbon number obtained with GCxGC technique

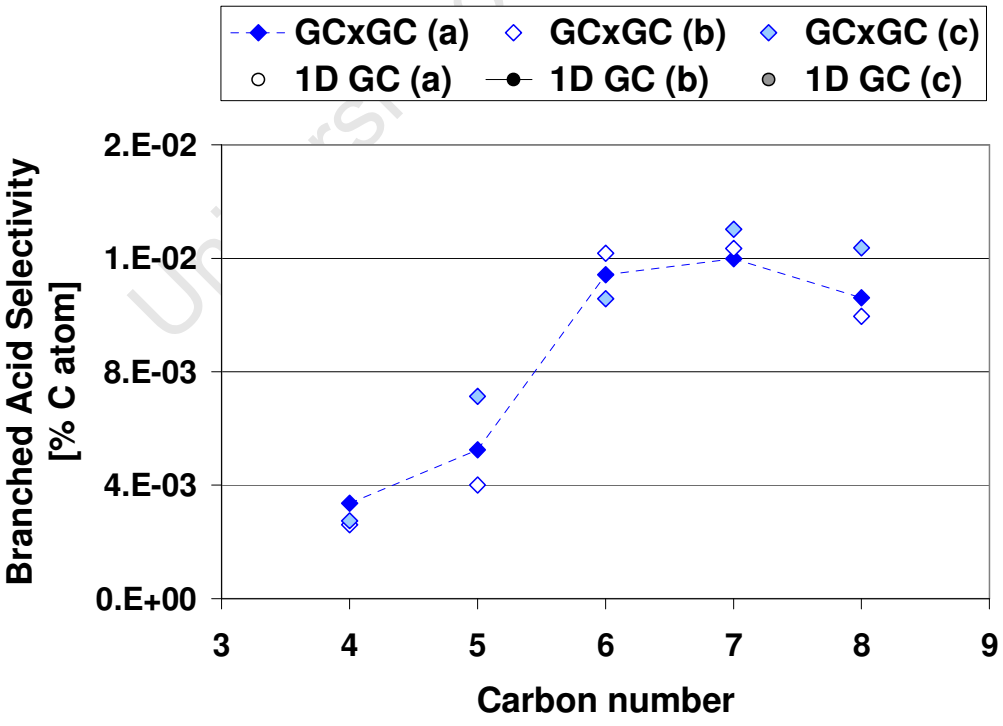

Figure 5.8: Selectivity for branched acids in the product range C_4 to C_8 as a function of carbon number obtained with GCxGC technique

Other oxygenates that were also more efficiently separated with GCxGC are the linear carboxylic acids, ketones and aldehydes. Figure 5.9 illustrates the selectivity of the linear carboxylic acids as a function of carbon number. The selectivity obtained for acetic acid and propionic acid with the GCxGC and the 1D GC technique correlate well. Deviations occur from C_4 onwards. Using GCxGC, linear carboxylic acids from C_2 to C_9 could be detected and quantified. For the 1D GC method C_2 to C_7 linear carboxylic acids could be detected. In comparison to the GCxGC product distribution, the 1D GC indicates a lower selectivity in C-%, due to the inability of the 1D GC technique to detect C_{3+} acid compounds in the oil fraction. Hence, the acid selectivity represents only acids present in the water fraction of the liquid product. With the GCxGC method the oil fraction could be analyzed for acids up to C_9, leading to a more complete linear carboxylic acid product distribution.

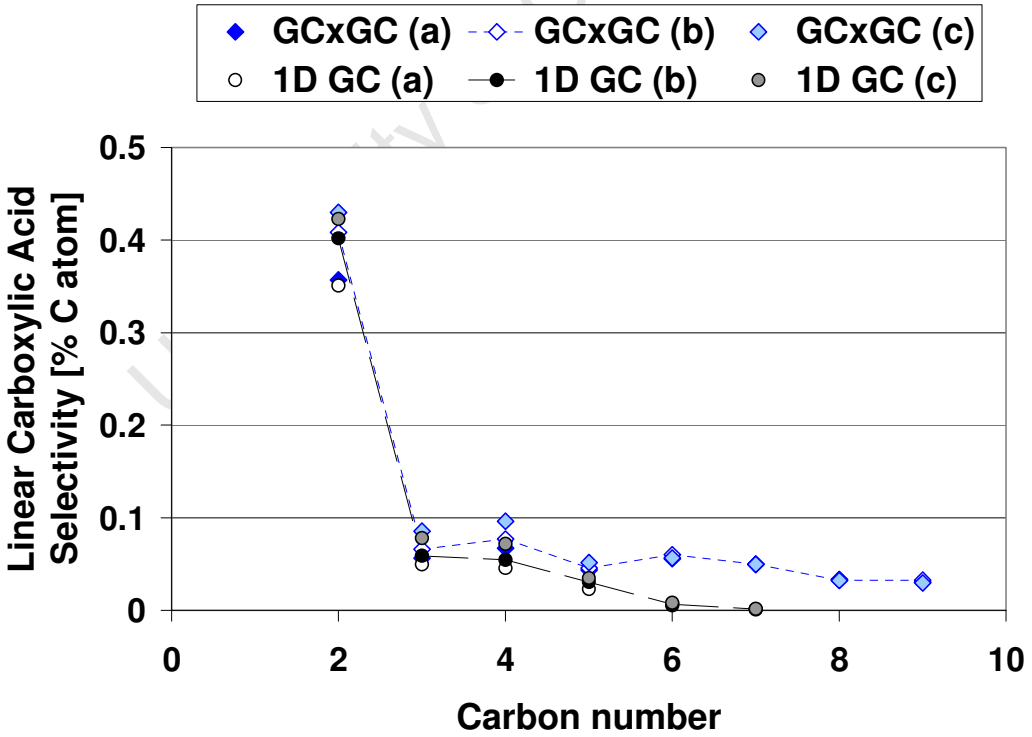

Figure 5.9: Linear carboxylic acid selectivity in product range C_1 to C_{15} as a function of carbon number obtained with the GCxGC and the 1D GC techniques

Methyl alkyl ketones ranging from C_3 – C_9 were separated and detected using the GCxGC technique, whereas with the 1D GC technique only the C_3 and C_4 ketones were detected (see Figure 5.10). A large deviation exists for acetone, on the 1D GC making accurate quantification difficult. The correlation between the selectivity for butanone-(2) obtained with the two different techniques is good.

The fact that only the C_3 and C_4 methyl alkyl ketones were detected using the 1D GC technique and up to C_9 methyl alkyl ketones could be detected using the GCxGC technique confirms that GCxGC has a greater ability to separate and detect oxygenated compounds in the Fischer-Tropsch product than 1D GC. Furthermore not only are we able to separate and group compounds of different functionalities but with GCxGC we are also now able to investigate the functionalities as a function of carbon number. This may be useful when investigating the contribution of secondary reactions which is more likely to occur as carbon number increases.

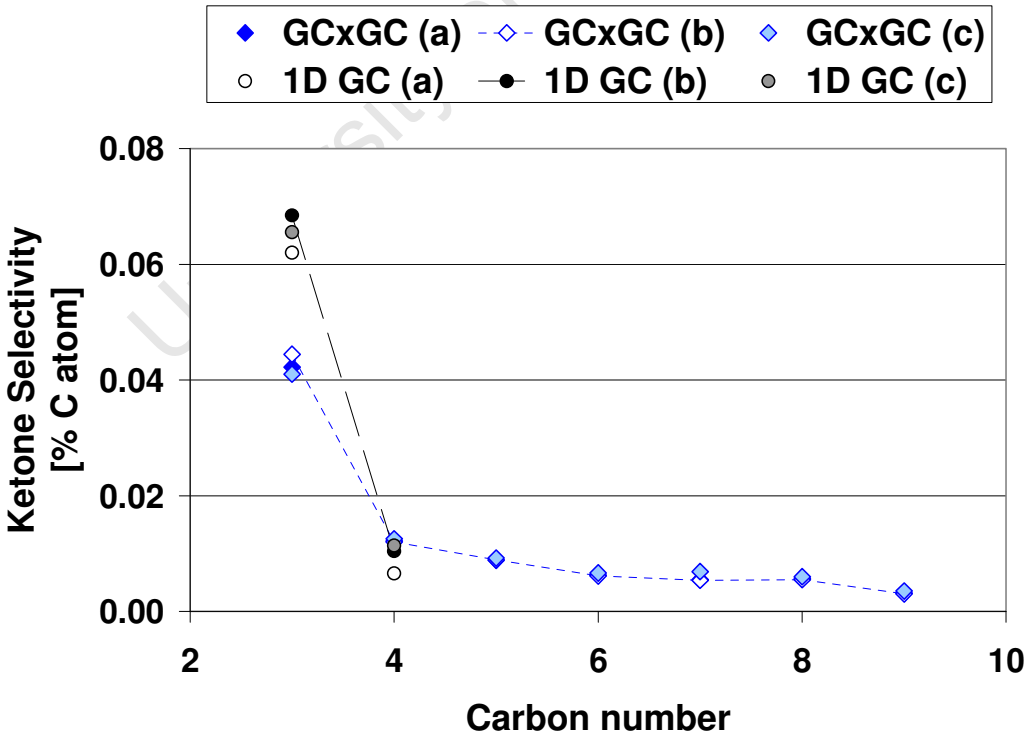

Figure 5.10: Methyl alkyl ketone selectivity in the product range C_1 to C_{15} as a function of carbon number obtained with the GCxGC and 1D GC techniques

The advantages of the GCxGC technique are further displayed when looking at the aldehyde selectivity, ranging from C_2 – C_{12}, in Figure 5.11. The figure clearly shows that the aldehyde selectivity could only be separated using the GCxGC technique and not by using the 1D GC technique. The aldehyde selectivity also did not vary much between the three data sets confirming that not only does GCxGC provide enhanced separation and detection but the data is also repeatable and accurate.

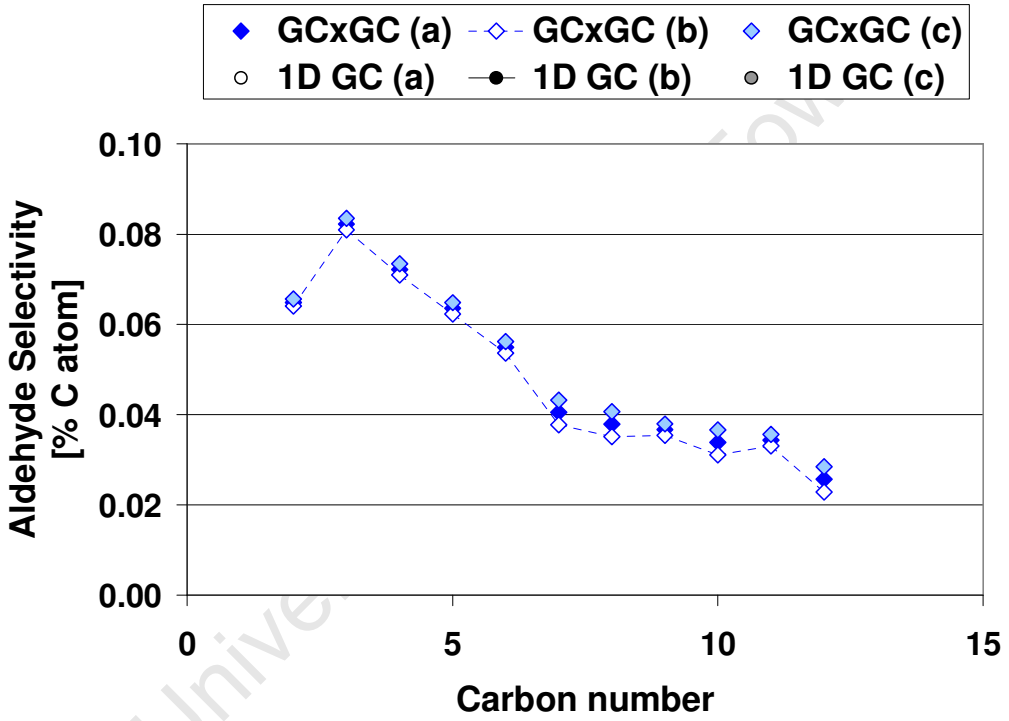

Figure 5.11: Aldehyde selectivity in the product range C_2 to C_{12} as a function of carbon number obtained with the GCxGC technique

With the enhanced separation power of GCxGC other minor compounds such as branched olefins and branched paraffins were also quantified using the GCxGC technique. Figure 5.12 displays a section of a two-dimensional chromatograph (contour plot) of a Fischer-Tropsch synthesis oil product injected off-line on to the GCxGC system. The encircled sections A and B indicate the areas on the GCxGC contour plot where the C_9 branched

paraffins and C_{10} branched olefins are found. In section A only two C_9 branched paraffins are displayed, but when the GCxGC plot is processed further and the resolution of the GCxGC graphic is increased, in order to see the compounds with very low concentrations, seven other branched compounds are viewed as seen in Figure 5.13. Similarly when section B of Figure 5.12 are further enhanced with the GC Image software to increase the resolution of the lower concentration compounds, quite a few other C_{10} branched olefins are observed as displayed in Figure 5.14.

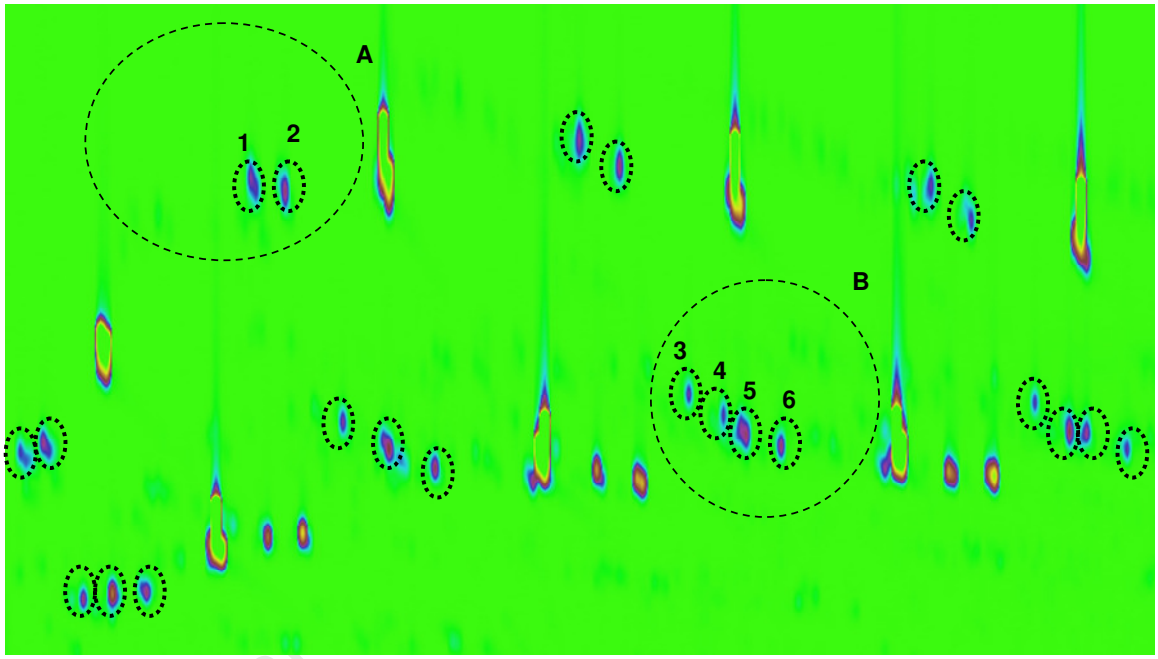

Figure 5.12: A section of a two-dimensional chromatograph (contour plot) of Fischer-Tropsch synthesis oil product injected off-line on to the GCxGC system illustrating the separation and grouping of branched paraffins and branched olefins (A: C_9 branched paraffins; B: C_{10} branched olefins)

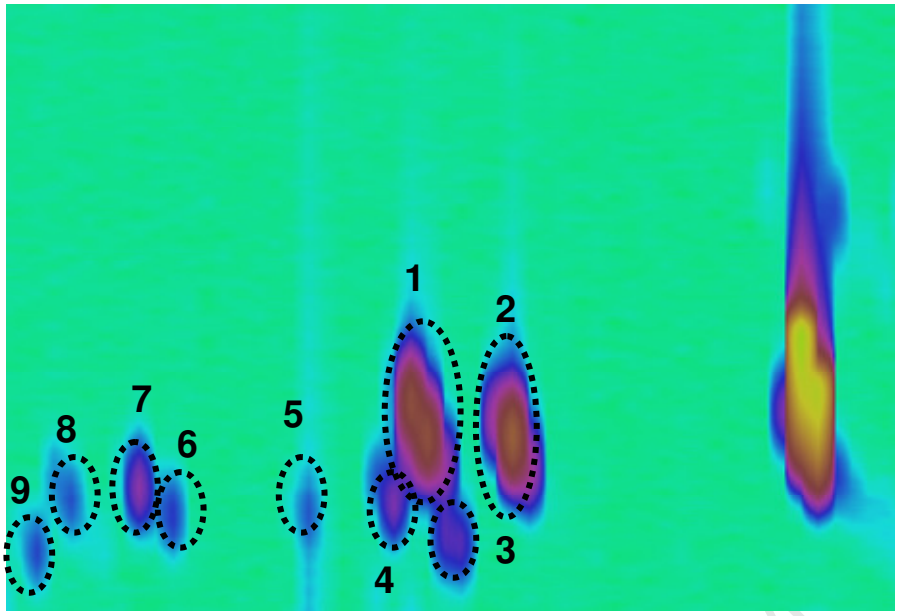

Figure 5.13: Section A of the GCxGC contour plot in Figure 5.12 are enhanced in order to show the rest of the low concentration C_9 branched paraffins

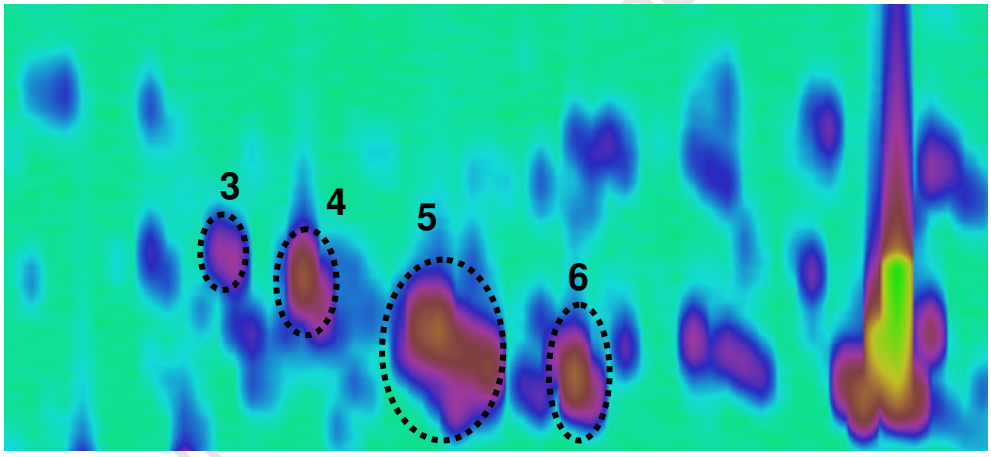

Figure 5.14: Section B of the GCxGC contour plot in Figure 5.12 are enhanced in order to show the rest of the low concentration C_{10} branched olefins

For the purpose of this study the various methyl-branched products were grouped and reported as such. Sufficient separation of the branched paraffins and branched olefins could not be achieved on the 1D GC; therefore the branched olefins and paraffins obtained from the GCxGC method was added together and compared with the data from the 1D GC. The selectivities of these compounds are displayed in Table 5.1. It is clear

from the table that not all the branched products were sufficiently detected using the 1D GC technique, thus resulting in lower C atom selectivity.

Table 5.1 is a summary of the Fischer-Tropsch product selectivities, ranging between C_1 and C_{15} of the total product (C_1 to C_{80}) displayed in the above graphs. The 95% confidence intervals (CI) with which the product selectivities can be determined using the GCxGC and 1 D GC technique are also indicated in this table. Confidence intervals (CI) are calculated values that define an interval around a measured value to indicate the reliability of this value. A result with a small confidence interval is more reliable than a result with a large confidence interval (Goldstein and Healey, 1995).

Taking the definition of confidence intervals in consideration it is clear that GCxGC gives more accurate and reliable results than the 1D GC because the 95% confidence intervals displayed with the selectivity data is much narrower for the data obtained by GCxGC techniques. Furthermore the superiority of the GCxGC technique above the 1D GC technique become apparent when focussing on the minor product compounds such as the acids, ketones, aldehydes, branched paraffins, olefins, alcohols, acids and secondary alcohols. From the above data one can see that aldehydes, secondary alcohols, branched alcohols and branched acids were not detected by the 1D GC. Furthermore, the efficient separation of branched paraffins and olefins, especially within the complex oil product, on the 1D GC is difficult. Therefore it can be concluded that given the confidence levels displayed in Table 5.1, the GCxGC technique displayed much narrower confidence levels which indicates a higher level of accuracy. All of these observations can be attributed to the resolving power of the GCxGC technique due to orthogonal separation and the use of modulation.

Table 5.1: Summary of Fischer-Tropsch product selectivities obtained from 1D GC and GCxGC systems in the product range C_1-C_{15} (*Note these selectivities are fractions of the total product which ranges from C_1 to C_{80} and will not count up to a 100% for only the C_1 to C_{15} range of this total product are used for the discussion*)

Compound Class	GCxGC [% C atom]	1D GC [% C atom]
n-Paraffins [$C_1 – C_{15}$]	8.56 ± 0.78	8.75 ± 1.32
1-Olefins [$C_2 – C_{15}$]	12.93 ± 0.45	13.304 ± 2.58
Internal Olefins [$C_4 – C_{15}$]	0.263 ± 0.052	0.371 ± 0.194
Branched Paraffins [$C_4 – C_{15}$]	0.293 ± 0.042	-
Branched Olefins [$C_4 – C_{15}$]	0.361 ± 0.053	-
Branched Paraffins and Olefins [$C_4 – C_{15}$]	0.654 ± 0.095	0.472 ± 0.272
n-Alcohols-(1) [$C_1 – C_{15}$]	2.80 ± 0.22	2.80 ±0.21
Linear carboxylic Acids [$C_2 – C_9$]	0.765 ± 0.220	0.549 ± 0.225
Ketones [$C_3 – C_9$]	0.093 ± 0.008	0.075 ± 0.017
Aldehydes [$C_2 – C_{12}$]	0.541 ± 0.070	-
n-Alcohols-(2) [$C_3 – C_{15}$]	0.0389 ± 0.005	-
Branched alcohols [$C_4 – C_{15}$]	0.301 ± 0.028	-
Branched acids [$C_4 – C_8$]	0.065 ± 0.008	-
C_{15+} Fischer-Tropsch product	72.34 ± 0.156	73.68 ± 0.688

5.2 THE EFFECT OF REACTION VARIABLES ON FISCHER-TROPSCH PRODUCT DISTRIBUTIONS

In the previous section the benefits of using GCxGC for Fischer-Tropsch research was illustrated by comparing product selectivities obtained from 1D GC methods with product selectivities obtained by GCxGC methods. It was highlighted that the real advantage in using GCxGC instead of 1D GC techniques was that with GCxGC minor Fischer-Tropsch compounds which

could not be detected or separated, especially in the oil fraction (C_6 to C_{30}), could be detected, efficiently separated and quantified using GCxGC. This makes GCxGC an attractive tool for Fischer-Tropsch research and can serve as an aid to investigate selectivity changes when reaction conditions changes or provide valuable information regarding product formation.

To illustrate the benefits that GCxGC can provide when applied in Fischer-Tropsch research, especially regarding selectivity and product formation, synthesis experiments were performed at different temperatures and different H_2/CO feed ratios. All the selectivity data portrayed in the discussion to follow were obtained using the GCxGC technique as described in Chapter 3 section 3.5.5. Because the real benefits of the GCxGC technique are evident when looking at the minor Fischer-Tropsch products the following section will focus on these compounds.

All experiments were run for the first 100 hours on stream at baseline conditions (T = 245ºC, H_2/CO feed ratio = 1.5, P_{total} = 27 bar) where after the specific parameter under investigation was changed. Therefore the focus is on the data obtained after 150 hours on line (i.e. data obtained after being exposed to 50 hours of the specified condition).

5.2.1. Oxygenate Selectivity

The products from Fischer-Tropsch synthesis are mainly applied to produce fuel but it can also be processed further to produce other high value chemicals such as olefins and oxygenates (Dry, 2002). For a commercial iron based Fischer-Tropsch process ca. 6 – 12 wt% of these products are oxygenates (Jager, 1997).

Although many researchers have proposed mechanisms that may account for the formation of these oxygenates (Pichler and Schulz, 1970; Johnston and Joyner, 1993; Schulz et al., 1990; Davis et al., 1990) little is still known of their formation. One of the reasons for this is the lack of experimental

data for oxygenate selectivity which is due to the difficulty of analyzing such complex products (Weitkamp et al., 1953). In recent years researchers such as Dry (2004) and Liu et al. (2007) have reported information on oxygenate selectivity and even went so far as to described the selectivity of the alcohols, acids and aldehydes separately, but in most cases oxygenates are grouped and reported together.

As discussed in the previous section (section 5.1), it is now possible with GCxGC to detect separate and quantify the various oxygenated compounds present in the Fischer-Tropsch products. This is achieved by the use of modulation (see Chapter 2 section 2.3.3) which allows for the enhanced resolution thus separation of oxygenated compounds. Furthermore the fact that separation on GCxGC is based on orthogonal separation (see Chapter 2 section 2.3.3) which independently separates compounds on the basis of volatility and polarity, oxygenated compounds can now be grouped as a function of carbon number and functionality. With GCxGC the following oxygenates formed from the Fischer-Tropsch synthesis experiments performed at different temperatures and H_2/CO feed ratios were detected and quantified: n-alcohols-(1), aldehydes, acids, ketones, secondary alcohols and branched oxygenated products.

In the literature, researchers usually mention the effect of synthesis parameters on oxygenates in general. In a few cases the selectivity of acids, ketones and aldehydes are mentioned, but mostly they refer to the linear alcohol selectivity which are calculated from the oxygenates detected in the water faction of the liquid product only, thus omitting the oxygenates in the oil product.

To show the true benefit that GCxGC can provide for selectivity and product formation research, the influence of changes in operating conditions (e.g. temperature and H_2/CO feed gas ratios) on oxygenate selectivity were investigated.

5.2.1.1. The effect of temperature

Various different observations have been reported in literature regarding the effect of temperature on oxygenate selectivity. In some instances an increase in total oxygenate selectivity was reported with increasing temperature (Liu et al., 2007), while in other cases a decrease in oxygenate selectivity was reported with increasing temperature (Roper, 1983; Claeys, 1997; Dry, 2004).

When plotting the % linear oxygenate selectivity which consist of the n-alcohols-(1), n-alcohols-(2), linear carboxylic acids, aldehydes and alkyl-methyl-ketones present in the linear products as a function of carbon number (Figure 5.15) a few things are observed:

- Firstly on a carbon number basis the linear Fischer-Tropsch products appear to comprise between 15 and 22 % of linear oxygenated products, except for the C_2 fraction which comprises ca. 20 to 40 % out of C_2 oxygenates. This is in accordance to observations in literature that the Fischer-Tropsch product consists largely out of linear paraffins and olefins and a small amount of oxygenates (Jager, 1997; Dry, 2004).

- Secondly at lower temperature (225ºC) the % linear oxygenates appear to increase (Figure 5.15). This observation is in contrast with Liu et al. (2007) but in accordance with the observations made by Roper (1983) and Claeys (1997).

- Thirdly, a maximum at C_2 and a minimum at C_3 are observed for the linear oxygenate selectivity. The oxygenate selectivity also appear to increase slightly with increasing carbon number.

The observations in Figure 5.15 can be explained as follows: for the Fischer-Tropsch experiments performed at various temperatures the conversion of CO + CO_2 to form Fischer-Tropsch products were kept

constant by varying the GHSV. To achieve the constant conversion at lower Fischer-Tropsch synthesis temperatures the GHSV were lowered, leading to higher surface coverage of CO which can be adsorbed to the catalyst surface to form oxygen containing surface species which is believed to be the species responsible for the formation of oxygenates (Pichler and Schulz, 1970; Johnston and Joyner, 1993; Claeys and Van Steen, 2004). The amount of oxygenates also increased with increasing carbon number, which may indicate the secondary re-adsorption of oxygenate species to form longer chain oxygenates which is especially favourable at lower temperatures.

The maximum observed at C_2 for the linear oxygenates in relation to linear hydrocarbons (Figure 5.15) may be explained when looking at the proposed kinetic scheme (see Chapter 4 Scheme 4.4) for the formation and re-adsorption of paraffins, olefins and oxygenates (Claeys and Van Steen, 2004). From this scheme it can be argued that species compete to form olefins, paraffins and oxygenates and that when it comes to the C_2 specie, the likelihood increases that the specie would desorb to form an oxygenate instead of participating in paraffin and olefin formation or chain growth.

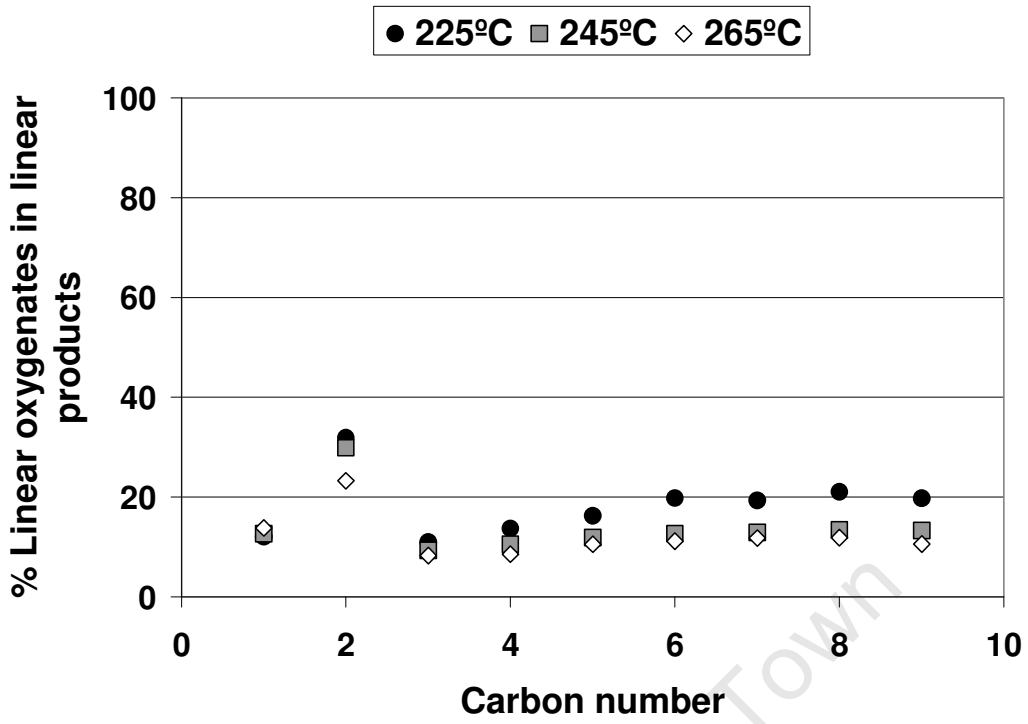

Figure 5.15: % Linear oxygenates in linear products for the C_1 to C_9 product range obtained from Fischer-Tropsch runs at 225ºC, 245ºC and 265ºC

Taking a closer look at oxygenate selectivity it is apparent that the linear oxygenates which include the n-alcohols-(1), aldehydes, linear carboxylic acids, n-alcohols-(2) and alkyl-methyl-ketones consist mostly (ca. 95%) of n-alcohols-(1), aldehydes and linear carboxylic acids and this seem to stay constant as carbon number increases (Figure 5.16). For the C_3 fraction however there appear to be a bit more n-alcohols-(2) and alkyl-methyl-ketones. In Figure 5.16 it appears as if temperature variations have no significant effect on the contents of n-alcohols-(1), aldehydes and linear carboxylic acids in the linear oxygenates.

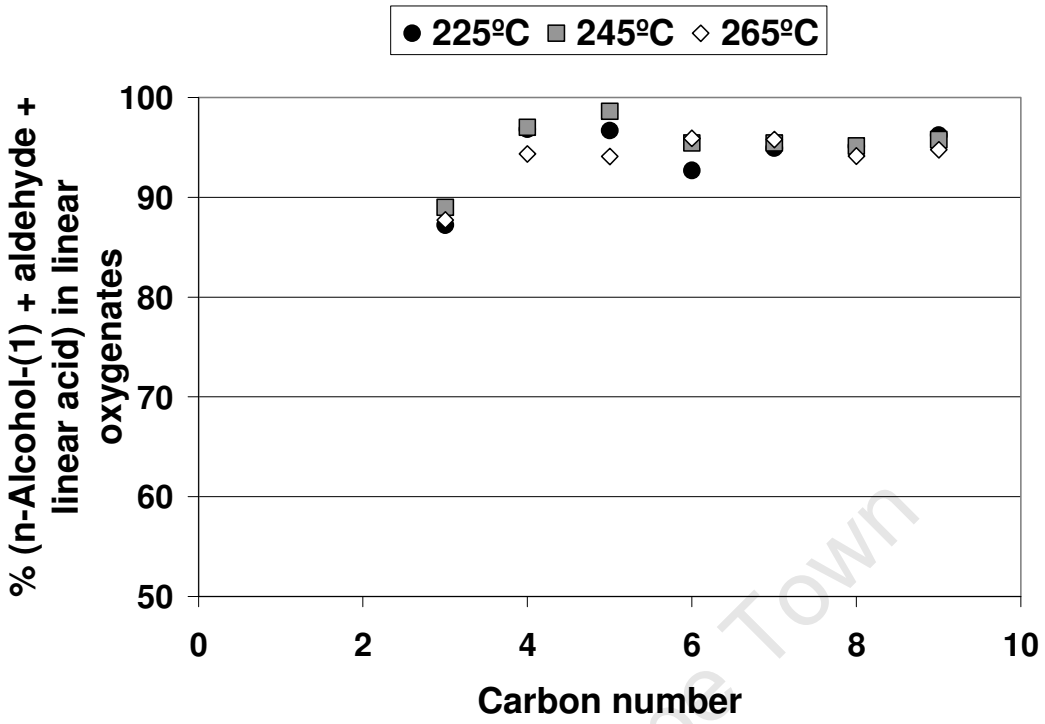

Figure 5.16: % n-Alcohol-(1) + aldehyde + linear carboxylic acid selectivity in linear oxygenates for the C_3 to C_9 product range for runs performed at 225ºC, 245ºC and 265ºC

n-Alcohol-(1), aldehyde and linear carboxylic acid selectivity may be interrelated to one another, especially at high (327ºC) Fischer-Tropsch reaction temperatures (Dry, 2004). Figures 5.17 to 5.20 portray these relationships if they exist at lower Fischer-Tropsch reaction conditions (225 - 265ºC).

If a reaction pathway between aldehydes and linear alcohols and between linear carboxylic acids and linear alcohols exists, then n-alcohols-(1) are formed from aldehydes and linear carboxylic acids, since with increasing carbon number the likelihood of secondary reactions increases as seen in Figure 5.17 where the n-alcohols-(1) increase with increasing carbon number.

Furthermore the n-alcohol-(1) selectivity appears to increase with increasing temperature (see Figure 5.17). This is in accordance with observations by

Liu et al. (2007) that the alcohol selectivity increases as temperature increases, but in contrast to Roper (1983) that alcohol selectivity decreases with increasing temperatures. Thus if one take the Schemes 4.3 and 4.4 in Chapter 4 into consideration then one can assume that n-alcohol-(1) formation is favoured at higher reaction temperatures.

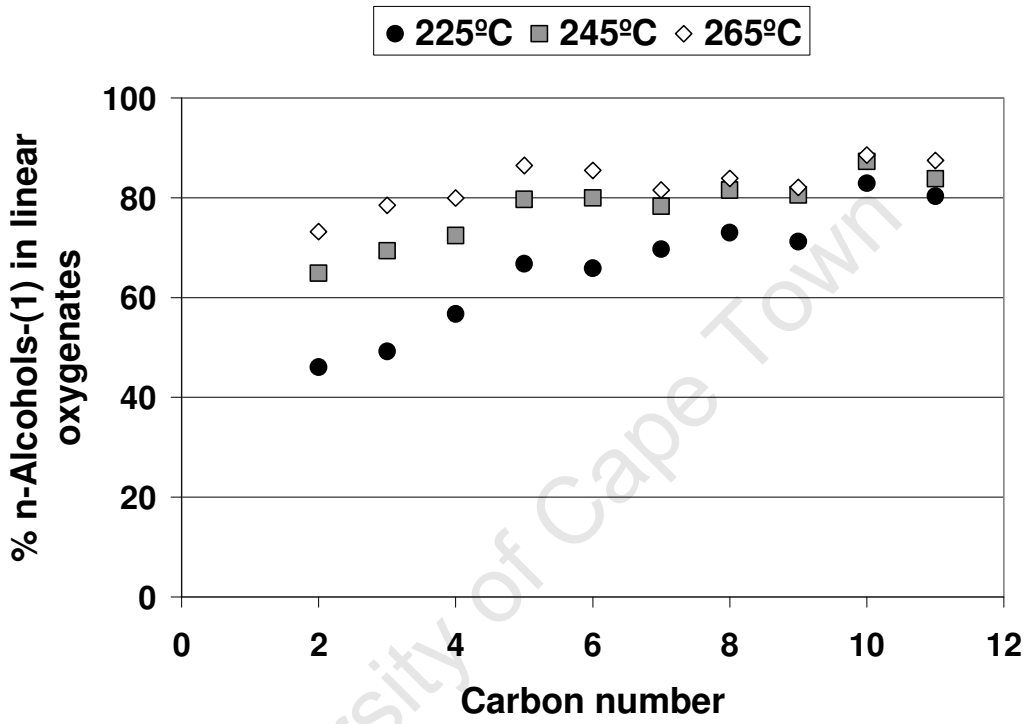

Figure 5.17: n-Alcohols-(1) content in the fraction of linear oxygenates (n-alcohol-(1), aldehyde and linear carboxylic acid) for the C_2 to C_{11} products in experiments performed at 225ºC, 245ºC and 265ºC

When looking at the % linear carboxylic acids present in the linear oxygenates (Figure 5.18) the acid selectivity increases as temperature decreases. This is in accordance with observations made by Liu et al. (2007) and Dry (1981). When looking at the linear carboxylic acid selectivity in relation to the n-alcohol-(1) selectivity (Figure 5.17) it appears that as the carbon number increases the acid selectivity decrease while the alcohol selectivity increases. Dry (2004) reported that at low Fischer-Tropsch temperatures (226ºC) acetic acid was not formed via the oxidation of primary ethanol but he indicated that hydrogenation of acetic acid to form

ethanol was possible. Taking this in consideration and that at long residence times, thus lower GHSV, secondary reactions are more prone to occur (Claeys and Van Steen, 2004), it can be said that at low temperatures acids may undergo secondary reactions to form n-alcohols-(1) and the likelihood of this occurring increase with increasing carbon number. From Figure 5.18 it is also clear that the observed C_2 maximum for the linear oxygenates in Figure 5.15 can be attributed to acetic acid selectivity.

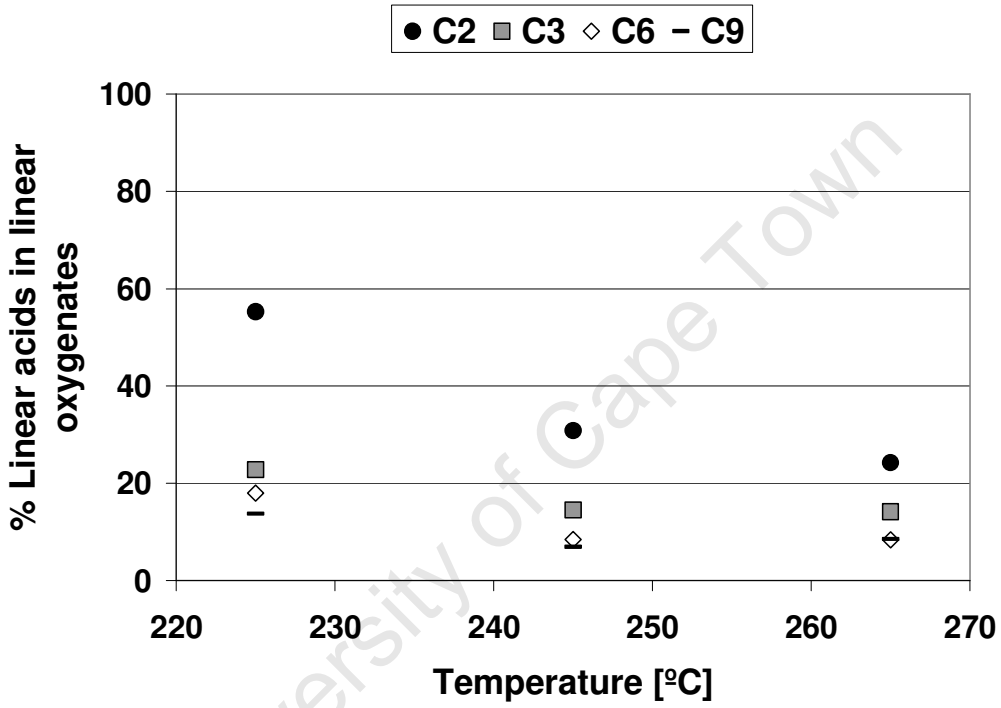

Figure 5.18: Linear carboxylic acid content in the fraction of linear oxygenates (n-alcohol-(1), aldehyde and linear carboxylic acid) for the C_2, C_3, C_6 and C_9 products in experiments performed at 225ºC, 245ºC and 265ºC

In Figure 5.19 the aldehyde to n-alcohol-(1) plus aldehyde ratio is displayed. It is clear from the figure that at lower Fischer-Tropsch temperatures aldehydes are more likely to form than at higher temperatures. Dry (2004) reported that at lower temperatures the hydrogenation of aldehydes to form alcohols are feasible this may explain the decrease in aldehyde selectivity as carbon number increases and the not so pronounced decrease when looking at the aldehyde selectivity at 265 ºC.

What is noticeable from the above figures are that the linear oxygenates consist mostly out of n-alcohols-(1). If aldehydes, alcohols and acids are formed primarily by the same mechanism (see Chapter 4 Schemes 4.3 and 4.4) then the formation rate of alcohols are must faster than the formation rate of the other oxygenated compounds.

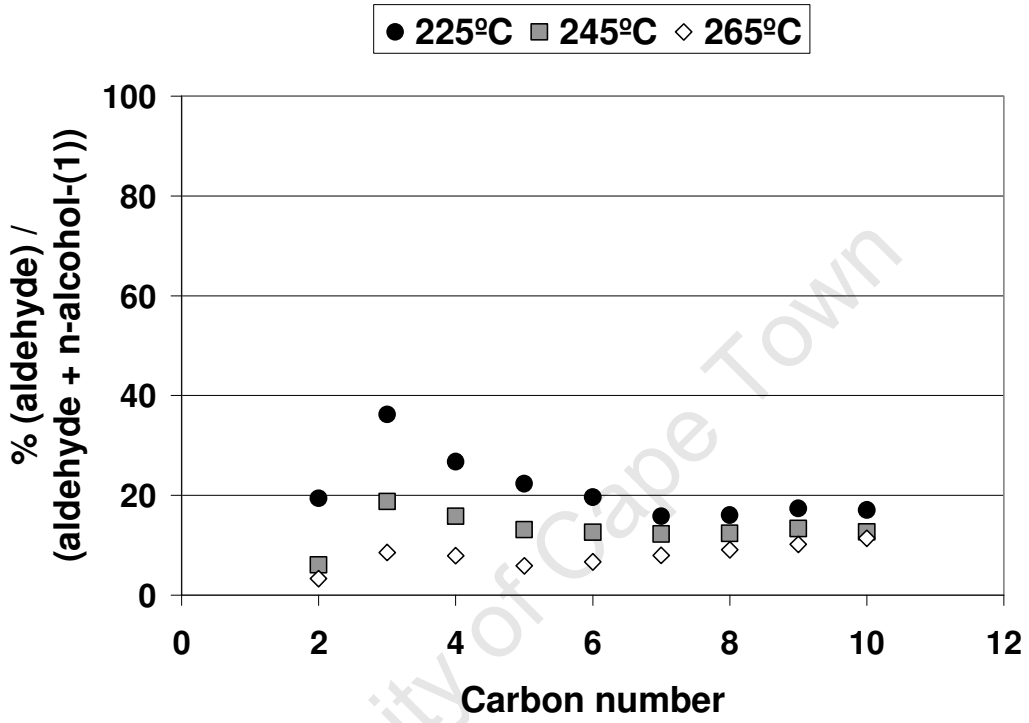

Figure 5.19: Aldehyde content in the fraction of n-alcohols-(1) plus aldehyde for the C_2 to C_{10} products in the Fischer-Tropsch synthesis performed at 225ºC, 245ºC and 265ºC

The percentage n-alcohol-(2) selectivity in the fraction of n-alcohol-(2) plus methyl alkyl ketone are displayed in Figure 5.20. In this figure one can see that the n-alcohol-(2) selectivity increases as carbon number increases. There is also not a clear relationship between the effects of synthesis temperature on the selectivity of the n-alcohols-(2), but there might be a slight decrease in n-alcohol-(2) selectivity as temperature decreases.

If there exist a relationship between methyl alkyl ketone and n-alcohol-(2) selectivity then it may be that with increasing carbon number the likelihood increases that ketones undergo secondary reactions to form n-alcohols-(2).

See equation 5.1. Secondary reactions of ketones to form n-alcohols-(2) have been observed by Dry (2004) at higher temperatures for the Fischer-Tropsch synthesis.

$$ketone + H_2 \leftrightarrow n - alcohol - (2) \quad (5.1)$$

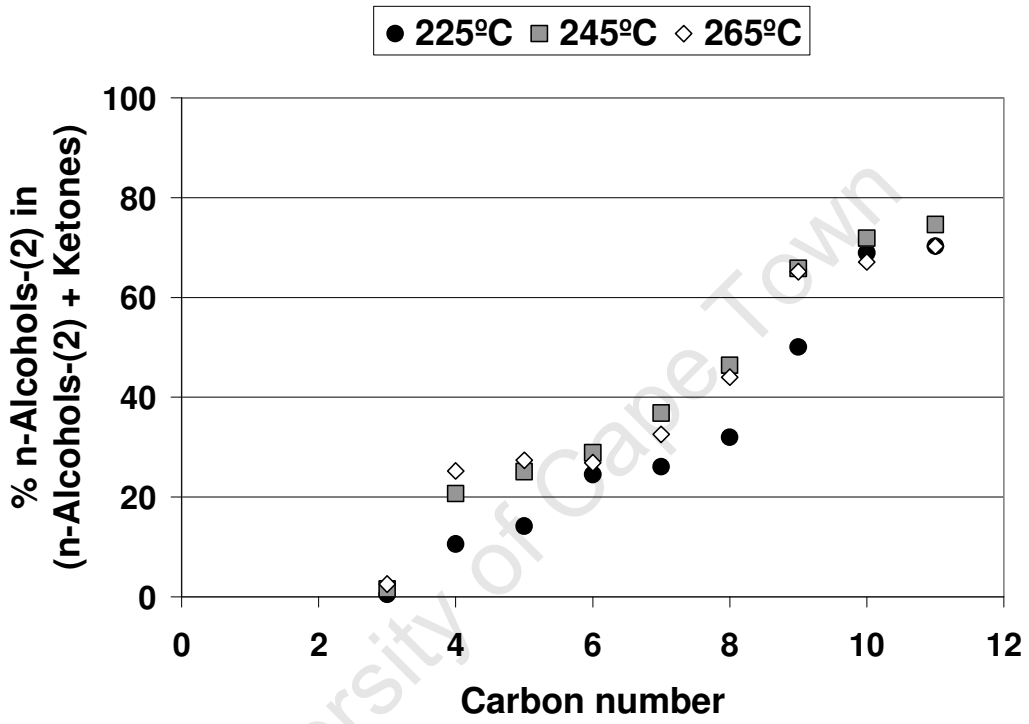

Figure 5.20: n-Alcohol-(2) content in the fraction of n-alcohol-(2) plus methyl alkyl ketone for the C_3 to C_{11} product of the Fischer-Tropsch synthesis at 225ºC, 245ºC and 265ºC

5.2.1.2. The effect of H_2/CO feed ratio

As with the investigation of the influence of temperature on oxygenate selectivity figures were constructed to investigate the influence of H_2/CO feed ratios on oxygenate selectivity.

For all the runs at different H_2/CO feed ratios the CO + CO_2 conversion were kept constant. To achieve this, the GHSV were lowered to keep a

constant conversion at low H_2/CO ratios and increased at higher H_2/CO ratios.

Taking the above in consideration one would expect the CO partial pressure to be higher at the H_2/CO feed ratio of 1.3 than at the feed ratio of 2.1. If this is so then the catalyst surface coverage by adsorbed monomers, whatever the chemical make-up of the monomers, will be higher (Dry, 2004). If one assumes that an oxygen containing surface specie is responsible for the formation of oxygenates (see Chapter 4 Scheme 4.3) then one can expect with higher surface coverage of this monomer the formation of oxygenates will increase.

In Figure 5.21 the % linear oxygenates (n-alcohol-(1), n-alcohol-(2), linear carboxylic acid, aldehyde and alkyl methyl ketone) in linear Fischer-Tropsch product is displayed which depicts a slight increase as H_2/CO feed ratio decreases which is consistent with the above discussion as well as with observations from Roper (1983), Claeys (1997) and Liu et al. (2007) that a general decrease are observed in total oxygenate selectivity as H_2/CO ratio increases.

Taking a closer look at oxygenate selectivity it is apparent that as observed from the selectivity trends of the runs at various temperatures, (Figures 5.15 to 5.20) the linear oxygenates consist mostly (ca. 95%) of n-alcohols-(1), aldehydes and linear carboxylic acids and this seem to stay constant as carbon number increases (see Figure 5.22). For the C_3 fraction however there appear to be a bit more n-alcohols-(2) and alkyl-methyl-ketones. Another observation is that no significant effects are noticed on the contents of n-alcohols-(1), aldehydes and linear carboxylic acids in the linear oxygenates as H_2/CO feed ratio varies.

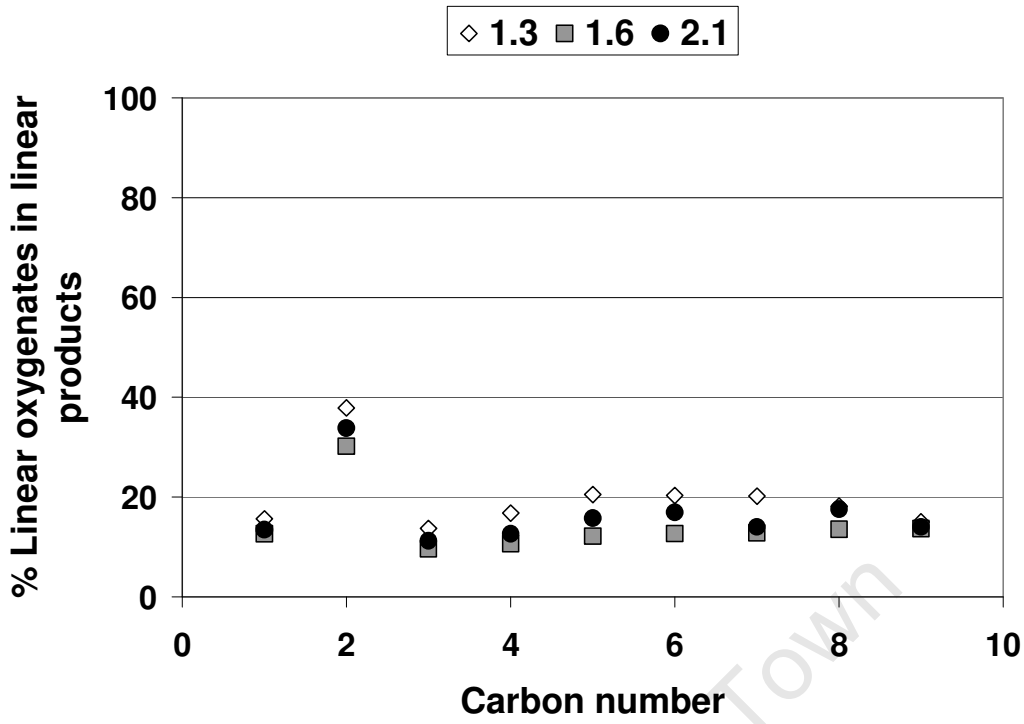

Figure 5.21: % Linear oxygenates in linear products for the C_1 to C_9 product range obtained from Fischer-Tropsch runs at H_2/CO ratios of 1.3, 1.6 and 2.1

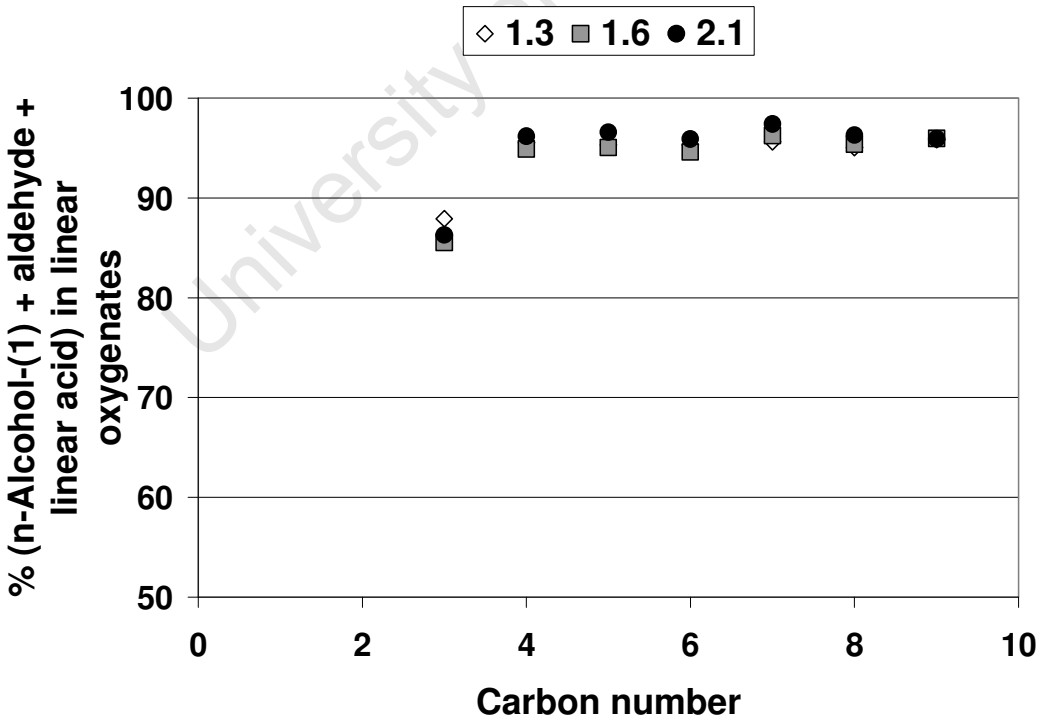

Figure 5.22: % n-Alcohol-(1) + aldehyde + linear carboxylic acid selectivity in linear oxygenates for the C_3 to C_9 product range for runs performed at 1.3, 1.6 and 2.1

In Figure 5.23 the content of n-alcohols-(1) in the fraction of linear oxygenates (n-alcohols-(1), linear carboxylic acids and aldehydes) are displayed. A few things are noticed. Firstly the n-alcohol-(1) selectivity appears to increase with decreasing H_2/CO feed ratios. Thus at a ratio of 2.1 the n-alcohol selectivity is lower. Similar observations were made by Roper (1983) and Claeys (1997). Liu et al. on the other hand observed a decrease in alcohol selectivity as H_2/CO ratios decreased. Secondly, the n-alcohol-(1) content in the fraction of linear oxygenates appear to increase with increasing carbon number.

If one can assume that if n-alcohols-(1), aldehydes and acids are formed via a primary reaction pathway and the formation of these compounds are interrelated, then n-alcohol-(1) formation appears to be favoured at lower H_2/CO feed ratios.

Regarding the increase in n-alcohol-(1) selectivity as carbon number increases, this may indicate the existence of a reaction pathway between aldehydes and linear alcohols and between linear carboxylic acids and linear alcohols for the n-alcohols-(1) may be formed from aldehydes and linear carboxylic acids through secondary reactions. The likelihood of secondary reactions usually increases with increasing carbon number. Furthermore the secondary reactions do not appear do be influenced by the changes in the H_2/CO feed ratio for all the trends feature a steady increase.

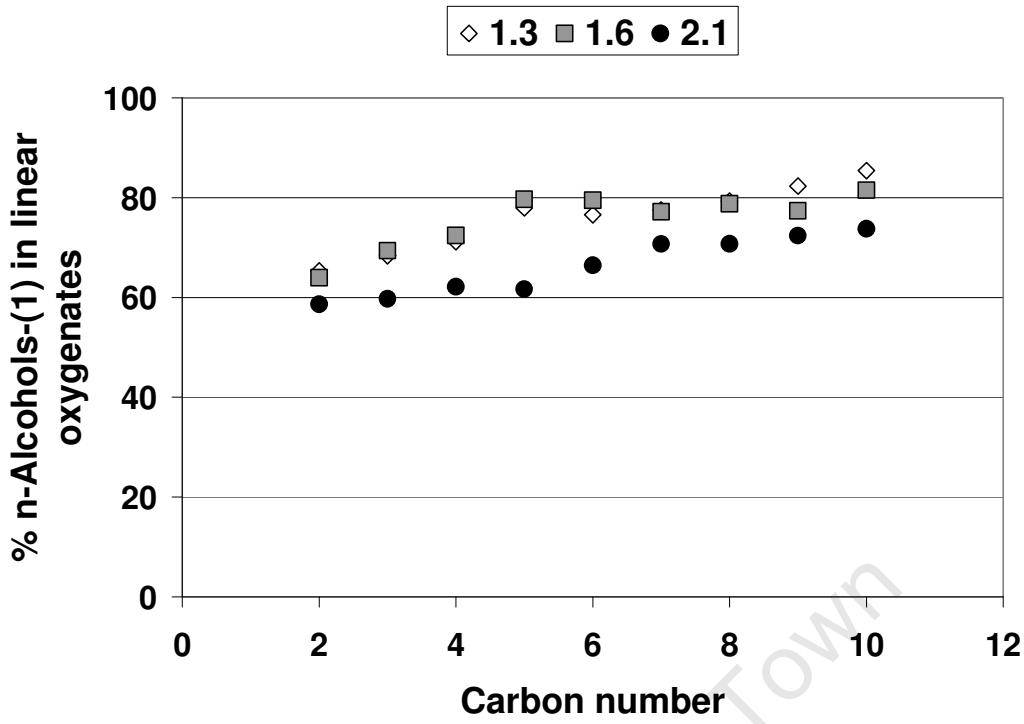

Figure 5.23: n-Alcohols-(1) content in the fraction of linear oxygenates (n-alcohol-(1), aldehyde and linear carboxylic acid) for the C_2 to C_{10} products in experiments performed at H_2/CO feed ratios of 1.3, 1.6 and 2.1

Figures 5.24 show the content of linear carboxylic acid in the fraction of linear oxygenates (n-alcohols-(1), linear carboxylic acids and aldehydes). The linear carboxylic acid content in the fraction of linear oxygenates generally appear to decrease as H_2/CO feed ratio increases. This is in accordance with observations by Liu et al. (2007). The acid selectivity also decreases as the carbon number increases.

If there exist a reaction pathway between linear carboxylic acids and linear alcohols then it is possible that linear carboxylic acids undergo secondary reactions, to form n-alcohols-(1) and the likelihood of this occurring increases with increasing carbon numbers. This can therefore explain the decrease in acid selectivity and increase in n-alcohol-(1) selectivity (Figure 5.23). Changes in H_2/CO ratio do not seem to influence the degree of secondary reactions if one assumes that it occurs.

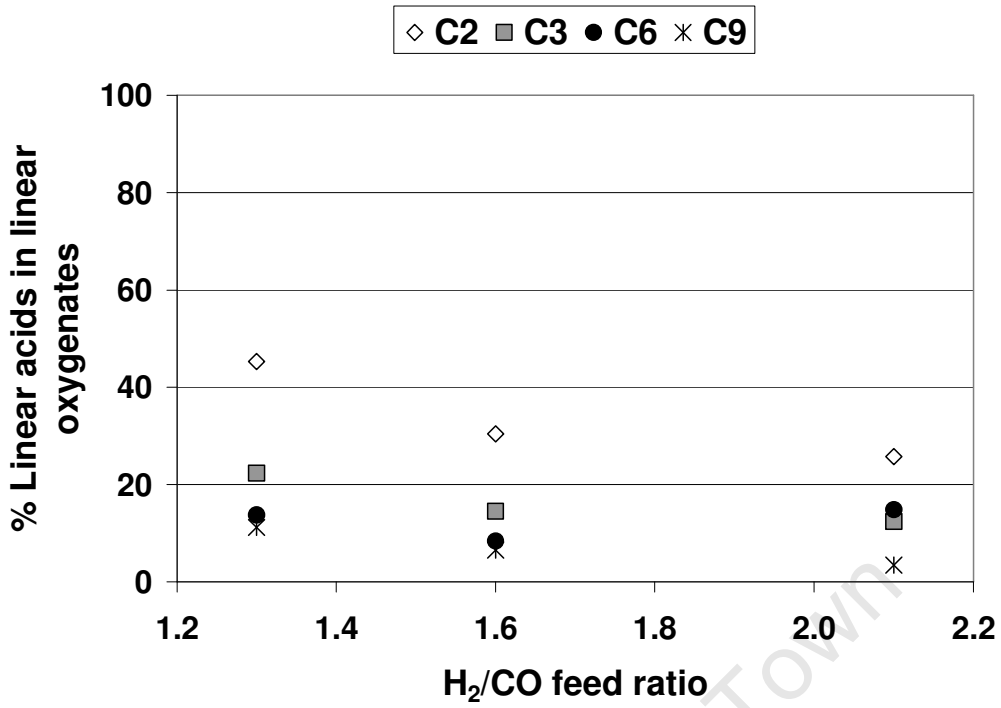

Figure 5.24: Linear carboxylic acid content in the fraction of linear oxygenates (n-alcohol-(1), aldehyde and linear carboxylic acid) for the C_2, C_3, C_6 and C_9 products in experiments performed at H_2/CO feed ratios of 1.3, 1.6 and 2.1

There might also be a relationship between the n-alcohol-(1) and aldehyde selectivity as eluded from the above discussion. In Figure 5.25 the aldehyde to n-alcohol-(1) ratio is displayed. It seems that at a high H_2/CO feed ratio such as 2.1, the aldehyde selectivity is higher than at a low H_2/CO feed ratio such as 1.3. This is in contrast to observations made by Liu et al. (2007).

Earlier the effect of temperature on aldehyde selectivity was discussed and it was mentioned that at low Fischer-Tropsch temperatures such as 237ºC the hydrogenation of aldehydes to form alcohols are feasible (Dry, 2004). The experiments to investigate the effect of H_2/CO ratio on selectivity were performed at 245ºC. Taking this in consideration at lower H_2/CO ratios it may be possible for aldehydes to undergo more secondary reactions to form n-alcohols-(1). Furthermore at the low H_2/CO feed ratio runs the GHSV were lowered to sustain a constant CO + CO_2 ratio and therefore increasing residence time of the products produced and therefore increasing the likelihood of secondary reactions occurring.

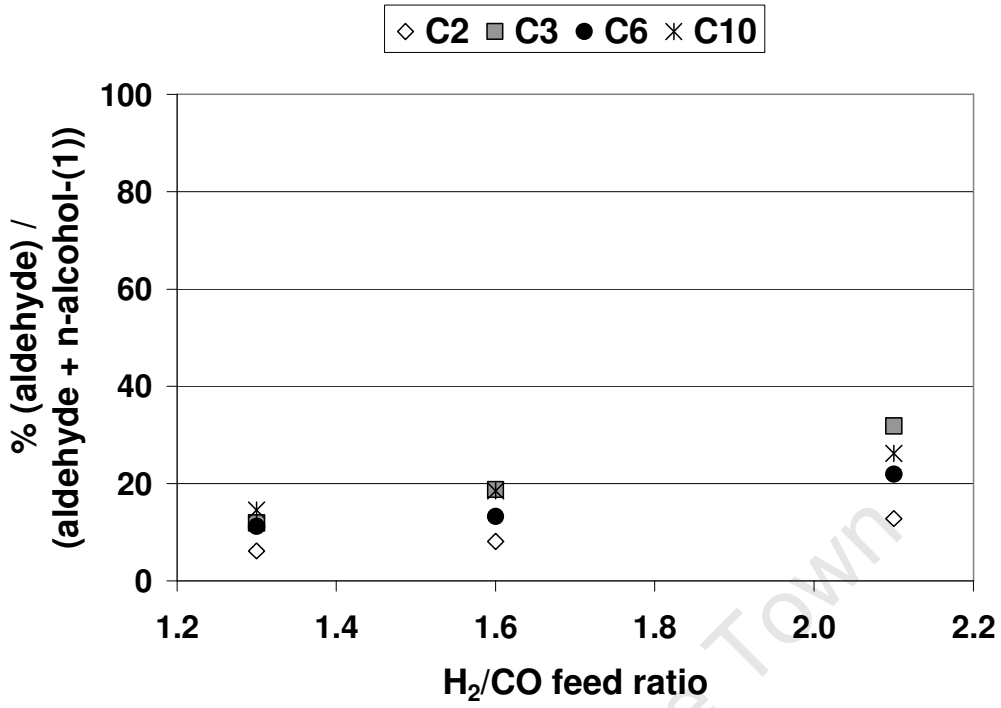

Figure 5.25: n-Alcohol-(1) content in the fraction of n-alcohol-(1) plus aldehyde for the C_2, C_3, C_6 and C_{10} products for runs at H_2/CO feed ratios of 1.3, 1.6 and 2.1

The percentage n-alcohol-(2) selectivity in the fraction of n-alcohol-(2) plus methyl alkyl ketone are displayed in Figure 5.26. In this figure one can see that the n-alcohol-(2) selectivity increases as carbon number increases. A slight increase in n-alcohol-(2) selectivity is also observed in relation to the methyl alkyl ketone selectivity as the H_2/O feed ratio decreases.

If there exist a relationship between methyl alkyl ketone and n-alcohol-(2) selectivity then it may be that with increasing carbon number the likelihood increases that ketones undergo secondary reactions to form n-alcohols-(2). See equation 5.1 in section 5.2.1.1. Furthermore as stated in the discussion about aldehyde selectivity, the GHSV was lowered to sustain a constant conversion therefore the residence time of the products and reactants increased and therefore also the likelihood of secondary reactions.

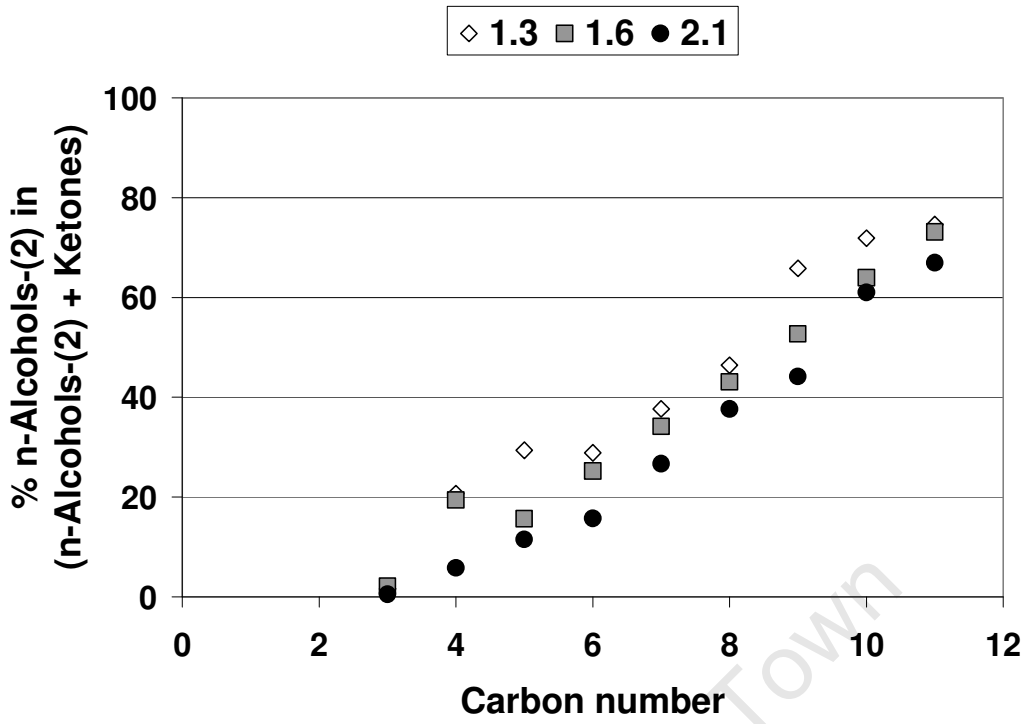

Figure 5.26: n-Alcohol-(2) content in the fraction of n-alcohol-(2) plus methyl alkyl ketone for the C_3 to C_{11} product of the Fischer-Tropsch synthesis using H_2/CO feed ratios of 1.3, 1.6 and 2.1

5.2.2. Other Selectivities

In the above section the application of GCxGC in the study of oxygenate selectivity and the factors that may influence the formation of the various oxygenated compounds were discussed. Although the focus on this study was mostly on the selectivity of oxygenates to illustrate the application of GCxGC, it also has the ability to separate and detect compounds such as linear olefins, paraffins and branched products present in the Fischer-Tropsch products.

Little is known about the effect of reaction conditions on the primary olefin content. Higher temperatures seem to favour the formation of olefins compared to paraffins (Dry, 2004) and an increase in H_2/CO feed ratio is expected to results in a decrease of primary olefin selectivities.

In Chapter 4 Figure 4.15 the linear olefins in the fraction of linear olefins plus linear paraffins were displayed as a function of carbon number for the various runs at 225ºC, 245ºC and 265ºC.

The linear olefins present in the fraction of linear hydrocarbons for C_2 decreases with increasing reaction temperature, but for C_3 to C_{12} increases with increasing reaction temperature (see also 4.3.3). One would expect as stated in literature (Dry, 2004), that primary olefin selectivity increases with temperature. The extent of secondary reactions may also increase. Therefore the decrease in C_2 olefin selectivity as temperature increase indicate that the secondary reaction of the C_2 specie is more likely to occur at higher temperatures whereas the increase in the C_3 to C_{12} ratio as temperature increase indicate that the primary formation of olefins were favoured more at the higher temperature.

The linear olefins in the fraction of linear olefins plus linear paraffins for runs at different H_2/CO feed ratios were shown in Chapter 4 Figure 4.16. For the C_2 product fraction the linear olefins does not appear to vary but for the C_3 to C_{12} fraction the ratio appear to decrease slightly as the H_2/CO feed ratio increases. Therefore the product produced at lower feed ratios appears to be more olefinic and it can be concluded that with increasing H_2/CO ratio more secondary reaction of the primary olefins occur. The result of the C_2 ratio is puzzling and needs to be investigated further.

In Chapter 4 section 4.3.3 Figure 4.17 the 1-olefin content in the fraction of linear olefins for the C_6 to C_{15} product cut obtained from the runs at different temperatures and different H_2/CO feed ratios respectively were displayed. From the graphs it appears as if at lower temperatures the linear olefin product consists mostly of 1-olefins and at higher temperatures more internal olefins are formed, thus more secondary double bond isomerisation occurs. When changing the H_2/CO feed ratio no significant changes were observed with regards to the 1-olefin content in the fraction of linear olefins. Thus, H_2/CO feed ratio does not seem to have a significant effect on olefin double bond isomerisation.

During Fischer-Tropsch synthesis branched products are also produced which includes branched paraffins, branched olefins, branched alcohols and branched acids. The principal of orthogonal separation which separates compounds, moving through a GCxGC system, on the basis of boiling point and functionality allows for the easy identification and quantification of branched products (see section 5.1). The amount of branched compounds produced during low temperature Fischer-Tropsch synthesis is very low and consist mainly of mono-methyl branched compounds (Claeys and Van Steen, 2004). Branched products may also form via a primary or secondary route (Schulz, 1990). In Tables 5.2 and 5.3 the branched product selectivities recorded for the C_4 to C_{15} product fraction of the Fischer-Tropsch product are displayed and it appears as if the branched functionality increases as temperature is raised in the order of: 225ºC < 245ºC < 265ºC and decreases as the H_2/CO feed ratio increases in the order of: 1.3 > 1.6 >2.1. Thus at higher temperatures the primary or secondary formation are enhanced this is in agreement with observations by Roper (1983) and Claeys (1997) that the selectivity towards branched products increase as Fischer-Tropsch synthesis reaction temperature increases. The observation of the increase in branching as the H_2/CO ratio decreases is however in disagreement with their observations (see Table 2.1 in Chapter 2).

Table 5.2: Summation of the selectivities of the branched products detected in the C_4 to C_{15} range of the Fischer-Tropsch product produced from runs at 225ºC, 245ºC and 265ºC *(Note selectivity is expressed as % C atom)*

Run	Branched Paraffins	Branched Olefins	Branched Alcohols	Branched Acids
225ºC	0.316	0.376	0.3145	0.046
245ºC	0.517	0.607	0.4894	0.064
265ºC	1.006	1.461	0.6589	0.045

Table 5.3: Summation of the selectivities of the branched products detected in the C_4 to C_{15} range of the Fischer-Tropsch product produced from runs at different H_2/CO feed ratios *(Note selectivity is expressed as % C atom)*

Run	Branched Paraffins	Branched Olefins	Branched Alcohols	Branched Acids
1.3	0.668	0.956	0.5958	0.058
1.6	0.557	0.675	0.5186	0.041
2.1	0.445	0.454	0.3801	0.019

CHAPTER 6

CONCLUSIONS AND RECOMMENDATIONS

6.1 CONCLUSIONS

The purpose of this thesis was to prove that two-dimensional gas chromatography (GCxGC) does offer improved separation and detection of especially trace compounds and that this analytical technique will benefit Fischer-Tropsch research as claimed in literature (Dallüge et. al., 2003; Vendeuvre et. al., 2005). To prove these claims the following issues were investigated:

- The comparison of GCxGC performance vs. 1D GC performance.
- The application of GCxGC vs. 1D GC for Fischer-Tropsch product analyses with special focus on the minor Fischer-Tropsch products such as oxygenates.

6.1.1 GCxGC performance versus 1D GC

Before comparing the performance of GCxGC with the performance of the 1D GC, on-line and off-line GCxGC methods for the analyses of the gaseous and liquid oil product of Fischer-Tropsch synthesis were developed. The validity of the methods were confirmed by injecting a test mixture several times on both the GCxGC and the 1D GC systems and then to compare the results of the two systems in terms of detection ability and accuracy (see Chapter 4).

It is evident from the results displayed in Chapter 4 that GCxGC and 1D GC display similar results for the detection of the major Fischer-Tropsch products such as n-paraffins, 1-olefins and n-alcohols-(1), thus both GCxGC and 1D GC methods are suitable for the analyses of the major product compounds. A distinct difference between GCxGC and 1D GC methods are

however observed when comparing the separation and detection of the minor compounds such as the acids, ketones, aldehydes, secondary alcohols and branched compounds (refer to Table 4.6). The performance of the GCxGC is more superior especially in terms of the analyses of the minor compounds. The advantages of GCxGC in relation to 1D GC can be summarized as follows:

- GCxGC has a greater ability to separate compounds with similar boiling points and functionality which tends to co-elute with each other when using 1D GC separation methods.
- Due to modulation GCxGC can detect and separate minor compounds which are present in low concentrations in the Fischer-Tropsch sample matrix. These compounds are not easily detected by 1D GC for the major compounds with high concentrations tend to absorb them.
- With GCxGC it is possible to separate the minor compounds in terms of their functional groups and as a function of carbon number.
- Although GCxGC and 1D GC both takes approximately 80 minutes to analyze a Fischer-Tropsch oil product, more compounds are separated and detected by the GCxGC thus more selectivity information is available for the construction of a Fischer-Tropsch synthesis product spectrum.
- With GCxGC it is possible to develop a method that allows for one analyses instead of three 1D GC analyses to analyze the C_1 to C_9 Fischer-Tropsch product range. This eliminates reduced accuracy due to the merging of various analyses required to construct a product spectrum for this range.

6.1.2 Application of GCxGC versus 1D GC for Fischer-Tropsch product analyses

The benefits of GCxGC as an application for Fischer-Tropsch research was further illustrated by performing synthesis experiments at various temperatures (225˚C, 245˚C and 265˚C) and H_2/CO feed ratios (1.3, 1.6 and 2.1). The products of these experiments were analyzed using both GCxGC and 1D GC and product distributions were constructed using methods described in Chapter 3.

When comparing the product selectivities obtained from the GCxGC and 1D GC methods (see Chapter 5) it is evident that GCxGC has a lot more to offer for Fischer-Tropsch research than 1D GC. Although it takes approximately the same amount of time to analyse the Fischer-Tropsch products and to translate the analyses into selectivity information, GCxGC generates more accurate information of not only the major compounds (n-paraffins, 1-olefins and n-alcohols-(1)) but it also delivers accurate information of the minor oxygenated and branched products which is very difficult to detect and separate with 1D GC.

Both GCxGC and 1D GC may be suitable for the analyses of the major compounds but GCxGC is a better technique to use when in depth Fischer-Tropsch selectivity studies are performed with a focus on both major and minor compound selectivities.

The real benefits of GCxGC are realised when Anderson-Schulz-Flory plots and other product selectivity graphs are constructed as a function of carbon number of especially the minor compounds (see Chapters 4 and 5). With this information researchers can now start to investigate the influence of synthesis parameters not only on the total product classes (for example ketones) of the minor compounds, but focus can also be shifted to each individual carbon number (for example C_9 ketones). Chain growth probabilities can also be constructed of each of the minor compound classes which may aid in product formation studies.

6.2 RECOMMENDATIONS AND FUTURE WORK

In this study the claims that were made regarding the improved separation and detection of GCxGC as an analytical technique for Fischer-Tropsch product analysis (Dallüge et. al., 2003; Vendeuvre et. al., 2005) were confirmed but this is not the end of the story. In order to really harvest the benefits of GCxGC, as a tool for Fischer-Tropsch research, selectivity and mechanistic research should be more focussed to answer specific defined research questions.

From this study it is recommended that a more in depth investigation be launched in the formation of branched products. In this study the branched products were grouped together but more work can be performed in identifying the individual branched compounds with the purpose of determining the position of the branching as well as the nature of the branching (methyl- or ethyl-branching) as depicted in section 5.1.

Furthermore chain growth probabilities of products, especially the minor products, can be studied in more depth.

The potential and benefits of GCxGC has been proven in this study, but it can also be applied in other Fischer-Tropsch processes such as HTFT and even in the analysis of refinery products or other petrochemical products streams.

REFERENCES

Adahchour, M., Beens, J., Brinkman, U.A.Th.
Recent developments in the application of comprehensive two-dimensional gas chromatography
Journal of Chromatography A 1186 (2008), 67

Adesina, A.A.
Hydrocarbon synthesis via Fischer-Tropsch reaction: travails and triumphs
Applied Catalysis A: General 138 (1996), 345

Amelse, J.A., Butt, J.B., Schwartz, L.H.
Carburization of supported iron synthesis catalysts
Journal of Physical Chemistry 82 (1978), 558

Amelse, J.A.
Silica-supported iron-bimetallic catalysts for the Fischer-Tropsch synthesis
PhD Thesis, Northwestern University, Evanston Illinois, USA (1980), 10

Anderson, R.B.
Catalysts for the Fischer-Tropsch synthesis
In "Catalysis" (P.H. Emmett, Ed.), Vol. 4, p.1, van Nostrand Reinhold, New York (1956)

Anderson, R. B., Seligman, B., Shultz, J. F., Kelly, R., Elliott, M. A.,
Fischer-Tropsch Synthesis. Some Important Variables of the Synthesis on Iron Catalysts
Industrial and Engineering Chemistry 44(2) (1952), 391

AOAC International
AOAC Peer Verified Methods Program - Manual on policies and procedures
Arlington VA 22201-3301, USA

Badische Analin u. Soda Fabrik

German Patent 293, 787 (1913)

Bartholomew, C.H., Farrauto, R.J.

(2006) *Fundamentals of Industrial Catalytic Processes.* 2nd ed., p. 398 – 467, New Jersey, John Wiley & Sons

BBC News

Energy: Meeting soaring demand

http://news.bbc.co.uk/go/pr/fr/-/1/hi/sci/tech/3995135.stm (2004)

Britannica Concise Encyclopedia

Gas chromatography

Encyclopedia Britannica, Inc., 2006. Answers.com 02 Jun. 2008.

http://www.answers.com/topic/gas-chromatography

Bruno, J.R.

Chromatography: Past, Present and Future

Presented at Contemporary Technology for Large Scale Chromatography, March 21-22, 2005

Bukur, D.B., Mukesh, D., Patel, S.A.

Promoter effects on precipitated iron catalysts for Fischer-Tropsch synthesis

Industrial Engineering Chemistry Research 29 (1990), 194

Bukur, D.B., Patel, S.A., Lang, X.

Promoter effects on precipitated iron catalysts for Fischer-Tropsch synthesis

Applied Catalysis A: General 61 (1990), 329

Bukur, D.B., Koranne, M., Lang, X., Rao, K.R.P.M., Huffman, G.P.

Pre-treatment effect studies with a precipitated iron Fischer-Tropsch catalyst

Applied Catalysis A: General 126 (1995a), 85

Bukur, D.B., Okabe, K., Rosynek, M.P., Li, C., Wang, D., Rao, K.R.P.M., Huffman, G.P.
Activation studies with a precipitated iron catalyst for Fischer-Tropsch synthesis. 1. Characterization studies
Journal of Catalysis 155 (1995b), 353

Bukur, D.B., Nowicki, L., Manne, R.K., Lang, X.
Activation studies with a precipitated iron catalyst for Fischer-Tropsch synthesis 2. Reaction studies
Journal of Catalysis 155 (1995c), 366

Bukur, D.B., Sivaraj, C.
Supported iron catalysts for slurry phase Fischer–Tropsch synthesis
Applied Catalysis A: General 231(1-2) (2002), *201*

Cady, W.E., Launer, P.J., Weitkamp, A.W.
Products of the Hydrogenation of Carbon Monoxide: Aromatic Hydrocarbons
Industrial and Engineering Chemistry 45 (1953), 350

Cain, D.G., Weitkamp, A.W., Bowman, N.J.
Products of the Hydrogenation of Carbon Monoxide: Oil-soluble Oxygenated Compounds
Industrial and Engineering Chemistry 45 (1953), 359

Chaumette, P., Courty, P.H., Kiennemann, A., Ernst, B.
Higher alcohol and paraffin synthesis on cobalt based catalysts: comparison of mechanistic aspects
Topics in Catalysis 2 (1995), 117

Claeys, M.
Selectivität, Elementarschritte und kinetische Modellierung bei der Fischer-Tropsch Synthesis
PhD Thesis, University of Karlsruhe, Karlsruhe, Germany (1997)

Claeys, M., Van Steen, E.
Basic studies
Elsevier: Amsterdam: A. Steynberg and M. Dry
Studies in Surface Science and Catalysis 152 (2004), 601

Crawford, K.E., Campbell, J.L., Fiddler, M.N., Duan, P., Qian, K., Gorbaty, M.L., Kenttämaa H.I.
Laser-Induced Acoustic Desorption/Fourier Transform Ion Cyclotron Resonance Mass Spectrometry for Petroleum Distillate Analysis
Analytical Chemistry 77 (24) (2005), 7916

Criddle, D. W., and Le Tourneau, R. L.
Analytical Chemistry 23 (1951), 1620

Davies, P.
Introduction and overview
Presentation for Analyst and investor site visit to Oryx GTL, February 2005
http://www.sasol.com/sasol_internet/downloads/1_PatDavies_Welcome_1109332901579.pdf

Davis, B.H.
Anderson-Schulz-Flory Product Distribution – Can it be avoided for Fischer-Tropsch Synthesis
Presentation at the AIChE 2003 Spring National Meeting, New Orleans, LA March 30 – April 3, 2003

Dallüge, J., Beens, J., Brinkman, U.A.T.
Comprehensive two-dimensional gas chromatography: a powerful and versatile analytical tool
Journal of Chromatography A 1000 (2003), 69

Dancuart, L.P., Steynberg, A.P.,
Fischer-Tropsch based GTL Technology: A New Process?
Presented in the 27th ACS National Meeting, Anaheim, CA, 2004

Dictor, R.A., Bell, A.T.
On-line analysis of Fischer-Tropsch synthesis products
Industrial and Engineering Chemistry Fundamentals 23 (1984), 252

Dictor, R.A., Bell, A.T.
Fischer-Tropsch synthesis over reduced and unreduced iron oxide catalysts
Journal of Catalysis 97 (1986), 121

Dietz, W.A.
Response factors for Gas Chromatographic Analyses
Journal of Gas Chromatography February (1967), 68

Donnelly, T. J., Satterfield, C. N.
Product distributions of the Fischer-Tropsch synthesis on precipitated iron catalysts
Applied Catalysis A: General 52 (1989), 93

Dry, M.E.
The Fischer-Tropsch synthesis
in "*Catalysis-Science and Technology" (J.R. Anderson, M. Boudart, Eds.), Vol.**1,** Springer-Verlag, New York (1981), 160*

Dry, M. E.
Practical and Theoretical Aspects of the Catalytic Fischer-Tropsch Process
Applied Catalysis A: General 138 (1996), 319

Dry, M. E.
Fischer-Tropsch Reactions and the Environment
Applied Catalysis A: General 189 (1999), 185

Dry, M.E.
The Fischer-Tropsch process: 1950-2000
Catalysis Today 71 (2002), 227

Dry, M.E.
Chemical concepts used for engineering
Studies in surface science and catalysis 152 (2004), 196

Dry, M.E.
FT Catalysts
Studies in surface science and catalysis 152 (2004), 523

DuBois, H.D. and Skoog, D.A.
Analytical Chemistry 20 (1948), 624

Duvenhage, D.J., Espinoza, R.L., Coville, N.J.
Fischer-Tropsch precipitated iron catalysts: Deactivation studies
Proceedings of the Sixth International Symposium: Catalyst deactivation, October 3-5 (1994), Ostend, Belgium, 351

Dwyer, D.J., Hardenbergh, J.H.
The catalytic reduction of carbon monoxide over iron surfaces: a surface science investigation
Journal of Catalysis 87 (1984), 66

Dwyer, D.J., Somorjai, G.A.
Hydrogenation of CO and CO_2 over iron foils. Correlations of rate, product distribution, and surface composition
Journal of Catalysis 52 (1978), 291

Elving, P.J., Warshowsky, B.
Analytical Chemistry 19 (1947), 1006

Elbashir, N.O., Roberts, C.B.
Selective control of hydrocarbon product distribution in supercritical phase Fischer-Tropsch synthesis
Preprints - American Chemical Society, Division of Petroleum Chemistry 49 (4) (2004), 422

Fischer, F., Pichler, H.
Ges. Abh. Kenntn. Kohle 13 (1937) 407

Fischer, F., Tropsch, H.
Uber die Herstellung von Ölgemische (Synthol) durch Aufbau aus Kohlenoxyd und Wasserhoff
Brennstoff-Chemie 4 (1923), 276

Fischer, F., Tropsch, H.
German patent 484, 337 (1925)

Fischer, F., Tropsch, H.
Die Erdölsynthese bei gewönlichen Druck aus den Vergassungsprodukten der Kohlen
Brennstoff-Chemie 7 (1926), 97

Flory, P.
Molecular Size Distribution in linear Condensation Products
Journal of American Chemical Society 58 (1936), 1877–1885

Friedel, R.A., Anderson, R.B.
Composition of synthetic liquid fuels, I. Production distribution and analyses of $C_5 – C_8$ paraffin isomers from cobalt catalyst
Journal of the American Chemical Society 72 (1950), 1212

Friedel, R.A., Anderson, R.B.
Journal of the American Chemical Society 2 (1950), 2307

Frohning, C.D.,
in Fischer-Tropsch-Synthese aus Kohle, J. Falbe (ed.), Stuttgart, Thieme (1977).

Frohning, C.D., Kölbel, H., Ralek, M., Rottig, W., Schnur, F., Schulz, H.
Fischer-Tropsch Synthese
In "*Chemierohstoffe aus Kohl*e" (J. Falbe, Ed.), Georg Thieme Verlag, Stuttgart (1977), 219

GC Image, LLC
GC Image™ Users' Guide © 2001–2007 by GC Image, LLC, and the University of Nebraska
http://www.gcimage.com/gcxgc/usersguide/index.html

Goldstein, H. and Healey, M.J.R.
The graphical presentation of a collection of means.
Journal of the Royal Statistical Society 158 (1995), 175-77

Govender, N.S.
Recycling the tail-gas during the Low Temperature Fischer-Tropsch Process
MSc Thesis, University of Cape Town, South Africa (2004)

Harynuk, J., Gorecki, T., Campbell, C.,
On the interpretation of GCxGC data
LCGC North America 20 (9) (2002), 876

Herrington, E.F.G.
The Fischer-Tropsch synthesis considered as a polymerisation reaction
Chemistry and Industry 65 (1946), 346

Hill, M.
Pre-feasibility study completed for Oz GTL plant-Sasol
Engineering News, 26 January 2007
http://www.engineeringnews.co.za/print_version.php?a_id=100641

Hinshaw, J.V.
Comprehensive Two-Dimensional Gas Chromatography
LCGC Europe: GC Connections, February 2004 edition
http://www.lcgceurope.com/lcgceurope/data/articlestandard//lcgceurope/072004/84877/article.pdf

Holbein, B.E., Stephen, J.D., Layzell, D.B.
Canadian Biodiesel Initiative: Aligning Research Needs and Priorities with the Emerging Industry
BIOCAP: Final Report August 23, 2004

Huang, C. S., Xu, L., Davis, B. H
Fischer-Tropsch synthesis: impact of pre-treatment of ultra fine iron oxide upon catalyst structure and selectivity
Fuel Science and Technology International 11 (5-6) (1993), 639

Iglesia, E., Reyes, S.C., Madon, R.J.
Journal of Catalysis 129 (1991), 238

Iglesia, E., Reyes, S.C., Soled, S.L.
Chapter 7: Reaction-transport Selectivity Models and the Design of Fischer-Tropsch Catalysts
In Computer-aided Design of Catalysts, Published by CRC Press, 1993

Iglesia, E., Reyes, S.C., Madon, R.J., Soled, S.L.
Advances in Catalysis 39 2(1993), 221

Jager, B.
Developments in Fischer-Tropsch technology
Studies in Surface Science and Catalysis 107 (1997), 219

Jager, B.
Developments in Fischer-Tropsch technology
Studies in Surface Science and Catalysis 119 (1998), 25

Jager, B., Espinoza, R.
Advances in low-temperature Fischer-Tropsch synthesis
Catalysis Today 23 (1995), 17

Janse van Vuuren, M.J., Govendor, G.N.S., Kotze, R., Masters, G.J., Pete, T.P.
The correlation between double bond isomerization, water gas shift and acid production during Fischer-Tropsch synthesis
ACS Div. Petroleum Chem.Preprints, 50(2), 200-202 (2005)

Janse van Vuuren, M.J., Huyser, J.J., Kupi, G.B., Grobler, T.
Understanding Fe-LTFT selectivity changes with catalyst age
Presented at 236th ACS National Meeting, August 17-21, 2008, Philadelphia, PA, USA

Johnston, O., Joyner, R.
Stud. Surf. Sci. Catal. 75 (1993) 165

Jothimurugesan, K., Goodwin, J.G. Jr., Gangwal, K.S., Spivey, J.J.
Development of iron Fischer-Tropsch catalysts for slurry bubble column reactors
Catalysis Today 58 (2000), 335

Jung H., Thomson W. J.
Dynamic X-Ray Diffraction Study of an Unreduced Iron Oxide Catalyst in Fischer-Tropsch Synthesis
Journal of Catalysis 139 (2) (1993), 375

Kölbel, H., Ralek, M.
The Fischer-Tropsch synthesis in the liquid phase
Catalysis Review-Science and Engineering 21 (1980), 225

Labhouse (PTY)LTD
Labouse GC training course
User Manual 1st ed., September 2003, p.14

Ledford, E.B., TerMaat, J.R., Billesbach, C.A.
Technical Note KT 030505-1: Introduction to GCxGC
http://www.zoex.com/TechnicalNote_word.doc

Liu, Y., Teng, B.T., Guo, X.H., Li, Y., Chang, J., Tian, L., Hao, X., Wang, Y., Xiang, H.W., Xu, Y.Y., Li, Y.W.,
Effect of reaction conditions on the catalytic performance of Fe-Mn catalyst for Fischer-Tropsch synthesis.
Journal of Molecular Catalysis A: Chemical 272 (2007) 182

Lox, E.S., Froment, G.F.
Kinetics of the Fischer-Tropsch reaction on a precipitated promoted iron catalyst. 1. Experimental procedure and results
Industrial Engineering Chemistry Research 32 (1993), 61

Lox, E.S., Marin, G.B., de Graeve, E., Bussiere, P.
Characterization of a promoted precipitated iron catalyst for Fischer-Tropsch synthesis
Applied Catalysis 40 (1988), 197

McGraw-Hill Encyclopedia of Science and Technology
Gas chromatography
Retrieved June 02, 2008, from Answers.com Web site:
http://www.answers.com/topic/gas-chromatography

McNaught, A.D., Wilkinson, A.
IUPAC Compendium of Chemical Terminology
The Gold Book, 2nd ed., Blackwell Science (1997)

Maitlis, P., Long, H., Quyoum, R., Turner, M., Whang, Z.Q.
Heterogeneous Catalysis of C-C Bond Formation: Black Art or organometallic Science
J. Chem.Soc., Chem. Comm. 1 (1996), 1

Maitlis, P., Quyoum, R., Long, H., Turner, M.
Towards a chemical Understanding of the Fischer-Tropsch Reaction: Alkene formation
Appl. Catal. A: Gen. 186 (1999), 363

Maitlis, P. M.
A new View of the Fischer-Tropsch Polymerization Reaction
Pure Appl. Chem. 61 (1989), 1747

Malherbe, J.A.
The effect of catalyst pre-treatment on the mechanical integrity and synthesis performance of an iron-based Fischer-Tropsch
MEng Thesis, University of Cape Town, *South Africa (2006)*

Masters, C.
The Fischer-Tropsch reaction
Advances in Organometallic Chemistry 17 (1979), 61

Newsome, D.S.
The water-gas shift reaction
Catalysis Review- Science and Engineering 21 (1980), 275

Niemantsverdriet, J.W., Van der Kraan, A.M., Van Dijk, W.L., Van der Baan, H.S.
Behaviour of metallic iron catalysts during Fischer-Tropsch synthesis studied with Mössbauer spectroscopy, X-ray diffraction, carbon content determination, and reaction kinetic measurements
Journal of Physical Chemistry 84 (1980), 3363

Nijs, H.H. and Jacobs, P.A.
On-line single run analysis of effluents from a Fischer-Tropsch Reactor
Journal of Chromatographic Science 18 (1981), 40

O'Brien, R.J., Xu, L., Bao, S., Raje, A., Davis, B.H.
Activity, selectivity and attrition characteristics of supported iron Fischer–Tropsch catalysts
Applied Catalysis A: General 196(2) (2000), 173

Pichler, H.
Über die Auffindung and Synthese neuer höchstmolecularer Paraffine
Brenstoff-Chemie 19 (1938), 226

Pichler, H. And Schulz, H.
Neue Erkenntnisse auf dem Gebiet der Synthese von Kohlenwasserstoffen aus CO und H_2
Chemie Ingenieur Technik 42(18) (1970), 1162

Puskas, I., Hurlbut, R.S.
Comments about the causes of deviations from the Anderson-Schulz-Flory distribution of the Fischer-Tropsch reaction products
Catalysis Today 84 (2003), 99

Rao, V.U.S., Stiegel, G.J., Cinquegrane, G.J., Srivastave, R.D.
Iron-based catalysts for slurry-phase Fischer-Tropsch process: Technology review
Fuel Processing Technology 30 (1992), 83

Rao, K.R.P.M., Huggins, F.E., Mahajan, V., Huffman, G.P., Rao, V.U.S.
Mössbauer spectroscopy study of CO-precipitated Fischer-Tropsch iron catalysts
Hyperfine Interaction 93 (1994), 1751

Bhatt, B.L., Bukur, D.B., Davis, B.H., O'Brien, R.J.
Mössbauer spectroscopy study of iron-based catalysts used in Fischer-Tropsch synthesis
Topics in Catalysis 2 (1995), 71

Raupp, G.B., Delgass, W.N.
Mössbauer investigation of supported Fe catalysts. III In-situ kinetics and spectroscopy during Fischer-Tropsch synthesis
Journal of Catalysis 58 (1979), 361

Reichenbach, S.E., Ni, M., Zhang, D., Ledford Jr.,E.B.
Image background removal in comprehensive two-dimensional gas chromatography
Journal of Chromatography, A 985 (1) (2003), 47

Reichenbach, S.E., Ni, M., Kottapalli, V., Visvanathan, A.
Information technologies for comprehensive two-dimensional gas chromatography
Chemometrics and Intelligent Laboratory Systems 71 (2004), 107

Roginski, S.
3rd Congress on Catalysis. Amsterdam, (1965) 939

Röper, M.
Fischer-Tropsch synthesis.
in "*Catalysis in C_1 Chemistry*" (W. Keim, Ed.), p. 41, D. Reidel, Dordrecht, The Netherlands (1983)

Sabatier, P., Senderens, J.B.
Comptes Rendus Hebd. Seances Acad. Sci. Paris, 134 (1902), 689

Satterfield, C.N., Huff Jr., G.A.
Usefulness of a slurry-type Fischer-Tropsch reactor for processing synthesis gas of low hydrogen-carbon monoxide ratios
Canadian Journal of Chemical Engineering 60 (1982), 159

Schulz, G. V.
Highly polymerized Compounds. CXXII The Relation between Reaction Rate and Composition of the Reaction Product in Macropolymerization Processes
Z. Phys. Chem. B30 (1930), 379–98.

Schulz, H.
Molekülaufbau bei der Fischer-Tropsch Synthese. Reaktionsschritte des Molekülsaufbau durch katalytische Umsetzung von Kohlenoxyd und Wasserstoff
Erdöl und Kohle. 30 (1977), 123

Schulz, H.
Selectivity and mechanism of the Fischer-Tropsch CO-hydrogenation
C1 Molecular Chemistry 1 (1985), 231

Schulz, H., Gökcebay, H.
Catalysis of Organic Reactions
J. Kosak (ed.), Marcel Dekker, New York (1984), p.153

Schulz, H.
Short history and present trends of Fischer-Tropsch synthesis
Applied Catalysis A: General 186 (1999), 3-12

Schulz, H. and Claeys, M.
Kinetic Modelling of Fischer-Tropsch Product Distributions
Applied Catalysis A: General 186 (1999a), 91

Schulz, H. and Claeys, M.
Reactions of α-olefins of different Chain Length added during Fischer-Tropsch Synthesis on a Cobalt Catalyst in a Slurry Reactor
Applied Catalysis A: General 186 (1999b), 71

Schulz, H., van Steen, E., Claeys, M.
Selectivity and mechanism of Fischer-Tropsch synthesis with iron and cobalt catalysts
Studies Surface Science and Catalysis 81 (1994), 455

Schulz, H., Erich, E., Gorre, H., van Steen, E.,
Regularities as a key for discriminating surface reactions and formation of the dynamic system
Catalysis Letters 7 (1990) 157

Shroff, M.D., Kalakkad, D.S., Coulter, K.E., Kohler, S.D., Harrington, M.S., Jackson, N.B., Sault, A.G., Datye, A.K.
Activation of Precipitated Iron Fischer-Tropsch Synthesis Catalyst
Journal of Catalysis 156 (1995), 185

Siggia, S.
Quantitative Organic Analysis via Functional Groups
p.4, 24, New York, John Wiley & Sons, 1949

Steitz, A. and Barnes, D.K.
Products of Hydrogenation of Carbon Monoxide: Water-soluble Oxygenated Compounds
Industrial and Engineering Chemistry 45 (1953), 353

Sternberg, A. and Wender, J.
Proc. Intern. Conf. Coordination Chem.
The Chemical Society, London (1959) 53

Steynberg, A.P., Espinoza, R.L., Jager, B., Vosloo, A.C.
High Temperature Fischer-Tropsch synthesis in commercial practice
Applied Catalysis A: General 186 (1999), 41

Steynberg, A.P.
Introduction to Fischer-Tropsch Technology
Studies in surface science and catalysis 152 (2004), 1-63

Storch, H.H., Golumbic, N., Anderson, R.B.
The Fischer-Tropsch and related synthesis
John Wiley & Sons, New York (1951), 610

Stranges, A.N.
AIChE 3rd Topical Conference on Natural Gas Utilization (Chen-Hwa Chiu, R.D. Srivastava and R. Mallison, Ed.), New Orleans (2003), 635-646

Sudsakorn, K., Goodwin, J.G, Jr., Jothimurugesan, K., Adeyiga, A.A.
Preparation of attrition-resistant spray-dried Fe Fischer-Tropsch catalyst using precipitated SiO2
Industrial Engineering Chemistry Research 40 (2001), 4778

Tau, L., Dabbagh, H., Davis, B.H.
Fischer-Tropsch synthesis: carbon-14 tracer study of alkene incorporation
Energy and Fuels 4 (1990), 94

Tau, L., Dabbagh, H., Davis, B.H.
Fischer-Tropsch synthesis: comparison of carbon-14 distributions when labelled alcohol is added to the synthesis gas
Energy Fuels 5 (1991), 174

Tillmetz, K.D.
Chem.-Ing.-Tech. 48 (1978), 1065

Van Berge, P.J., Everson, R.C.
Cobalt as an alternative Fischer-Tropsch catalyst to iron for the production of middle distillates
Studies in Surface Science and Catalysis 107 (1997), 207

Vannice, M.A.
Catalytic synthesis of hydrocarbons from hydrogen-carbon monoxide mixtures over group VIII metals. I. Specific activities and product distributions of supported metals
Journal of Catalysis 37 (1975), 449

Van der Laan, G.P., Beenackers, A.A.C.M.
Kinetics and selectivity of the Fischer-Tropsch synthesis: A literature review
Catalysis Reviews - Science and Engineering 41 (1999), 255

Van der Laan, G.P., Beenackers, A.A.C.M.
Intrinsic kinetics of the gas–solid Fischer–Tropsch and water gas shift reactions over a precipitated iron catalyst
Applied Catalysis A: General 193 (2000), 39

Van der Merwe, C.
Sasol to spend R300m on coal-to-liquids feasibility study
Engineering News, 10 March 2008
http://www.engineeringnews.co.za/print_version.php?a_id=128825

Vendeuvre, C., Bertoncini, F., Duval, L., Duplan, J-L., Thiébaut, D., Hennion, M-C.
Comparison of conventional gas chromatography and comprehensive two-dimensional gas chromatography for the detailed analysis of petrochemical samples
Journal of Chromatography A, 1056 (2004), 155

Vendeuvre, C., Ruiz-Guerrero, R., Bertoncini, F., Duval, L., Thiébaut, D., Hennion, M-C.
Characterisation of middle-distillates by comprehensive two dimensional gas chromatography (GCxGC): A powerful alternative for performing various standard analysis of middle-distillates
Journal of Chromatography A, 1086 (2005), 21

Venkatramani, C.J., Xu, J.Z., Phillips, J.B.,
Analytical chemistry 68 (1996), 1486

Von Christoffel, E., Surjo, I., Baerns, M.
Chemiker-Z 102 (1978)

Weitkamp, A.W., Seelig, H.S., Bowman, N.J., Cady, W.E.
Products of the Hydrogenation of Carbon Monoxide over and Iron Catalyst
Industrial and Engineering Chemistry 45 (1953), 343

Weitkamp, A.W., Frye, C.G.
Products of the Hydrogenation of Carbon Monoxide: Relation of Product composition to Reaction Mechansim
Industrial and Engineering Chemistry 45 (1953), 363

Xu, L., Bao, S., Houpt, D. J., Lambert, S. H., Davis, B. H.
Role of CO_2 in the initiation of chain growth and alcohol formation during the Fischer-Tropsch synthesis
Catalysis Today 36(3) (1997), 347

Xu, L., Bao, S., O'Brien, R.J., Raje, A., Davis, B.H.
Don't rule out iron catalysts for Fischer-Tropsch synthesis
Chemtech 28 (1998), 47

Yang, Y., Xiang, H.W., Xu, Y.Y., Bai, L., Li, Y.W.
Effect of potassium promoter on precipitated iron-manganese catalyst for Fischer-Tropsch synthesis
Applied Catalysis A: General, 266 (2) (2004), 181

Zhang, H.B., Schrader, G.L.,
Characterisation of a fused iron catalyst for Fischer-Tropsch synthesis by in situ laser Raman spectroscopy
Journal of Catalysis 95 (1985), 325

Zhang, Y., Davis, B.,
Indirect Liquefaction-Where do we stand?
Catalysis 15 (2000), 183

Zhang, C.H., Teng, B.T., Yang, Y., Tao, Z., Hao, Q., Wan, H., Yi, F., Xu, B., Xiang, H., Li, J.
Effect of air-exposure on reduction behaviour of a Fe–Mn–Cu–K/SiO_2 Fischer-Tropsch synthesis catalyst
Journal of Molecular Catalysis A: Chemical 239 (2005), *15*

Zhang, C.H., Yang, Y., Teng, B.T., Li, T.Z., Zheng, H.Y., Xiang, H.W., Li, Y.W.
Study of an iron-manganese Fischer–Tropsch synthesis catalyst promoted with copper
Journal of Catalysis 237 (2006), *405*

Zhao, R., Goodwin jr., J.G, Jothimurugesan, K., Gangwal, S.K., Spivey, J.J.
Spray dried iron Fischer-Tropsch catalyst. 1. Effect of structure on the attrition resistance of the catalyst in the calcined state.
Industrial Engineering Chemistry Research 40 (2001a), 1065

Zimmerman, W.H., Bukur, D.B.

Reaction kinetics over iron catalysts used for the Fischer-Tropsch synthesis

Canadian Journal of Chemical Engineering 68 (1990), 292

APPENDICES

APPENDIX A

RAW FISCHER-TROPSCH SYNTHESIS DATA

In Tables A1 to A6 the performance data for the Fischer-Tropsch runs at various temperatures and H_2/CO feed ratios are displayed.

A.1. The effect of synthesis temperature

A.1.1. Experiment at 225°C

Table A.1: Fischer-Tropsch synthesis conditions for experiment at 225ºC

Time on stream [h]	27.9	43.3	67.7	165.4	190.0	213.8	238.0
Catalyst Inventory [g]	10	10	10	10	10	10	10
Reactor stirrer speed [rpm]	400	400	400	400	400	400	400
Reactor temperature [ºC]	245	245	245	225	225	225	225
GHSV syngas [ml (STP) / gcat / h]	9471	9615	9471	4778	4803	4797	4797
pH_2O /(pH_2+pCO)	0.1	0.11	0.1	0.08	0.1	0.09	0.09
CO_2 selectivity [% C atom]	22.4	21	22.4	22.2	20.2	20.4	20.4
FT Reaction Rate [mole CO / g-cat / s]	1.13E-05	1.24E-05	1.13E-05	5.32E-06	5.61E-06	5.50E-06	5.49E-06
WGS Reaction Rate [mole CO_2 formed / g-cat / s]	3.21E-06	3.21E-06	3.21E-06	1.45E-06	1.44E-06	1.38E-06	1.38E-06

Note: The part highlighted grey indicate when conditions were changed to experimental conditions

A.1.2. Experiment at 245°C

Table A.2: Fischer-Tropsch synthesis conditions for experiment at 245ºC

Time on stream [h]	15.0	38.9	63.0	162.2	185.8	210.1	229.6
Catalyst Inventory [g]	10	10	10	10	10	10	10
Reactor stirrer speed [rpm]	400	400	400	400	400	400	400
Reactor temperature [ºC]	245	245	245	245	245	245	245
GHSV syngas [ml (STP) / gcat / h]	9631	9551	9716	9744	9796	9800	9800
pH_2O /(pH_2+pCO)	0.1	0.12	0.13	0.1	0.1	0.08	0.09
CO_2 selectivity [% C atom]	24.4	22.4	20.2	21.5	17.9	21.1	21.1
FT Reaction Rate [mole CO / g-cat / s]	1.27E-05	1.25E-05	1.35E-05	1.19E-05	1.21E-05	1.10E-05	1.06E-05
WGS Reaction Rate [mole CO_2 formed / g-cat / s]	3.75E-06	3.79E-06	3.43E-06	3.06E-06	2.51E-06	2.70E-06	2.66E-06

A.1.3. Experiment at 265°C

Table A.3: Fischer-Tropsch synthesis conditions for experiment at 265ºC

Time on stream [h]	22.5	41.9	66.1	162.5	185.5	210.0	234.0
Catalyst Inventory [g]	5	5	5	5	5	5	5
Reactor stirrer speed [rpm]	400	400	400	400	400	450	400
Reactor temperature [ºC]	245	245	245	265	265	265	265
GHSV syngas [ml (STP) / gcat / h]	9301	9980	9864	18957	18957	18957	18843
pH_2O /(pH_2+pCO)	0.2	0.1	0.1	0.1	0.1	0.1	0.1
CO_2 selectivity [% C atom]	21.3	21.3	19.6	24.2	24.6	25.3	25.3
FT Reaction Rate [mole CO / g-cat / s]	1.20E-05	1.27E-05	1.26E-05	2.34E-05	2.34E-05	2.31E-05	2.34E-05
WGS Reaction Rate [mole CO_2 formed / g-cat / s]	2.31E-06	3.19E-06	3.10E-06	7.19E-06	7.27E-06	7.44E-06	7.19E-06

Note: The part highlighted grey indicate when conditions were changed to experimental conditions

A.2. The effect of H_2/CO ratio

A.2.1. Experiment with Feed gas H_2/CO ratio of 1.3

Table A.4: Fischer-Tropsch synthesis conditions for experiment with a Feed gas H_2/CO ratio of 1.3

Time on stream [h]	22.8	46.1	150.0	171.8	191.9
Catalyst Inventory [g]	10	10	10	10	10
Reactor stirrer speed [rpm]	400	400	400	400	400
GHSV syngas [ml (STP) / gcat / h]	9451	9818	4014	4078	4107
H_2/CO in feed gas	1.52	1.51	1.25	1.25	1.27
pH_2O /(pH_2+pCO)	0.09	0.11	0.12	0.13	0.09
CO_2 selectivity [% C atom]	27.5	24.4	31.4	30.3	33.8
FT Reaction Rate [mole CO / g-cat / s]	1.30E-05	1.40E-05	6.80E-06	7.00E-06	6.30E-06
WGS Reaction Rate [mole CO_2 formed / g-cat / s]	4.40E-06	4.30E-06	3.00E-06	3.00E-06	3.00E-06

Note: The part highlighted grey indicate when conditions were changed to experimental conditions

A.2.2. Experiment with Feed gas H_2/CO ratio of 1.6

Table A.5: Fischer-Tropsch synthesis conditions for experiment with a Feed gas H_2/CO ratio of 1.6

Time on stream [h]	38.9	63.0	162.2	185.8	210.1	229.6
Catalyst Inventory [g]	10	10	10	10	10	10
Reactor stirrer speed [rpm]	400	400	400	400	400	400
GHSV syngas [ml (STP) / gcat / h]	9551	9716	9744	9796	9800	9800
H_2/CO in feed gas	1.56	1.56	1.56	1.57	1.56	1.56
pH_2O /(pH_2+pCO)	0.12	0.13	0.1	0.1	0.08	0.09
CO_2 selectivity [% C atom]	22.4	20.2	21.5	17.9	21.1	19.9
FT Reaction Rate [mole CO / g-cat / s]	1.25E-05	1.35E-05	1.19E-05	1.21E-05	1.10E-05	1.06E-05
WGS Reaction Rate [mole CO_2 formed / g-cat / s]	3.79E-06	3.43E-06	3.06E-06	2.51E-06	2.70E-06	2.66E-06

A.2.3. Experiment with Feed gas H_2/CO ratio of 2.1

Table A.6: Fischer-Tropsch synthesis conditions for experiment with a Feed gas H_2/CO ratio of 2.1

Time on stream [h]	23.0	47.7	142.7	167.2	190.7
Catalyst Inventory [g]	10	10	10	10	10
Reactor stirrer speed [rpm]	400	400	400	400	400
GHSV syngas [ml (STP) / gcat / h]	9981	10072	15517	15518	14519
H_2/CO in feed gas	1.50	1.51	2.12	2.12	2.10
pH_2O /(pH_2+pCO)	0.1	0.11	0.08	0.07	0.08
CO_2 selectivity [% C atom]	19.6	19.9	16.0	15.6	16.3
FT Reaction Rate [mole CO / g-cat / s]	1.22E-05	1.26E-05	1.47E-05	1.40E-05	1.43E-05
WGS Reaction Rate [mole CO_2 formed / g-cat / s]	2.87E-06	3.07E-06	2.71E-06	2.52E-06	2.23E-06

Note: The part highlighted grey indicate when conditions were changed to experimental conditions

APPENDIX B

FISCHER-TROPSCH PRODUCT SELECTIVITY DATA

The data displayed in the tables below (Tables B1 to B24) were used to construct the selectivity (as a function of carbon number) graphs in Chapter 5. The Anderson-Schulz-Flory plots (displayed in Chapter 4) were also derived from these C atom selectivities. The C atom percentages were determined using methods described in Chapter 3 section 3.5.5.

B.1. Fischer-Tropsch synthesis runs at different temperature

Table B.1: n-Paraffin selectivity data obtained from GCxGC analysis for experiments at 225ºC, 245 ºC and 265ºC

n-Paraffins [C-atom %]															
Run	**Carbon number**														
	1	**2**	**3**	**4**	**5**	**6**	**7**	**8**	**9**	**10**	**11**	**12**	**13**	**14**	**15**
225ºC	2.208	0.340	0.700	0.644	0.526	0.447	0.427	0.281	0.396	0.453	0.480	0.489	0.490	0.488	0.472
245ºC	3.975	0.739	1.102	1.078	0.892	0.829	0.750	0.496	0.629	0.693	0.719	0.777	0.789	0.804	0.820
265ºC	5.235	1.302	1.385	1.258	0.995	0.885	0.776	0.614	0.716	0.753	0.772	0.772	0.773	0.767	0.749

Table B.2: 1-Olefin selectivity data obtained from GCxGC analysis for experiments at 225ºC, 245 ºC and 265ºC

1-Olefins [C-atom %]															
Run	**Carbon number**														
	1	**2**	**3**	**4**	**5**	**6**	**7**	**8**	**9**	**10**	**11**	**12**	**13**	**14**	**15**
225ºC	-	1.212	1.967	1.572	1.195	0.984	0.818	0.714	0.681	0.740	0.729	0.677	0.640	0.577	0.502
245ºC	-	1.918	3.792	3.196	2.486	2.073	1.773	1.550	1.263	1.261	1.150	1.043	0.934	0.802	0.655
265ºC	-	2.815	5.530	4.589	3.393	2.730	2.206	1.853	1.706	1.624	1.461	1.263	1.133	0.946	0.766

Table B.3: n-Alcohol-(1) selectivity data obtained from GCxGC analysis for experiments at 225ºC, 245 ºC and 265ºC

n-Alcohols-(1) [C-atom %]															
Run	**Carbon number**														
	1	**2**	**3**	**4**	**5**	**6**	**7**	**8**	**9**	**10**	**11**	**12**	**13**	**14**	**15**
225ºC	0.331	0.361	0.180	0.239	0.248	0.235	0.208	0.188	0.168	0.153	0.136	0.122	0.117	0.100	0.082
245ºC	0.576	0.736	0.311	0.354	0.358	0.322	0.280	0.246	0.224	0.201	0.171	0.153	0.163	0.132	0.120
265ºC	0.841	0.917	0.429	0.414	0.421	0.373	0.312	0.263	0.223	0.189	0.172	0.149	0.133	0.111	0.085

Table B.4: Linear carboxylic acid selectivity data obtained from GCxGC analysis for experiments at 225ºC, 245 ºC and 265ºC

Linear Carboxylic Acids [C-atom %]									
Run	**Carbon number**								
	1	**2**	**3**	**4**	**5**	**6**	**7**	**8**	**9**
225ºC	-	0.408	0.066	0.077	0.045	0.060	0.050	0.033	0.033
245ºC	-	0.350	0.065	0.068	0.037	0.034	0.038	0.021	0.019
265ºC	-	0.303	0.077	0.068	0.040	0.036	0.043	0.024	0.023

Table B.5: Ketone selectivity data obtained from GCxGC analysis for experiments at 225ºC, 245 ºC and 265ºC

Ketones [C-atom %]											
Run	**Carbon number**										
	1	**2**	**3**	**4**	**5**	**6**	**7**	**8**	**9**	**10**	**11**
225ºC	-	-	0.042	0.012	0.009	0.006	0.006	0.006	0.003	0.002	0.002
245ºC	-	-	0.054	0.018	0.014	0.014	0.011	0.008	0.004	0.003	0.003
265ºC	-	-	0.074	0.023	0.022	0.021	0.016	0.011	0.005	0.005	0.004

Table B.6: Aldehyde selectivity data obtained from GCxGC analysis for experiments at 225ºC, 245 ºC and 265ºC

Aldehydes [C-atom %]											
Run	**Carbon number**										
	1	**2**	**3**	**4**	**5**	**6**	**7**	**8**	**9**	**10**	**11**
225ºC	-	0.064	0.081	0.071	0.062	0.054	0.038	0.035	0.036	0.031	0.033
245ºC	-	0.048	0.072	0.066	0.054	0.047	0.039	0.035	0.035	0.029	0.033
265ºC	-	0.032	0.040	0.036	0.026	0.027	0.027	0.026	0.025	0.024	0.025

Table B.7: Internal Olefin selectivity data obtained from GCxGC analysis for experiments at 225ºC, 245 ºC and 265ºC

Internal Olefins [C-atom %]										
Run	**Carbon number**									
	6	**7**	**8**	**9**	**10**	**11**	**12**	**13**	**14**	**15**
225ºC	0.006	0.010	0.016	0.022	0.027	0.035	0.037	0.039	0.037	0.034
245ºC	0.023	0.044	0.072	0.102	0.130	0.161	0.184	0.199	0.196	0.197
265ºC	0.055	0.092	0.134	0.168	0.197	0.241	0.257	0.262	0.246	0.244

Table B.8: Branched Olefin selectivity data obtained from GCxGC analysis for experiments at 225ºC, 245 ºC and 265ºC

Branched Olefins [C-atom %]										
Run	**Carbon number**									
	6	**7**	**8**	**9**	**10**	**11**	**12**	**13**	**14**	**15**
225ºC	0.008	0.021	0.038	0.051	0.055	0.056	0.051	0.039	0.032	0.024
245ºC	0.017	0.041	0.068	0.082	0.084	0.086	0.076	0.061	0.052	0.039
265ºC	0.049	0.113	0.171	0.196	0.200	0.199	0.181	0.146	0.119	0.085

Table B.9: Branched Paraffin selectivity data obtained from GCxGC analysis for experiments at 225ºC, 245 ºC and 265ºC

Branched Paraffins [C-atom %]										
Run	**Carbon number**									
	6	**7**	**8**	**9**	**10**	**11**	**12**	**13**	**14**	**15**
225ºC	0.008	0.016	0.027	0.037	0.042	0.042	0.045	0.046	0.033	0.020
245ºC	0.008	0.029	0.047	0.056	0.063	0.063	0.069	0.074	0.061	0.049
265ºC	0.036	0.065	0.098	0.111	0.121	0.120	0.125	0.128	0.110	0.092

Table B.10: n-Alcohol-(2) selectivity data obtained from GCxGC analysis for experiments at 225ºC, 245 ºC and 265ºC

n-Alcohols-(2) [C-atom %]													
Run	**Carbon number**												
	3	**4**	**5**	**6**	**7**	**8**	**9**	**10**	**11**	**12**	**13**	**14**	**15**
225ºC	0.000	0.000	0.001	0.002	0.002	0.003	0.003	0.004	0.004	0.005	0.005	0.005	0.006
245ºC	0.001	0.005	0.005	0.006	0.006	0.007	0.008	0.009	0.009	0.010	0.012	0.012	0.012
265ºC	0.002	0.008	0.008	0.008	0.008	0.009	0.010	0.010	0.010	0.012	0.015	0.015	0.014

Table B.11: Branched Alcohol selectivity data obtained from GCxGC analysis for experiments at 225ºC, 245 ºC and 265ºC

Branched Alcohols [C-atom %]												
Run	**Carbon number**											
	4	**5**	**6**	**7**	**8**	**9**	**10**	**11**	**12**	**13**	**14**	**15**
225ºC	0.001	0.015	0.039	0.046	0.042	0.041	0.038	0.023	0.024	0.023	0.013	0.009
245ºC	0.002	0.023	0.055	0.063	0.058	0.062	0.058	0.040	0.035	0.044	0.026	0.022
265ºC	0.005	0.038	0.082	0.093	0.082	0.077	0.063	0.048	0.051	0.055	0.035	0.029

Table B.12: Branched Acid selectivity data obtained from GCxGC analysis for experiments at 225ºC, 245 ºC and 265ºC

Branched Acids [C-atom %]					
Run	**Carbon number**				
	4	**5**	**6**	**7**	**8**
225ºC	0.003	0.007	0.011	0.013	0.012
245ºC	0.008	0.015	0.019	0.014	0.008
265ºC	0.004	0.008	0.013	0.012	0.009

B.2. Fischer-Tropsch synthesis runs at different H_2/CO ratios

Table B.13: n-Paraffin selectivity data obtained from GCxGC analysis for experiment at Feed gas H_2/CO ratios of 1.3, 1.6 and 2.1

n-Paraffins [C-atom %]															
Run	**Carbon number**														
	1	**2**	**3**	**4**	**5**	**6**	**7**	**8**	**9**	**10**	**11**	**12**	**13**	**14**	**15**
1.3	3.755	0.606	0.916	0.785	0.611	0.562	0.482	0.448	0.512	0.527	0.519	0.518	0.521	0.562	0.595
1.6	4.010	0.778	1.136	1.127	0.926	0.810	0.751	0.551	0.699	0.771	0.799	0.807	0.796	0.754	0.695
2.1	5.721	1.915	1.184	1.147	0.919	0.747	0.823	0.496	0.601	0.648	0.690	0.716	0.744	0.770	0.806

Table B.14: 1-Olefin selectivity data obtained from GCxGC analysis for experiment at Feed gas H_2/CO ratios of 1.3, 1.6 and 2.1

1-Olefins [C-atom %]															
Run	**Carbon number**														
	1	**2**	**3**	**4**	**5**	**6**	**7**	**8**	**9**	**10**	**11**	**12**	**13**	**14**	**15**
1.3	-	1.635	2.840	2.285	1.617	1.399	1.120	1.025	1.048	0.985	0.864	0.732	0.601	0.545	0.480
1.6	-	1.984	3.927	3.286	2.530	2.092	1.784	1.542	1.370	1.366	1.246	1.075	0.938	0.753	0.563
2.1	-	0.875	3.379	2.649	1.909	1.500	1.137	0.840	0.910	0.896	0.845	0.776	0.699	0.615	0.532

Table B.15: n-Alcohol-(1) selectivity data obtained from GCxGC analysis for experiment at Feed gas H_2/CO ratios of 1.3, 1.6 and 2.1

n-Alcohols-(1) [C-atom %]															
Run	**Carbon number**														
	1	**2**	**3**	**4**	**5**	**6**	**7**	**8**	**9**	**10**	**11**	**12**	**13**	**14**	**15**
1.3	0.695	0.701	0.360	0.425	0.430	0.370	0.305	0.252	0.208	0.171	0.155	0.132	0.136	0.086	0.097
1.6	0.793	0.812	0.314	0.357	0.381	0.353	0.308	0.271	0.246	0.219	0.187	0.169	0.146	0.118	0.100
2.1	0.892	0.924	0.299	0.330	0.317	0.294	0.223	0.197	0.174	0.152	0.135	0.125	0.119	0.124	0.099

Table B.16: Linear carboxylic acid selectivity data obtained from GCxGC analysis for experiment at Feed gas H_2/CO ratios of 1.3, 1.6 and 2.1

Linear Carboxylic Acid [C-atom %]									
Run	**Carbon number**								
	1	**2**	**3**	**4**	**5**	**6**	**7**	**8**	**9**
1.3	-	0.618	0.118	0.128	0.076	0.066	0.049	0.031	0.030
1.6	-	0.350	0.065	0.068	0.037	0.034	0.038	0.021	0.019
2.1	-	0.345	0.058	0.065	0.094	0.070	0.023	0.014	0.010

Table B.17: Ketone selectivity data obtained from GCxGC analysis for experiment at Feed gas H_2/CO ratios of 1.3, 1.6 and 2.1

Ketones [C-atom %]											
Run	**Carbon number**										
	1	**2**	**3**	**4**	**5**	**6**	**7**	**8**	**9**	**10**	**11**
1.3	-	-	0.071	0.023	0.022	0.018	0.012	0.009	0.004	0.004	0.003
1.6	-	-	0.075	0.022	0.019	0.017	0.008	0.008	0.005	0.004	0.003
2.1	-	-	0.079	0.020	0.016	0.016	0.005	0.007	0.006	0.004	0.002

Table B.18: Aldehyde selectivity data obtained from GCxGC analysis for experiment at Feed gas H_2/CO ratios of 1.3, 1.6 and 2.1

Aldehydes [C-atom %]											
Run	**Carbon number**										
	1	**2**	**3**	**4**	**5**	**6**	**7**	**8**	**9**	**10**	**11**
1.3	-	0.046	0.049	0.044	0.045	0.047	0.039	0.035	0.035	0.029	0.033
1.6	-	0.065	0.072	0.066	0.054	0.049	0.044	0.045	0.051	0.046	0.037
2.1	-	0.136	0.140	0.134	0.108	0.083	0.072	0.068	0.058	0.054	0.074

Table B.19: Internal Olefin selectivity data obtained from GCxGC analysis for experiment at Feed gas H_2/CO ratios of 1.3, 1.6 and 2.1

Internal Olefins [C-atom %]										
Run	**Carbon number**									
	6	**7**	**8**	**9**	**10**	**11**	**12**	**13**	**14**	**15**
1.3	0.015	0.010	0.016	0.022	0.027	0.035	0.037	0.039	0.037	0.034
1.6	0.025	0.044	0.072	0.102	0.130	0.161	0.184	0.199	0.196	0.197
2.1	0.012	0.031	0.046	0.058	0.068	0.080	0.091	0.104	0.113	0.118

Table B.20: Branched Olefin selectivity data obtained from GCxGC analysis for experiment at Feed gas H_2/CO ratios of 1.3, 1.6 and 2.1

Branched Olefins [C-atom %]										
Run	**Carbon number**									
	6	**7**	**8**	**9**	**10**	**11**	**12**	**13**	**14**	**15**
1.3	0.039	0.085	0.124	0.137	0.136	0.129	0.114	0.085	0.064	0.042
1.6	0.019	0.046	0.076	0.094	0.094	0.096	0.087	0.065	0.057	0.042
2.1	-	0.012	0.040	0.055	0.065	0.066	0.067	0.061	0.044	0.044

Table B.21: Branched Paraffin selectivity data obtained from GCxGC analysis for experiment at Feed gas H_2/CO ratios of 1.3, 1.6 and 2.1

Branched Paraffins [C-atom %]										
Run	**Carbon number**									
	6	**7**	**8**	**9**	**10**	**11**	**12**	**13**	**14**	**15**
1.3	0.031	0.057	0.077	0.084	0.091	0.085	0.083	0.081	0.038	0.042
1.6	0.016	0.032	0.051	0.063	0.069	0.071	0.077	0.082	0.042	0.053
2.1	-	0.020	0.035	0.048	0.055	0.061	0.060	0.060	0.053	0.052

Table B.22: n-Alcohol-(2) selectivity data obtained from GCxGC analysis for experiment at Feed gas H_2/CO ratios of 1.3, 1.6 and 2.1

n-Alcohols-(2) [C-atom %]													
Run	**Carbon number**												
	3	**4**	**5**	**6**	**7**	**8**	**9**	**10**	**11**	**12**	**13**	**14**	**15**
1.3	0.0009	0.0046	0.0048	0.0056	0.0063	0.0072	0.0081	0.0087	0.0089	0.0102	0.0122	0.0125	0.0117
1.6	0.0006	0.0046	0.0042	0.0061	0.0059	0.0071	0.0076	0.0076	0.0082	0.0090	0.0098	0.0101	0.0099
2.1	0.0004	0.0012	0.0021	0.0030	0.0037	0.0040	0.0045	0.0056	0.0049	0.0067	0.0068	0.0068	0.0082

Table B.23: Branched Alcohol selectivity data obtained from GCxGC analysis for experiment at Feed gas H_2/CO ratios of 1.3, 1.6 and 2.1

Branched Alcohols [C-atom %]												
Run	**Carbon number**											
	4	**5**	**6**	**7**	**8**	**9**	**10**	**11**	**12**	**13**	**14**	**15**
1.3	0.0040	0.0353	0.0816	0.0873	0.0754	0.0709	0.0624	0.0579	0.0431	0.0364	0.0238	0.0175
1.6	0.0027	0.0256	0.0603	0.0696	0.0643	0.0655	0.0574	0.0418	0.0389	0.0441	0.0252	0.0231
2.1	0.0016	0.0162	0.0447	0.0516	0.0509	0.0459	0.0367	0.0302	0.0262	0.0272	0.0228	0.0260

Table B.24: Branched Acid selectivity data obtained from GCxGC analysis for experiment at Feed gas H_2/CO ratios of 1.3, 1.6 and 2.1

Branched Acids [C-atom %]					
Run	**Carbon number**				
	4	**5**	**6**	**7**	**8**
1.3	0.004	0.008	0.016	0.015	0.015
1.6	0.003	0.007	0.010	0.009	0.011
2.1	0.001	0.004	0.004	0.004	0.007

APPENDIX C

STATISTICAL CONCEPTS AND EQUATIONS

Average

$$\bar{X} = \frac{\sum Xi}{n}$$

Where

$\bar{X}$	=	Average of data points
Xi	=	Data point i
n	=	Number of data points

Standard Deviation

$$S = \pm \sqrt{\frac{\sum (Xi - \bar{X})^2}{n-1}}$$

Where

S	=	Standard Deviation, S, of data points
$\bar{X}$	=	Average of data points
Xi	=	Data point i
n	=	Number of data points

%Relative Standard Deviation

$$\%RSD = \frac{S}{\bar{X}} \times 100$$

Where

$\%RSD$	=	% Relative Standard Deviation of data points
S	=	Standard Deviation, S, of data points
$\bar{X}$	=	Average of data points

Acceptance Criteria for precision utilizing %RSD estimates

The *AOAC* manual for the Peer Verified Methods program presents a table (see Table C.1) with %RSD estimates that can be used to determine the precision of data as a function of analyte concentration.

Table C.1: Acceptance criteria for precision utilizing %RSD estimates

Analyte Concentration	Unit	RSD (%)
100	100%	1.3
≥10	10%	2.8
≥1	1%	2.7
≥0.1	0.10%	3.7
0.01	100 ppm	5.3
0.001	10 ppm	7.3
0.0001	1 ppm	11
0.00001	100 ppb	15
0.000001	10 ppb	21
0.0000001	1 ppb	30

Accuracy

$$Accuracy = \%\ Recovery = \frac{measured\ result}{true\ value} \times 100$$

The *AOAC* manual for the Peer Verified Methods program presents a table (see Table C.2) with % Recovery estimates that can be used to determine the accuracy of data as a function of analyte concentration.

Table C.2: Acceptance criteria for accuracy as % Recovery

Analyte Concentration	Unit	Mean % Recovery
100	100%	98-102
10 - 99	10%	98-102
1 - 10	1%	97-103
0.1 – 1	0.10%	95-105
0.01	100 ppm	90-107
0.001	10 ppm	80-110
0.0001	1 ppm	80-110
0.00001	100 ppb	80-110
0.000001	10 ppb	60-115
0.0000001	1 ppb	40-120

Confidence limits

Confidence limits are calculated values that define an interval around a measured value. This calculated interval will contain the 'true value' at a specified probability, usually at 90%, 95%, or 99%.

$$CL_P = \pm t \times S$$

Where

CL_P	=	Confidence Limit at probability *(%p)*
t	=	α-Value for a double sided Student's t-test at probability (*%p)*
S	=	Standard Deviation, S, of data points

Table C.3: t-Values for Confidence limits

Degrees of Freedom	Confidence Level 90%	95%	99%
3	2.353	3.182	5.841
4	2.132	2.776	4.604
5	2.015	2.571	4.032
6	1.943	2.447	3.707
7	1.895	2.365	3.499
8	1.860	2.306	3.355
9	1.833	2.262	3.250
10	1.812	2.228	3.169
12	1.782	2.179	3.055
15	1.753	2.131	2.947